UNIVERSITY OF CALIFORNIA, MERCED

Periodontal Bacteria Influence Inflammasome Activation and Cytokine Secretion During Oral Infection

A dissertation submitted in partial satisfaction of the requirements for the degree Doctor of Philosophy

in

Quantitative and Systems Biology

by

Larry Johnson, M.Sc.

Committee in charge:
Professor Néstor J. Oviedo, Chair
Professor Wei-Chun Chin
Professor Katrina K. Hoyer

2016

The dissertation of Larry Johnson is approved, and it is acceptable in quality and form for publication on microfilm and electronically:

_____

Dr. Wei-Chun Chin

_____

Dr. Katrina K. Hoyer

_____

Dr. Néstor J. Oviedo, Chair

University of California, Merced

2016

DEDICATION

I would like to dedicate this to my mother and father, Joanna Tsai and Richard Johnson, for their sacrifices and support. I would also like to thank my brother, Peter Johnson, and my extended family as they are always there for me.

TABLE OF CONTENTS

LIST OF FIGURES

ACKNOWLEDGEMENTS

This studies were supported by intramural funds from the University of the Pacific, NIDCR grants R01DE019444, R01DE016593, T90DE021990, R01DE019444, University of California Presidential Chair, and the Fundação de Amparo à Pesquisa do Estado do Rio de Janeiro (FAPERJ). Additional funding also included from UC Merced Graduate Division and UC Merced Quantitative and Systems Biology Program.

I would also like to acknowledge the following collaborators:

Dr. Özlem Yilmaz at the Medical University of South Carolina, South Carolina, USA

Dr. Robson Coutinho-Silva at the Federal University of Rio de Janeiro, Rio de Janeiro, Brazil

Dr. Christina Maeda Takiya at the Federal University of Rio de Janeiro, Rio de Janeiro, Brazil

I would like to thank my undergraduate students:

Fiona Bui, Caitlin David, Cassandra Hernandez, Jeffrey Ly, Paul Barghouth, Javier Sanchez, and Natalia Barghouth

Permissions to reproduce and use copyright materials in this dissertation were obtained from *Cellular Microbiology*, *Microbes and Infection*, and *PLOS ONE*.

CURRICULUM VITAE

EDUCATION

Doctorate of Philosophy 2016
University of California, Merced
Quantitative and Systems Biology

Master of Science 2009
University of California, Merced
Quantitative and Systems Biology

Bachelor of Science 2007
University of California, Merced
Biological Sciences
Emphasis: Immunology

PUBLICATIONS

Johnson, L., Takiya C.M., Almeida-da-Silva C.L.C., Rocha G.M., Weissmüller G., Scharfstein J., Coutinho-Silva R., Ojcius D.M. Macrophage activation contributes to inflammatory response of *Fusobacterium nucleatum* oral infection in BALB/c mice. (Submitted for publication)

Bui, F.Q., **Johnson, L.**, Roberts, J., Hung, S.C., Lee, J., Atanasova, K.R., *et al.* (2015). Fusobacterium nucleatum infection of gingival epithelial cells leads to NLRP3 inflammasome-dependent secretion of IL-1beta and the danger signals ASC and HMGB1. *Cellular microbiology*.

Johnson, L., Atanasova, K.R., Bui, P.Q., Lee, J., Hung, S.C., Yilmaz, O. and Ojcius, D.M. (2015). *Porphyromonas gingivalis* attenuates ATP-mediated inflammasome activation and HMGB1 release through expression of a nucleoside-diphosphate kinase. *Microbes and infection / Institut Pasteur* 17, 369-377.

Johnson, L., Gaab, E.M., Sanchez, J., Bui, P.Q., Nobile, C.J., Hoyer, K.K., Peterson, M.W., and Ojcius, D.M. (2014). Valley fever: danger lurking in a dust cloud. *Microbes and infection / Institut Pasteur 16*, 591-600.

Hung, S.C., Choi, C.H., Said-Sadier, N., **Johnson, L.**, Atanasova, K.R., Sellami, H., Yilmaz, O., and Ojcius, D.M. (2013). P2X4 assembles with P2X7 and pannexin-1 in gingival epithelial cells and modulates ATP-induced reactive oxygen species production and inflammasome activation. *PloS one 8*, e70210.

Cain C.J., Conte D.A., García-Ojeda M.E., Daglio L.G., **Johnson L.**, Lau, E.H., *et al.* (2008). What Systems Biology Is (Not, Yet). *Science* 320,1013-1014.

FELLOWSHIPS AND FUNDING

Fundação Carlos Chagas Filho de Amparo à Pesquisa do Estado do Rio de Janeiro (FAPERJ) Research Fellowship	2015-2016
Fee and Tuition Fellowship (UC Merced Graduate Division/Quantitative and Systems Biology	2015-2016
Quantitative and Systems Biology Summer Research Fellowship	2014
Quantitative and Systems Biology Summer Research Fellowship	2013
Quantitative and Systems Biology Summer Need-Based Supplement	2013

PRESENTATIONS

Fiona Q. Bui, **Larry Johnson**, Kalina Rosenova Atanasova, Shu-Chen Hung, JoAnn Roberts, Jungnam Lee, OzlemYilmaz, and David M. Ojcius. "*Fusobacterium nucleatum* Infection of Gingival Epithelial Cells Leads to NLRP3 Inflammasome-Dependent Secretion of IL-1β and the Danger Signals ASC and HMGB1". 2nd Quantitative and Systems Biology Annual Retreat. Yosemite Bug Rustic Mountain Resort, Yosemite, California. 20 May 2015.

Larry Johnson, Kalina R. Atanasova, Phuong Q. Bui, Jungnam Lee, Shu-Chen Hung, Özlem Yilmaz, David M. Ojcius. "Porphyromonas gingivalis inhibits ATP-mediated inflammasome activation and HMGB1 release through expression of a nucleoside-diphosphate kinase." 1st Quantitative and Systems Biology Annual Retreat. Gateway Gardens Monte Carlo Ballroom, Merced, California. 6 November 2014.

Larry Johnson, & David M. Ojcius.
"Pregnancy and its Influence on the Course of *Chlamydia* Infection." 1st Annual Research Week. University of California, Merced. 4 March 2008.

Cruz Cristiane, **Larry Johnson**, Najwane Said, David Ojcius.
"Pro-inflammatory responses in response to ligation of a toll like receptor and the purinergic receptor $P2X_7$ in alveolar macrophages requires production of reactive oxygen species" 13th International Congress of Immunology, Rio de Janeiro, Brazil. 21 August 2007.

ABSTRACT OF THE DISSERTATION

Periodontal Bacteria Influence Inflammasome Activation and Cytokine Secretion During Oral Infection

by

Larry Johnson

Doctor of Philosophy in Quantitative and Systems Biology

University of California, Merced, 2016

Professor David M. Ojcius, Dissertation Advisor

Porphyromonas gingivalis and *Fusobacterium nucleatum*, Gram-negative anaerobic bacteria, have been identified as major contributing pathogens in the etiology of mild to acute periodontitis. They are opportunistic pathogens that are highly adapted to colonize the oral epithelial tissues. *P. gingivalis* has also been associated with a variety of other chronic and inflammatory conditions including orodigestive cancers, rheumatoid arthritis, liver disease, and diabetes. Whereas, *F. nucleatum* has been linked to Lemierre's syndrome and skin ulcers. Recognition and clearance of these pathogens are regulated by inflammation and host immune response. We aimed to study the mechanisms and inflammatory responses (focusing on the effect with intracellular complexes known as inflammasomes) used by *P. gingivalis* and *F. nucleatum* to survive and persist during infection in gingival epithelial cells (GECs). Our findings indicate *P. gingivalis* infection inhibits inflammasome activation and release of pro-inflammatory cytokines by secretion of nucleoside-diphosphate kinase (NDK) to hydrolyze extracellular ATP. By defining NDK as a key enzyme for influencing inflammation in *P. gingivalis* infection, therapeutic methods can be designed to possibly target NDK to prevent and treat periodontitis. On the other hand, GECs infected with *F. nucleatum* induce an opposite immune response of upregulated cytokine production and release as a result of inflammasome activation. *In vivo* studies with BALB/c and C57BL/6 mice also show pro-inflammatory response during infection. Our findings can be used as a model of invasion during *F. nucleatum* infection *in vitro* and *in vivo*. Expanding our understanding of host response to pathogenic bacteria is important for limiting progression of periodontitis and other emerging systematic disease linked to these bacteria.

LIST OF ABBREVIATIONS

Symbol	Definition
ASC	Apoptosis-associated speck-like protein
ATP	Adenosine triphosphate
BMDMs	Bone marrow-derived macrophages
Ca^{2+}	Calcium
Caspases	Cysteine-aspartic acid proteases
cDNA	Complementary DNA
CFU	Colony-forming unit
Cl^-	Chloride
CLRs	C-type lectin receptors
CTB	Cholera toxin B
DAMPs	Danger-associated molecular patterns
DNA	Deoxyribonucleic acid
dsRNA	double-stranded RNA
FadA	*Fusobacterium nucleatum ad*hesin A
GECs	Gingival epithelial cells
H&E	Hematoxylin-eosin
H^+	Hydrogen
HMGB1	High-motility group box protein 1
HRP	Horseradish peroxidase
IFNs	type I interferons
IgG	Immunoglobulin G
IL	Interleukin
IRFs	Interferon-regulatory factors
K^+	Potassium
KO	Knock-out
LeTx	Lethal toxin
LPS	Lipopolysaccharide
LRR	Leucine-rich repeat
MDP	Muramyl dipeptide
MSU	Monosodium urate
NDK	Nucleotide-diphosphate kinase
NF-kB	nuclear factor-kB
NLRs	NOD-like receptors
OD	Optical density
PAMPs	Pathogen-associated molecular patterns
PBS	Phosphate-buffered saline

PCR	Polymerase chain reaction
PRRs	Pattern recognition receptors
PVDF	Polyvinylidene fluoride
RLRs	Retinoic acid-inducible gene RIG-1-like receptors
RNA	Ribonucleic acid
ROS	Reactive oxygen species
RT-PCR	Reverse Transcription polymerase chain reaction
SDS-PAGE	Sodium dodecyl sulfate polyacrylamide gel electrophoresis
ssRNA	Single-stranded RNA
TGF	Transforming growth factor
TLRs	Toll-like receptors
TNF	Tumor necrosis factor
TRAP	Tartrate-resistant acid phosphatase
TRIF	TIR-domain-containing adapter-inducing interferon-β

Chapter 1: Overview

1.1 Background

Periodontitis

Mild to severe periodontitis afflicts about 15-20% of middle-aged adults worldwide [1]. This disease arises from multiple factors which include diet, tobacco use, oral hygiene, and heavy alcohol use [1]. Some of these causes can be prevented or a decrease in progression of disease with lifestyle changes. However, there are limitations to those individuals of lower-income countries. Many countries put regular dental care as a low priority in their decisions for policy making [2]. Therefore, the cost falls to the individual for periodontal surgery, which can range from $4000 to $5000 to those who can afford it [3]. For those suffering with persistent oral infection, it can contribute to other systemic problems or diseases such as cardiovascular diseases, diabetes, pregnancy complications, and respiratory diseases [4]. As a result, this can contribute to additional medical costs.

Most cases of periodontitis in humans are diagnosed when the observation of the gingiva, or gums, show signs of swelling, redness, or chronically bleeding [5]. These are characteristics of inflammation. At this stage of disease, pathogenic bacteria have induced a chronic inflammatory response. Without treatment, the outcome increases chances of tooth loss and persistent infection, which may affect overall health. Preceding the disease, one can develop gingivitis. It is characterized with similar symptoms to periodontitis, but without tooth loss. To understand how to prevent either of these diseases, it is important to study host response and survival mechanisms of the pathogens in the host oral cavity. This can provide methods to control and suppress inflammation after clearance of infection and avoid development of autoinflammatory diseases.

Oral cavity as a first line of defense

Microorganisms are found throughout the oral cavity and attach to surfaces within the mouth such: cheeks, tongue, and teeth [6]. The junctional epithelium, which is located between the tooth and gingival connective tissue, is a gingival crevicular fluid-filled area for bacteria to reside [7]. This periodontal pocket contains various microorganisms including: *Porphyromonas gingivalis*, *Streptococcus gordonii*, *Fusobacterium nucleatum, and Aggregatibacter actinomycetemcomitans* [8-10]. The bacteria most commonly found is *F. nucleatum* and can form biofilms on teeth [11-13]. Biofilms provide opportunity for bacteria adhere, where they compete for nutrients and space. *P. gingivalis* is one of these organisms to attach and coaggregate in this anaerobic environment [14, 15]. Both *F. nucleatum* and *P. gingivalis* are commonly found in high frequencies in periodontal patients [16-18].

Bacteria colonize the oral cavity as commensal or infectious organisms. Dr. Sigmund Socransky pioneered two distinct ideas correlating oral pathogens and the oral cavity. The first is to distinguish an organism as an infectious oral pathogen. There are five parts to the criteria, which are adapted from Koch's postulates. 1) The pathogen must be present in high numbers in those afflicted by disease in comparison to healthy individuals showing a presence of low frequency [19]. 2) When eliminating the organism, the progression of disease should stop [19]. 3) A host immune response is required in the presence of the pathogen to show it influences development of disease [19]. 4) The

organism can be cultivated outside the host and pathogenesis can be observed when it is reintroduced to another host [19]. 5) The last criteria is the pathogen has a number of unique mechanisms or virulence factors to cause destructive periodontal disease [19].

Socransky's second significant contribution to understanding dental disease is categorizing the communities of microbial complexes based on their clinical measurement of disease with pocket depth and bleeding on probing [20]. The complexes are separated into five numeric or color groups. The 1st complex (red complex) describes *Porphyromonas gingivalis, Bacteroides forsythus*, and *Treponema denticola* as most predominant deep in the periodontal pocket and clinically associated with periodontal diagnosis [20]. *Fusobacterium nucleatum*, *Prevotella intermedia*, and *Streptococcus constellatus* are a few examples of the bacteria as part of the 2nd complex (orange complex), which are close in relationship to the red complex and show clinical signs of pocket depth [20]. The remaining categories are the 3rd complex (yellow complex), 4th complex (green complex), and 5th complex (purple complex) [20]. Although these last complexes aren't described as highly significant in diagnosis of periodontal disease, they are suggested playing a role in early colonization of pathogenic bacteria [20]. Collectively, these methods aid to distinguish commensal and pathogenic bacteria and allow to focus studies on pathogens, which may lead to a better understanding of periodontal disease.

Epithelial cells are found throughout the body covering the intestinal tract, respiratory airways, and skin [21]. These cells act as physical and chemical barrier to protect against pathogens. Gingival epithelial cells (GECs) are the first types of cells to encounter and be invaded by microorganisms in the oral cavity. Their structures are compact with cell-cell junctions and are distinguished by their keratin intermediate filaments [22]. GECs are now known to provide more functionality than acting as not only a barrier, but also contributing to immune recognition and response [22, 23]. They express a complexity of receptors to recognition pathogens and respond with release of inflammatory mediators to recruit other immune cells, such as neutrophils and macrophages [24]. However, their cytokines secretion levels fluctuate depending if tissues are inflamed or uninflamed [24, 25]. The basal levels of cytokines are low to regulate localized inflammation, limit tissue destruction, and maintain homeostasis with commensal microorganisms [25]. However, it is dysregulation of this system, which allows pathogenic organism to colonize and propagate the oral cavity. When this is left uncontrolled, localize and systemic disease can arise.

Overview of immune response and release of pro-inflammatory cytokines

The immune system recognizes and responds to foreign microbes with innate and adaptive immunity. While some characteristic of innate immunity is nonspecific and is triggered within hours, adaptive immunity is antigen-specific and develops over days. As part of innate immunity, inflammation can be induced at the site of infection. This contributes to recruitment of immune cells to fight the pathogens in an attempt to resolve the infection quickly. Inflammation is amplified by release of pro-inflammatory cytokines from uninfected and infected cells as a response to recognition of foreign antigen. The secretion of theses cytokines requires two signals for production and release.

Signal 1- Pathogen-associated molecular patterns and pattern recognition receptors

First, the host cell must recognize non-self antigens or pathogen-associated molecular patterns (PAMPs), which bind to pattern recognition receptors (PRRs). When a PRR is stimulated by a PAMP, the receptor triggers intracellular signaling cascades to activate transcription factors such as nuclear factor- κB (NF-κB) or interferon-regulatory factors (IRFs). The result is upregulation of gene transcription for pro-inflammatory cytokines [26].

There is a vast diversity of PAMPs derived from bacteria, viruses, fungi, and protozoans. A few examples are lipopolysaccharide (LPS), bacterial flagellin, double-stranded RNA (dsRNA), single-stranded RNA (ssRNA), peptidoglycan, or unmethylated CpG DNA [27]. The immune system has developed ways to distinguish live and dead microbes, secretion of PAMPs into the cytosol, and cytoskeleton rearrangement to shape its response to infection [28]. These PAMPs can be sensed by both surface and cytosolic receptors. The dual recognition from one PAMP can contribute to transcriptional and post-translational pathways without redundancy of downstream effects [28]. Thus, the immune system can establish a more effective response whether the microbe is intracellular or extracellular.

PRRs are divided into families which include Toll-like receptors (TLRs), C-type lectin receptors (CLRs), retinoic acid-inducible gene (RIG)-1-like receptors (RLRs), and NOD-like receptors [29]. These receptors can be found on the cell surface as transmembrane receptors or within the cell as cytosolic receptors. TLRs are the most studied of the PRRs [30, 31]. There are 10 TLRs in humans and 13 in mice characterized [32-34]. Each TLR has specificity for different pathogen components. Some examples are the binding of flagellin to TLR5, unmethylated CpG DNA to TLR9, and dsRNA to TLR3 [27]. TLR2 and TLR4 are most commonly associated with recognition of LPS from Gram-negative and Gram-positive bacteria [35, 36]. Activated TLRs commonly lead to the MyD88 signaling pathway and induction of pro-inflammatory cytokines by translocation of NF-κB into the nucleus [37]. However, an antiviral pathway, TIR-domain-containing adapter-inducing interferon-β (TRIF), can be signaled by stimulation of TLR3 and TLR4 [38]. This response activates production of type I interferons (IFNs), IFN-α and IFN-β [38].

Signal 2- Danger-associated molecular patterns and inflammasome

A secondary danger signal is needed to cleave the cytokines to a mature form for secretion. These molecules are danger-associated molecular patterns (DAMPs), can be released from damaged or necrotic cells, such as adenosine triphosphatase (ATP), monosodium urate (MSU) crystals, DNA, or high-motility group box protein 1 (HMGB1) [39-41]. DAMPs contribute to generation of reactive oxygen species (ROS) within the cell and activates the inflammasome to produce mature cysteine-aspartic acid proteases (caspases), like caspase-1, required to cleave pro-inflammatory cytokines to a mature form. Once released into the extracellular medium, these cytokines can contribute to an increase in inflammation and immune cell recruitment.

Canonical Inflammasome

The NLRs are a family of cytosolic receptors consisting of 23 human genes and at least 34 mouse genes [42, 43]. They are expressed mainly in macrophages and neutrophils, but can found in other immune cells and epithelial cells [43, 44]. There are five characterized inflammasomes within the NLR subfamilies: NLRP1 (NALP1b), NLRP3 (NALP3), NLRC4 (IPAF), AIM2, and Pyrin [45, 46]. Their structures are comprised of three similar components: the central nucleotide-binding and oligomerization (NOD or NACHT) domain, N-terminal caspases recruitment (CARD) domain, and C-terminal leucine–rich repeat (LRR) motif [42, 46, 47]. All these structures contribute to downstream signaling by protein-protein interaction and ligand sensing [42, 46, 48].

Each inflammasome has a variety of activators. NLPR1 is signaled by *Bacillus anthracis* lethal toxin (LeTx), *Toxoplasma gondii*, and muramyl dipeptide (MDP) [45, 46, 48, 49]. NLRP3 is the most studied inflammasome and has been shown to activated by *Staphylococcus aureus* and *Listeria monocytogenes*, which induce pore-forming toxins [42, 46]. Sendai virus, adenovirus, and influenza A virus can also trigger NLRP3 [42, 46]. Within the cell, there are activators such as ATP, ROS, fatty acid, and amyloid polypetides for NLRP3 [45]. NLRC4 responds to flagellin and Gram-negative bacteria, such as *Salmonella typhimurium* and *Shigella flexneri*, utilizing a type III or type IV secretion systems [45, 46, 49]. AIM2 is induced by cytosolic double-stranded DNA [45, 46, 50]. The pyrin inflammasome is activated by *Clostridium difficile* toxin B and Rho-inactivating toxins from *Vibrio parahaemolyticus*, *Histophilus somni*, and *Clostridium botulinum* [50].

Upon activation, apoptosis-associated speck-like protein (ASC) and caspase-1 assemble with the other domains to form the macromolecular protein complex, inflammasome [37, 42, 46]. ASC attracts additional pro-caspase-1 into close proximity and triggers autocleavage into caspase-1 [48]. Active caspase-1 then induces proteolysis of cytokines, pro-IL-1β and pro-IL-18, to their mature forms allowing their release from the cell [42, 48]. As a result, the secretion of inflammatory cytokines contributes to localized inflammation. A model of canonical inflammasome activation pathway is depicted below (Fig. 1). However, uncontrolled inflammation can increase inflammasome activation and lead to pyroptosis or pyronecrosis, which is a caspase-1 dependent cell death [42, 46, 51]. Normally cells are removed through the process of apoptosis with characteristics of cell shrinkage, DNA fragmentation, and condensation of chromatin occurring without inducing an immune response. On the other hand, pyroptosis is associated with cellular swelling, rupture of plasma membrane, and release of pro-inflammatory molecules within the cell (ATP or HMGB1) [42, 46, 51]. Both cytokines and pyroptosis are important for clearance of intracellular pathogens [44, 52].

Figure 1 Model showing the role of $P2X_4$ and $P2X_7$ in ROS production and inflammasome activation in GEC stimulated with extracellular ATP [59]

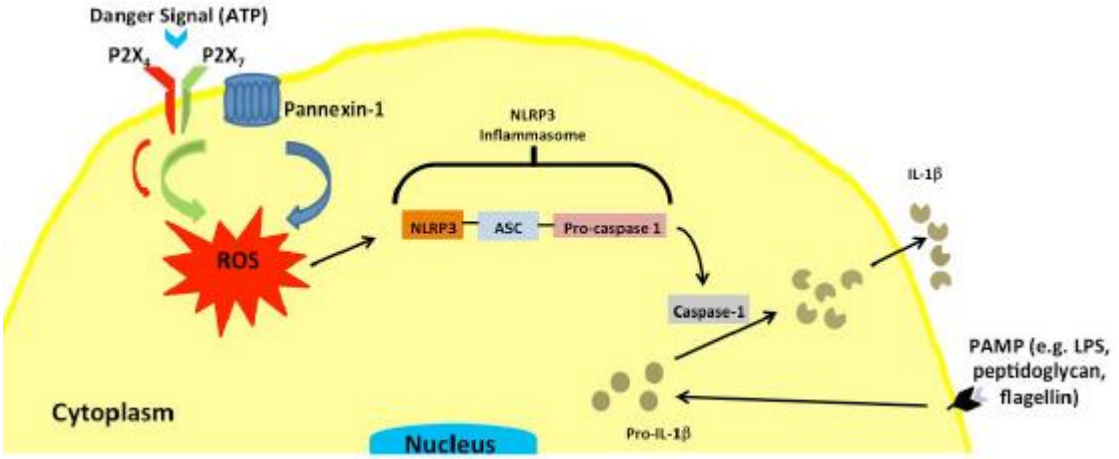

Non-Canonical Inflammasome

It has recently been described the non-canonical inflammasome, caspase-11, can also contribute to caspase-1-dependent IL-1β and IL-18 production [53]. NLRP3 inflammasome is the most characterized to have been shown to play a role through this non-canonical pathway [48, 50, 54-56]. Caspase-11 in mice is homologous to caspase-4 and caspase-5 in humans [45]. Activation of caspase-11 is critical for Gram-negative bacteria recognition and caspase-1 activation [48, 50].

The mechanism of triggering caspase-11 is controversial as different publications suggest activation upstream or downstream of NLRP3 [48, 56]. However, its activators include cholera toxin B (CTB), bacterial RNA, and LPS [11, 43, 57]. The signaling cascade model for caspase-11 begins with the stimulation of a TLR to induce expression of type I interferons, NLRP3, and pro-IL-1β [11, 48]. Then activation of caspase-11 occurs independent of TLR signaling and recognizes cytosolic LPS as one proposed model [11, 39, 43]. It is also speculated caspase-11 can autoactivate once it surpasses a level of concentration [56]. Activated caspase-11 will lead to pyroptosis and/or caspase-1 activation [48, 50, 56]. Without caspase-1 activation, caspase-11 can induce pyroptosis and release of IL-1α and HMGB1 [45, 56]. However, caspase-11 alone cannot cleave pro-IL-1β or pro-IL-18 [45, 50, 56, 58]. Both caspase-11 and caspase-1 work synergistically to recognize and respond to intracellular pathogens through pyroptosis and pro-inflammatory cytokine release.

For my Ph.D. research, I set out to fulfill the following specific aims:

1.2 Specific Aims

Specific Aim 1.
To evaluate the influence of *Porphyromonas gingivalis* infection with ATP-induced inflammasome activation and cytokine secretion.

Hypothesis: *Porphyromonas gingivalis* inhibits ATP-induced inflammasome activation and cytokine secretion by secretion of NDK.

We investigated how *P. gingivalis* influences innate immune response by conducting experiments to assess ATP-induced inflammasome activation with the presence of wild-type *P. gingivalis* and *ndk*-deficient (ΔNDK) *P. gingivalis* infection in GECs. Additionally, we measured pro-inflammatory cytokine secretion upon activation of the inflammasome due to *P. gingivalis* infection. The findings of the elevated cytokine secretion levels allowed us to target pathways with specific inhibitors to regulate host cell mediators of the cytokine secretion pathway. The combined results provide a new perspective to local inflammation during initial infection in the oral cavity. It emphasizes the significance of NDK release from *P. gingivalis* as a component of inhibiting ATP-induced inflammasome activation and cytokine secretion.

Specific Aim 2.

A) To characterize pro-inflammatory response to *F. nucleatum* oral infection *in vivo*
B) To evaluate the role of inflammasome activation and during *F. nucleatum* oral infection

Hypothesis. *Fusobacterium nucleatum* upregulates pro-inflammatory cytokine expression and induces release of cytokines modulated by inflammasome activation during infection in BALB/c and C57BL/6 mice.

F. nucleatum oral infection has not been described in either BALB/c or C57BL/6 mice, so we set out to investigate how *F. nucleatum* influences innate immune responses during infection for both strains. We measured pro-inflammatory cytokine production during *F. nucleatum* infection. Then we evaluated the effects of infection on the oral cavity by histology. Because we observed an increase of pro-inflammatory response during *F. nucleatum* infection, we also aimed to assess the role of inflammasome activation. These experiments are the first to characterize *F. nucleatum* oral infection in mice. Using these perspectives, we can begin to develop strategies for earlier clearance of the bacteria before it proliferates into a systemic problem.

Chapter 2: Purinergic Receptors

2.1 Introduction

The purinergic receptors, also known as purinoceptors, are plasma membrane receptors expressed throughout the body in skeletal muscle, the cardiovascular and central nervous systems, epithelial cells, and immune cells [59-64]. They play an important role in cell proliferation, inflammation, embryonic development, apoptosis, and cancer [62, 65]. There are three classes of purinergic receptors: P1, P2Y, and P2X [65, 66]. Both P1 (adenosine) and P2Y receptors are G protein-coupled receptors, while P2X receptors are ligand ion-gated channel receptors [66, 67]. P1 receptors have four subtypes A_1, A_2A, A_2B, and A_3, which can recognize adenosine [66, 67]. P2 receptors are comprised of seven P2X ($P2X_{1-7}$) receptors and eight P2Y receptors ($P2Y_1$, $P2Y_2$, $P2Y_4$, $P2Y_6$, and $P2Y_{11-14}$) [67, 68]. Both P2Y and P2X are activated by ATP, ADP, UTP, UDP, and diadenosine polyphosphates [62, 65, 67].

For the purpose of our studies, we focused on the P2X receptors and their significance during inflammasome activation. $P2X_7$ is a ligand-gated ion channel, which is triggered by ATP [66, 69]. Stimulation of $P2X_7$ receptors can lead to Ca^{2+} influx through the ion gates and membrane depolarization [64, 66, 70]. This rapid change in polarization can increase with more stimuli, but is reversible. Activation can also result in other intracellular and extracellular exchanges of ions, Na^+ and K^+ [66, 67]. Upon $P2X_7$ activation, there is recruitment of large pore formations on the cellular membrane, known as pannexin-1 hemichannels [69]. These hemichannels contribute to ATP release from the cell and triggering intracellular signaling of the inflammasome [69, 71, 72]. The signaling cascade can continue downstream leading to IL-1β release as a response to recognition of extracellular ATP by the purinergic receptor [69, 72].

The activation and assembly of the inflammasome can be triggered within the cell by ROS production and oxidative stress [57, 73, 74] . ROS are free radicals generated from oxygen metabolism in the mitochondria or NADPH oxidases [73, 74]. It is proposed that K^+ efflux during inflammasome activation can further induce ROS generation [74]. In our study, we aimed to characterize the involvement between $P2X_7$, $P2X_4$, and pannexin-1 to generate ROS and to activate the inflammasome in GECs. ATP has also been described to be the ligand for $P2X_4$ receptor [75, 76]. However, it had not been characterized in its association with ATP-mediated inflammasome activation. We also evaluated inhibiting these purinergic receptors and hemichannel to determine its influence on cytokine production in *P. gingivalis* infected GECs.

We published our findings in *PLOS ONE* showing ATP-induced ROS production and inflammasome activation was associated with $P2X_7$, $P2X_4$, and pannexin-1 in GECs. This response was specific to ATP and occurred within a few minutes after stimulation. Depletion of $P2X_7$ or $P2X_4$ led to a decrease in inflammasome activation. Inhibition of $P2X_7$ or $P2X_4$ also effected *P. gingivalis*-infected cells, which resulted in a decrease in IL-1β secretion. Overall, $P2X_7$, $P2X_4$, and pannexin-1 modulate ROS production and caspase-1 activation.

2.2 P2X4 Assembles with P2X7 and Pannexin-1 in Gingival Epithelial Cells and Modulates ATP-induced Reactive Oxygen Species Production and Inflammasome Activation

$P2X_4$ Assembles with $P2X_7$ and Pannexin-1 in Gingival Epithelial Cells and Modulates ATP-induced Reactive Oxygen Species Production and Inflammasome Activation

Shu-Chen Hung[1,2], Chul Hee Choi[3], Najwane Said-Sadier[1,2], Larry Johnson[1,2], Kalina Rosenova Atanasova[3], Özlem Yilmaz[3,4], and David M. Ojcius[1,2]

[1] Molecular Cell Biology and [2] Health Sciences Research Institute, University of California, Merced, CA 95343, USA; [3] Department of Periodontology and [4] Emerging Pathogens Institute, University of Florida, Gainesville, FL 32610, USA

Running head: $P2X_4$ modulates ATP-induced inflammasome activation

To whom correspondence should be addressed: David Ojcius, Molecular Cell Biology, University of California, 5200 North Lake Road, Merced, CA 95343, USA. Telephone: (209) 228-2948. E-mail: dojcius@ucmerced.edu.

Background: The purinergic receptor $P2X_7$ mediates ATP-dependent inflammasome activation. Other purinergic receptors have never been shown to have this ability.
Result: ATP stimulation of $P2X_4$ or $P2X_7$ leads to ROS production, but only ligation of $P2X_7$ leads to inflammasome activation. Depletion or inhibition of $P2X_4$ abrogates $P2X_7$-dependent inflammasome activation.
Conclusion: $P2X_4$ is present in a complex with $P2X_7$ and its associated pore, pannexin-1.
Significance: Due to its presence in the $P2X_7$ complex, $P2X_4$ can modulate $P2X_7$-dependent ROS production and inflammasome activation.

We have previously reported that *Porphyromonas gingivalis* infection of gingival epithelial cells (GEC) requires an exogenous danger signal such as ATP to activate an inflammasome and caspase-1, thereby inducing secretion of interleukin (IL)-1β. Stimulation with extracellular ATP also stimulates production of reactive oxygen species (ROS) in GEC. However, the mechanism by which ROS is generated in response to ATP, and the role that different purinergic receptors may play in inflammasome activation, is still unclear. In this study, we revealed that the purinergic receptor $P2X_4$ is associated with the receptor $P2X_7$ and its associated pore, pannexin-1. ATP induces ROS production through a complex consisting of $P2X_4$, $P2X_7$, and pannexin-1. $P2X_7$-mediated ROS production can activate the NLRP3 inflammasome and caspase-1. Furthermore, separate depletion or inhibition of $P2X_4$, $P2X_7$, or pannexin-1 complex blocks IL-1β secretion in *P. gingivalis*-infected GEC following ATP treatment. However, activation via $P2X_4$ alone induces ROS generation but not inflammasome activation. These results suggest that ROS is generated through stimulation of a $P2X_4$/$P2X_7$/pannexin-1 complex, and reveal an unexpected role for $P2X_4$, which acts as a positive regulator of inflammasome activation during microbial infection.

Innate immunity is the first line of defense used by the host against microbial infection. In human tissues, epithelial cells play a major role in innate immunity. Epithelial cells can not only form physical

barriers, but also secrete inflammatory cytokines and chemokines in response to infection following recognition of microbial products by pattern-recognition receptors (PRRs), such as Toll-like receptors (TLR) and Nod-like receptors (NLR) (1-4).

The proinflammatory cytokines IL-1β and IL-18 have been linked to atherosclerosis, systemic inflammatory diseases, and autoimmune disease. Their expression and secretion are stringently controlled by pathogen-associated molecular patterns (PAMPs) and danger signals (5-7). Some PAMPs like lipopolysaccharide (LPS), peptidoglycan, lipoteichoic acid, flagellin, and microbial nucleic acids induce pro-IL-1β and pro-IL-18 expression and intracellular accumulation (8,9). However, the maturation and secretion of these cytokines requires a danger signal like ATP or uric acid crystal, which comes from stressed or infected cell and leads to the activation of inflammasomes (10-13).

Inflammasomes are large multiprotein complexes that act as a caspase-1-activating platform for IL-1β and IL-18 maturation. They can be categorized by the composition of their integral PRR family member, which acts as a scaffold protein that contributes to caspase-1 recruitment, clustering, and auto-activation (12-17). The best characterized inflammasome is the NLRP3 inflammasome. It contains NLRP3 as a scaffold protein, an apoptosis-associated speck-like protein containing a caspase recruitment domain (ASC) adaptor, and caspase-1 (18,19). Danger-associated molecular patterns (DAMPs), such as extracellular ATP, can activate the NLRP3 inflammasome through ATP-gated $P2X_7$ ion channels (11,12,20). Upon ATP stimulation, the $P2X_7$ receptor opens a cation channel, which permits K^+ efflux, and gradually forms a larger pore on the membrane by recruiting the hemichannel pannexin-1 to activate the NLRP3 inflammasome (21-23). Although $P2X_4$ is also an ATP-gated ion channel, it has not been previously described to participate in ATP-mediated caspase-1 activation.

Several downstream mechanisms have been proposed to induce NLRP3 inflammasome activation, including reactive oxygen species (ROS) production, lysosomal destabilization, K^+ efflux, and apoptosis (12,24-26). In particular, ATP stimulation of cells has been shown to induce caspase-1 activation following ROS production, and treatment with the $P2X_7$ antagonist, oxATP, attenuates ATP-induced ROS generation (12,27-32). In addition to $P2X_7$ agonists, agonists of other purinergic receptors also promote ROS generation, implying that other purinergic receptors may also contribute to ATP-induced ROS production (31,33,34). However, until now, no other purinergic receptor has been implicated in ATP-induced activation of the NLRP3 inflammasome other than $P2X_7$.

Gingival epithelial cells (GEC) represent the first barrier to infection and are a prominent component of the innate immune system in the oral cavity. The GEC are also targets of infection, and can be infected by common periodontopathogens such as *Porphyromonas gingivalis*, *Tannerella forsythia*, and *Actinobacillus actinomycetemcomitans* (35-38). Previously, we showed that *P. gingivalis*-infected GEC overexpress pro-IL-1β, but secretion of the cytokine requires a second stimulus, such as treatment with exogenous ATP, to activate caspase-1 through the NLRP3 inflammasome (34,39). Characterizing the cell signaling events activated by pathogens in GEC provides potential candidates to control inflammatory responses associated with periodontal disease. However, the molecular mechanisms by which the GEC

respond to bacterial infections remain to be elucidated. Thus, we here investigate which purinergic receptors contribute to ATP-induced ROS production and inflammasome activation in GEC, and reveal an unexpected modulatory role for $P2X_4$.

EXPERIMENTAL PROCEDURES

Cells and chemical reagents

Porphyromonas gingivalis ATCC 33277 was cultured anaerobically for 24 h at 37°C in trypticase soy broth (TSB) supplemented with yeast extract (1 mg/ml), haemin (5 μg/ml) and menadione (1 μg/ml) and used for infection as described (34).

The human immortalized gingival keratinocyte (IHGK) cell line (40), was obtained as previously described (40,41). Cells were cultured in serum-free defined keratinocyte-SFM (Gibco) at 37 °C in a humidified incubator containing 5% CO_2.

Primary GEC were obtained after oral surgery from healthy gingival tissue as previously described (42). Cells were cultured as monolayers in serum-free keratinocyte growth medium (KGM) (Lonza) at 37°C in 5% CO_2. Primary GEC were used for experimentation at ~75–80% confluence and cultured for 24 h or 48 h before infection with *P. gingivalis* at a multiplicity of infection (M.O.I.) of 100 (34).

ATP, ADP, UTP, oxATP, PPADS, and probenecid were from Sigma-Aldrich. AMP was from Santa Cruz Biotech. 5-BDBD was from Tocris Bioscience. All primers were purchased from Fisher Scientific. Antibodies against $P2X_4$ (APR-002) and $P2X_7$ (APR-008) were obtained from Alomone Labs.

RNA extraction, reverse transcription PCR, and quantitative PCR

Total RNA was isolated from 10^6 IHGK cells using RNeasy Mini kit (Qiagen) according to the manufacturer's protocol. cDNA was amplified from 2 μg RNA by random hexamers using TagMan Reverse Transcription Reagents kit (Applied Biosystems). The following primers were used in PCR: 5′-CGCCTTCCTCTTCGAGTATGA-3′ and 5′-AGATAACGCCCACCTTCTTATTACG-3′ for $P2X_1$; 5′-GCCTACGGGATCCGCATT-3′ and 5′-TGGTGGGAATCAGGCTGAAC-3′ for $P2X_2$; 5′-GCTGGACCATCGGGATCA-3′ and 5′-GAAAACCCACCCTACAAAGTAGGA-3′ for $P2X_3$; 5′-CCTCTGCTTGCCCAGGTACTC-3′ and 5′-CCAGGAGATACGTTGTGCTCAA-3′ for $P2X_4$; 5′-CTGCCTGTCGCTGTTCGA-3′ and 5′-GCAGGCCCACCTTCTTGTT-3′ for $P2X_5$; 5′-AGGCCAGTGTGTGGTGTTCA-3′ and 5′-TCTCCACTGGGCACCAACTC-3′ for $P2X_6$; 5′-TCTTCGTGATGACAAACTTTCTCAA-3′ and 5′-GTCCTGCGGGTGGGATACT-3′ for $P2X_7$; and 5′-GGTGAGACAAGACCCAGAGC-3′ and 5′-GGCATCGGACCTTACACCTA-3′ for pannexin-1.

The PCR cycling protocol for all primers was 94°C at 5 s, 55°C at 5 s and 68°C at 15 s. The protocol was repeated for 40 cycles and included an initial 5 min enzyme activation step at 94 °C and a final 10 min extension step at 72 °C. PCR products were separated by electrophoresis on a 2% agarose gel and visualized by ethidium bromide staining.

Quantitative PCR (qPCR) was carried out with 1/50 of the cDNA preparation in the Mx3000P (Stratagene) in 25 μl final volumes with the Brilliant QPCR Master Mix (Stratagene). cDNA was amplified using 200 nM of each specific sense and antisense primers. Quantitative

PCR was conducted at 95°C for 10 min, followed by 40 cycles at 95°C for 30 s, 55°C for 1 min and 72°C for 30 s. The expression levels of $P2X_4$, $P2X_7$, and pannexin-1 were normalized to GAPDH by the comparative cycle threshold method, as described by the manufacturer (Stratagene). The primers for the genes coding $P2X_4$, $P2X_7$, and pannexin-1 were as above. For GAPDH, the primers were: 5′-TTAAAAGCAGCCCTGGTGAC-3′ and 5′-CTCTGCTCCTCCTGTTCGAC-3′.

Lentiviral infection of IHGK cells

Immortalized GEC (IHGK) stably expressing shRNA against $P2X_4$ (TRCN0000044960 and TRCN0000044962), $P2X_7$ (TRCN0000045095 and TRCN0000045097), and pannexin-1 (TRCN0000156046 and TRCN0000155348) were generated by transducing the cells with lentiviral particles purchased from Sigma-Aldrich. Transduction was performed following the manufacturer's instructions. Nontarget shRNA control cells were also generated using an irrelevant sequence (SHC002V, Sigma). Briefly, GEC were plated at 70% confluency 24 h prior to transduction, and the corresponding lentiviral transduction particles were added at M.O.I. of 3 overnight. Fresh media was added the next day, and stably infected cells were selected by addition of media containing 5 μg/ml puromycin (Sigma-Aldrich).

Transient RNA depletion with siRNA in primary GEC

Expression of $P2X_4$ and $P2X_7$ in primary GEC was repressed with different siRNA sequences as previously described (43). The siRNA sequences were: 5'-GCUUUCAACGGGUCUGUCATT-3' and 5'-UGACAGACCCGUUGAAAGCTA-3' for $P2X_4$ (Ambion, LifeCell Technologies, S9957, Cat. #: 4392420); and 5'-ACAAUGUUGAGAAACGGACUCUGAT-3' for $P2X_7$ (27 mer siRNA duplexes OriGene Technologies, Cat. #: SR303325). Briefly, cells were treated with siRNA using Glycofect Transfection Reagent (Kerafast) mixed with 10 nM siRNA (stock concentration of siRNA was 20 nM) in a total volume of 100 μl. Four hours later, new cell-medium was added to the cells without removal of the transfection mixture, and cells were incubated for 36 hours. qPCR was performed to confirm the knockdown efficiency.

ROS measurement

ROS measurement was assayed with the ROS indicator dye, CM-H_2-DCFDA DCF, Invitrogen) as described previously (43). In brief, cells were loaded with 2.5 μM DCF in PBS for 30 min at 37 °C, washed with PBS, and treated with 100 μM or 3 mM ATP for 1 h at 37 °C. Cells were counter-stained with Hoechst33342 in order to reveal the nucleus. Finally, the cells were observed by wide-field fluorescence microscope (Leica, Deerfield, IL).

Measurement of caspase-1 activation by ELISA

GEC were treated with 100 μM or 3 mM ATP for 3 h and supernatants were collected and subjected to human caspase-1 immunoassay (R&D) according to manufacturer's instructions. In brief, the caspase-1 ELISA uses monoclonal and polyclonal antibodies specific for the caspase-1 p20 subunit as capture and detection antibodies, respectively. One hundred μl of supernatant were first mixed with 50 μl of RD1W buffer and loaded onto caspase-1 monoclonal antibody coated-wells for 1.5 hrs. One hundred μl of caspase-1 antiserum was then used as detection antibodies. Anti-rabbit IgG-HRP conjugate

was used for quantification. Activated caspase-1 was measured using a plate reader at 450 nm with wavelength correction at 540 nm.

Measurement of IL-1β secretion by ELISA

Secretion of IL-1β was measured using a commercial cytokine ELISA kit (BD Biosciences Pharmingen) as described (39).

Co-Immunoprecipitation of purinergic receptors

Co-immunoprecipitation was performed with Dynabeads (Invitrogen) according to the manufacturer's instructions. Cells were lysed with the extraction buffer, and cell extracts were incubated for 3 h at 4°C with beads pre-coupled overnight with $P2X_4$ antibody. Precipitates were washed with extraction buffer and LWB with the use of a magnet and were subjected to 2X sample buffer and heated to 99°C for 10 min. The eluted proteins were analyzed by Western blot as previously described (44).

RESULTS

ATP induces ROS generation in GEC

It has been shown stimulation with ATP results in high levels of ROS generated in alveolar macrophages and primary GEC (27,34). In order to characterize ATP-induced ROS production in GEC, we used a stable GEC cell line, the human immortalized gingival keratinocyte cell line (HIGK) (40), stained with carboxy-H_2DCFDA (DCF), which remains nonfluorescent until its deacetylation and oxidation. Fluorescence microscopy images showed a significant increase of DCF fluorescence in 3 mM ATP stimulated HIGK cells (Fig. 1A). Quantitative analysis of fluorescence microscopy data showed that the fluorescence in ATP-treated cells was about 9 times higher than in cells without treatment. Furthermore, the cells responded quickly to ATP stimulation within 5 minutes and reached a steady state from 30 minutes to at least 3 hours (Fig. 1, B and C). Treatment with other extracellular nucleotides such as ADP, AMP, or UTP was unable to induce significant ROS generation in the cells (Fig. 1C). These results suggest that stimulation with ATP, unlike other nucleotides, can induce ROS production in GECs.

Purinergic receptors involved in ATP-induced ROS generation

It has been proposed that extracellular ATP induces ROS production through ligation of the ATP-gated $P2X_7$ ion channel, in association with the pore-forming hemi-channel, pannexin-1, in macrophages and neurons (19,21,45). To investigate whether ATP-induced ROS production in GEC takes place through $P2X_7$, we examined the gene expression levels of purinergic receptors in HIGK cells. In agreement with our previous description of primary GEC (46), the HIGK cells express $P2X_1$ throuh $P2X_7$. In addition, the HIGK cells express pannexin-1 (Fig. 2A).

P2X- and pannexin-1-dependent responses in HIGK cells were next examined by fluorescence microscopy (Fig. 2B). Consistent with previous results, 3 mM ATP stimulated a large level of ROS production, suggesting that ATP mediates ROS production through $P2X_7$ ligation (Fig. 2, B and C). A role for P2X7 was further confirmed by showing that ATP-induced ROS production was inhibited by pretreatment with the $P2X_7$ and pannexin-1 antagonists, oxATP and probenecid, respectively (Fig. 2D). Moreover, as illustrated in Fig. 2E, treatment with the selective $P2X_7$ antagonist, PPADS, significantly blocked ATP-induced ROS generation. These data suggest that $P2X_7$ may be involved in ATP-induced ROS generation in GEC.

Unexpectedly, treatment with 100

μM ATP also elicited ROS generation but to a lower extent than with 3 mM ATP (Fig. 2, A and B). $P2X_4$ is considered to mediate high affinity responses to ATP stimulation, at lower concentrations than for $P2X_7$ (31,33,47,48). Thus, these results suggested that $P2X_4$ may be involved in ATP-mediated ROS production. To test this possibility, we pretreated cells with the potent $P2X_4$ antagonist, 5-BDBD. As shown in Fig. 2E, pretreatment with 5-BDBD significantly blocked ATP-induced ROS generation. Taken together, these results suggest that ATP may elicit ROS generation through $P2X_4$ and $P2X_7$ ligation in GEC.

Confirmation by RNA interference for role of $P2X_7$, $P2X_4$ and pannexin-1 in ATP-mediated ROS production

As inhibitor studies suggested that $P2X_4$may be involved in ATP-dependent ROS responses, we examined this unexpected result by stably depleting $P2X_4$, $P2X_7$ and pannexin-1 by lentiviral delivery of specific shRNA. Depletion efficiency in each cell line was validated individually by qPCR. As shown in Fig. 3A, the mRNA levels of $P2X_4$, $P2X_7$, and pannexin-1 were reduced by at least ~70% in comparison to cells transduced with control shRNA virus particles. In agreement with Fig. 2, depletion of $P2X_7$ or pannexin-1 resulted in attenuation of ROS production after ATP stimulation, compared to GEC transduced with control shRNA. Although depletion of $P2X_4$ by RNA interference was less efficient than for $P2X_7$, $P2X_4$ depletion resulted in a dramatic decrease in ATP-mediated ROS production (Fig. 3, B and C). Collectively, these findings indicate that both $P2X_4$ and $P2X_7$ contribute to ROS generation after ATP treatment of GEC.

ATP ligation by $P2X_4$/$P2X_7$/pannexin-1 complex leads to inflammasome activation in GEC

We previously showed that ATP treatment of GEC leads to NLRP3 inflammasome activation (39). As ROS production has been associated with inflammasome and caspase-1 activation (12,27,29,30), we evaluated whether ATP-mediated caspase-1 activation in GEC takes place through $P2X_4$/$P2X_7$ ligation. Using ELISA to measure secretion of activated caspase-1, we observed that treatment of GEC with 100 μM ATP was insufficient for caspase-1 activation, even though ROS generation was induced. In contrast, 3 mM ATP treatment resulted in high levels of caspase-1 activation in GEC stably-expressing the control shRNA (Fig. 4A); but the activation of caspase-1 by 3 mM ATP treatment was abrogated when either $P2X_4$ or $P2X_7$ were depleted in GEC (Fig. 4A). Thus, treatment with 3 mM ATP induced ROS production via the $P2X_4$/$P2X_7$ complex and activated the NLRP3 inflammasome. However, 100 μM ATP stimulation induced ROS generation through $P2X_4$ ligation, but stimulation with this concentration of ATP was not sufficient to activate the inflammasome.

The non-redundant roles of $P2X_4$ and $P2X_7$ in ATP-induced ROS generation led us to hypothesize that $P2X_4$ and $P2X_7$ may be associated in the membrane and function as a physical complex in ATP-mediated responses in GEC. Therefore, we examined physical associations between $P2X_4$ and $P2X_7$ in GEC by performing co-immunoprecipitation experiments. After precipitating endogenous $P2X_4$ using an anti-$P2X_4$ antibody, we observed that $P2X_7$ and pannexin-1 were detected in the immunoprecipitate (Fig. 4B). Taken together, these data indicate that $P2X_4$, $P2X_7$, and pannexin-1 form a heterocomplex in GEC, and play non-redundant roles in ATP-induced ROS generation.

ATP ligation of $P2X_4$/$P2X_7$/pannexin-1 contributes to secretion of pro-

inflammatory cytokines secretion in primary GEC infected with *P. gingivalis*

Previously we had reported that infection of GEC with *P. gingivalis* leads to expression of pro-IL-1β and its accumulation within the infected cell. However, secretion of IL-1β requires a second signal, such as the danger signal ATP, in order to activate the NLRP3 inflammasome and caspase-1, allowing processing and secretion of the mature IL-1β (39).

Given the unexpected observation that $P2X_4$ can modulate ATP-dependent caspase-1 activation in the immortalized HIGK cells, we examined whether a similar effect could be observed in immortalized (HIGK) cells and primary GEC during infection with *P. gingivalis*. As in our previous studies, neither *P. gingivalis* infection alone nor infection combined with 100 μM ATP treatment could induce IL-1β secretion by HIGK cells. Only infected cells treated with 3 mM ATP, but not other nucleotides, could promote Il-1β secretion (Fig. 5A). Similarly, using primary GEC, we found that ATP, but not other nucleotides, could promote IL-1β secretion by infected cells (Fig. 5C). We also consistently observed that primary GEC produce and secrete higher levels of IL-1β than HIGK cells (Fig. 5).

Furthermore, pretreatment of infected HIGK or primary GEC with the $P2X_7$ antagonists, PPADS and oxATP, blocked ATP-dependent IL-1β secretion. In addition, the pannexin-1 inhibitor, probenecid, also abrogated IL-1β secretion. Finally, inhibition of $P2X_4$ by 5-BDBD reduced the amount of IL-1β secretion, even though the cells were treated with 3 mM ATP, which stimulates signaling via $P2X_7$ (Fig. 5B and D).

To further confirm a role for $P2X_4$ and $P2X_7$ in IL-1β, we used siRNA to deplete $P2X_4$ and $P2X_7$ in primary GEC individually. (In our hands, siRNA treatment is more effective than shRNA delivery for RNA interference in primary GEC.) Fig. 5E showed that $P2X_4$ or $P2X_7$ mRNA levels were depleted with an efficiency of over 80% in primary GEC. Similarly to our previous results (39), *P. gingivalis* infection followed by 3 mM ATP treatment caused IL-1β secretion by the primary GEC that had been treated with control siRNA. However, depletion of $P2X_4$ or $P2X_7$ reduced significantly IL-1β secretion, which again showed a non-redundant role for $P2X_4$ and $P2X_7$ in ATP-dependent IL-1β secretion. Probenecid treatment prior to ATP stimulation repressed even further the IL-1β secretion in $P2X_4$ and $P2X_7$ knockdown cells, consistent with a role for pannexin-1 in IL-1β secretion by primary GEC. All these results imply that a $P2X_4$/$P2X_7$/pannexin-1 complex is required for IL-1β secretion in response to ATP treatment of *P. gingivalis*-infected cells.

DISCUSSION

Our results show that $P2X_4$, $P2X_7$, and pannexin-1 contribute to ROS generation and are associated with inflammasome activation in GEC. Consistent with this possibility, previous studies have suggested that $P2X_4$ and $P2X_7$ may behave as heteromeric receptors on bone marrow derived macrophages (BMDM) (49,50). Similarly, ATP-induced cell death of mouse macrophages was shown to involve the $P2X_4$ receptor, initiating Ca^{2+} influx upon stimulation with ATP and contributing to pore formation by activation of the $P2X_7$ receptor (51,52). These findings suggest the functionality and dependence of the $P2X_4$ and $P2X_7$ receptors on each other.

In GEC, we found that extracellular nucleotide-induced ROS production occurred within a few minutes and was specific for ATP stimulation. We then characterized expression of possible target receptors and tested whether specific inhibitors for these receptors could block ROS generation. Inhibitors of $P2X_4$, $P2X_7$, and pannexin-1 reduced significantly ATP-dependent production of ROS. To further evaluate the functionality of the receptors, we depleted either purinergic receptor or pannexin-1 by RNA interference, and find that both purinergic receptors and pannexin-1 are required for efficient ATP-induced ROS production in primary or immortalized GEC. Our findings differ from another study, which showed that depletion of the $P2X_4$ receptor increased ATP-mediated ROS production in the macrophage cell line, RAW264.7 cells (51,52). The conflicting results may be attributed to different cells lines, but we also used primary GEC and found similar results as with the HIGK cells.

We have previously reported that treatment of GEC with ATP concentrations that stimulate $P2X_7$ leads to activation of the inflammasome and caspase-1 (39). However, we now find that depletion of either $P2X_4$ or $P2X_7$ results in decreased caspase-1 activation in GEC. ROS is produced when either $P2X_4$ or $P2X_7$ are stimulated, but caspase-1 is activated only when GEC are treated with ATP concentrations that activate $P2X_7$. Similarly, IL-1β secretion from *P. gingivalis*-infected cells, which requires caspase-1 activation, could be induced by treatment of the infected cells with ATP concentrations that stimulate $P2X_7$, but inhibiting or depleting either $P2X_4$ or $P2X_7$ resulted in significantly lower levels of IL-1β secretion.

Taken together, these results suggested that $P2X_4$ stimulation may not be sufficient for activation of caspase-1, but $P2X_4$ may form a complex with $P2X_7$, which could explain why $P2X_4$ depletion results in loss of $P2X_7$-mediated signaling. We confirmed this hypothesis by demonstrating by co-immunprecipitation experiments that $P2X_4$ is physically associated with $P2X_7$ and pannexin-1 in GEC. $P2X_4$ and $P2X_7$ have previously been shown to also form heteromeric receptors in BMDM (49). Thus, these results suggest that $P2X_7$ stimulation is required for caspase-1 activation, but $P2X_4$, through its presence in the $P2X_4$/$P2X_7$/pannexin-1 complex, modulates the activity of $P2X_7$ (Fig. 6).

Here, we provide an initial insight into how signaling through $P2X_4$, $P2X_7$, and pannexin-1 may activate caspase-1 in GEC. The same complex is involved in secretion of IL-1β from GEC that had been primed by *P. gingivalis* infection. Thus, understanding the triggers for $P2X_7$-dependent ROS generation and caspase-1 activation could aid in drug discovery and development of therapeutic approaches for diseases associated with *P. gingivalis*, such as periodontal disease and cardiovascular disease.

An obvious question is the intracellular source of ROS in GEC, which has been postulated to originate from mitochondria and/or the NADPH oxidase on the plasma membrane (34). A larger challenge may be to identify the molecular mechanisms that allow caspase-1 to be activated only after $P2X_7$ stimulation, even though both $P2X_4$ and $P2X_7$ ligation leads to ROS production.

REFERENCES

1. Hornef, M. W., and Bogdan, C. (2005) *J Endotoxin Res* **11**, 124-128
2. Viala, J., Chaput, C., Boneca, I. G., Cardona, A., Girardin, S. E., Moran, A. P., Athman, R., Memet, S., Huerre, M. R., Coyle, A. J., DiStefano, P. S., Sansonetti, P. J., Labigne, A., Bertin, J., Philpott, D. J., and Ferrero, R. L. (2004) *Nat Immunol* **5**, 1166-1174
3. Chamaillard, M., Inohara, N., and Nunez, G. (2004) *Trends Microbiol* **12**, 529-532
4. Philpott, D. J., Girardin, S. E., and Sansonetti, P. J. (2001) *Curr Opin Immunol* **13**, 410-416
5. Gerdes, N., Sukhova, G. K., Libby, P., Reynolds, R. S., Young, J. L., and Schonbeck, U. (2002) *J Exp Med* **195**, 245-257
6. Dinarello, C. A. (2005) *J Exp Med* **201**, 1355-1359
7. Dinarello, C. A. (2006) *Am J Clin Nutr* **83**, 447S-455S
8. Ishii, K. J., Koyama, S., Nakagawa, A., Coban, C., and Akira, S. (2008) *Cell Host Microbe* **3**, 352-363
9. Franchi, L., Eigenbrod, T., Munoz-Planillo, R., and Nunez, G. (2009) *Nat Immunol* **10**, 241-247
10. Zitvogel, L., Kepp, O., Galluzzi, L., and Kroemer, G. (2012) *Nat Immunol* **13**, 343-351
11. Lich, J. D., Arthur, J. C., and Ting, J. P. (2006) *Immunity* **24**, 241-243
12. Said-Sadier, N., and Ojcius, D. M. (2012) *Biomed. J.* **35**, 437-449
13. Ciraci, C., Janczy, J. R., Sutterwala, F. S., and Cassel, S. L. (2012) *Microbes Infect* **14**, 1263-1270
14. Martinon, F., Burns, K., and Tschopp, J. (2002) *Mol Cell* **10**, 417-426
15. Kanneganti, T. D. (2010) *Nat Rev Immunol* **10**, 688-698
16. Lupfer, C., and Kanneganti, T. D. (2012) *Virulence* **3**
17. Broz, P., and Monack, D. M. (2011) *Immunol Rev* **243**, 174-190
18. Davis, B. K., Wen, H., and Ting, J. P. (2011) *Annu Rev Immunol* **29**, 707-735
19. Schroder, K., and Tschopp, J. (2010) *Cell* **140**, 821-832
20. Meylan, E., Tschopp, J., and Karin, M. (2006) *Nature* **442**, 39-44
21. Kanneganti, T. D., Lamkanfi, M., Kim, Y. G., Chen, G., Park, J. H., Franchi, L., Vandenabeele, P., and Nunez, G. (2007) *Immunity* **26**, 433-443
22. Locovei, S., Scemes, E., Qiu, F., Spray, D. C., and Dahl, G. (2007) *FEBS Lett* **581**, 483-488
23. Kahlenberg, J. M., and Dubyak, G. R. (2004) *Am J Physiol Cell Physiol* **286**, C1100-1108
24. Shi, Y., Mucsi, A. D., and Ng, G. (2010) *Immunol Rev* **233**, 203-217
25. Halle, A., Hornung, V., Petzold, G. C., Stewart, C. R., Monks, B. G., Reinheckel, T., Fitzgerald, K. A., Latz, E., Moore, K. J., and Golenbock, D. T. (2008) *Nat Immunol* **9**, 857-865
26. Hornung, V., Bauernfeind, F., Halle, A., Samstad, E. O., Kono, H., Rock, K. L., Fitzgerald, K. A., and Latz, E. (2008) *Nat Immunol* **9**, 847-856
27. Cruz, C. M., Rinna, A., Forman, H. J., Ventura, A. L., Persechini, P. M., and Ojcius, D. M. (2007) *J Biol Chem* **282**, 2871-2879
28. Arlehamn, C. S., Petrilli, V., Gross, O., Tschopp, J., and Evans, T. J. (2010) *J Biol Chem* **285**, 10508-10518
29. Zhou, R., Tardivel, A., Thorens, B., Choi, I., and Tschopp, J. (2010) *Nat Immunol* **11**, 136-140
30. Zhou, R., Yazdi, A. S., Menu, P., and Tschopp, J. (2011) *Nature* **469**, 221-225
31. Bowler, J. W., Bailey, R. J., North, R. A., and Surprenant, A. (2003) *Br J Pharmacol* **140**, 567-575
32. Rayah, A., Kanellopoulos, J. M., and Di Virgilio, F. (2012) *Microbes Infect* **14**, 1254-1262

33. North, R. A. (2002) *Physiol Rev* **82**, 1013-1067
34. Choi, C. H., Spooner, R., Deguzman, J., Koutouzis, T., Ojcius, D. M., and Yilmaz, O. (2012) *Cell Microbiol* **in press**
35. Lamont, R. J., and Yilmaz, O. (2002) *Periodontol 2000* **30**, 61-69
36. Nisapakultorn, K., Ross, K. F., and Herzberg, M. C. (2001) *Infect Immun* **69**, 4242-4247
37. Socransky, S. S., Haffajee, A. D., Cugini, M. A., Smith, C., and Kent, R. L., Jr. (1998) *J Clin Periodontol* **25**, 134-144
38. Christersson, L. A., Wikesjo, U. M., Albini, B., Zambon, J. J., and Genco, R. J. (1987) *J Periodontol* **58**, 540-545
39. Yilmaz, O., Sater, A. A., Yao, L., Koutouzis, T., Pettengill, M., and Ojcius, D. M. (2010) *Cell Microbiol* **12**, 188-198
40. Oda, D., Bigler, L., Lee, P., and Blanton, R. (1996) *Exp. Cell Res.* **226**, 164-169
41. McMahon, L., Schwartz, K., Yilmaz, O., Brown, E., Ryan, L. K., and Diamond, G. (2011) *Infect Immun* **79**, 2250-2256
42. Yilmaz, O., Jungas, T., Verbeke, P., and Ojcius, D. M. (2004) *Infect Immun* **72**, 3743-3751
43. Abdul-Sater, A. A., Said-Sadier, N., Lam, V. M., Singh, B., Pettengill, M. A., Soares, F., Tattoli, I., Lipinski, S., Girardin, S. E., Rosenstiel, P., and Ojcius, D. M. (2010) *J Biol Chem* **285**, 41637-41645
44. Huang, P. R., Hung, S. C., and Wang, T. C. (2010) *Biochim Biophys Acta* **1803**, 1164-1174
45. Silverman, W. R., de Rivero Vaccari, J. P., Locovei, S., Qiu, F., Carlsson, S. K., Scemes, E., Keane, R. W., and Dahl, G. (2009) *J Biol Chem* **284**, 18143-18151
46. Yilmaz, O., Yao, L., Maeda, K., Rose, T. M., Lewis, E. L., Duman, M., Lamont, R. J., and Ojcius, D. M. (2008) *Cell Microbiol* **10**, 863-875
47. Negulyaev, Y. A., and Markwardt, F. (2000) *Neurosci Lett* **279**, 165-168
48. Soto, F., Garcia-Guzman, M., Gomez-Hernandez, J. M., Hollmann, M., Karschin, C., and Stuhmer, W. (1996) *Proc Natl Acad Sci U S A* **93**, 3684-3688
49. Guo, C., Masin, M., Qureshi, O. S., and Murrell-Lagnado, R. D. (2007) *Mol Pharmacol* **72**, 1447-1456
50. Boumechache, M., Masin, M., Edwardson, J. M., Gorecki, D. C., and Murrell-Lagnado, R. (2009) *J Biol Chem* **284**, 13446-13454
51. Kawano, A., Tsukimoto, M., Mori, D., Noguchi, T., Harada, H., Takenouchi, T., Kitani, H., and Kojima, S. (2012) *Biochem Biophys Res Commun* **420**, 102-107
52. Kawano, A., Tsukimoto, M., Noguchi, T., Hotta, N., Harada, H., Takenouchi, T., Kitani, H., and Kojima, S. (2012) *Biochem Biophys Res Commun* **419**, 374-380

ACKNOWLEDGMENTS

This study was supported by NIDCR grants R01DE019444 (to D.M.O) and R01DE016593 (to Ö.Y), and a University of California Presidential Chair.

FIGURE LEGENDS

Fig. 1. ROS production in response to ATP in GEC. (A) Immortalized GEC (HIGK) were treated for 1 hour with 3 mM ATP or left untreated as a control and stained with DCF (green) to detect ROS by fluorescence microscopy. Hoechst (blue) was used to stain nuclei. (B) ROS generation was measured with DCF at the indicated time points after 3 mM ATP stimulation. The mean fluorescence was quantified by image J and normalized for the number of cells. (C) Quantification of ROS production induced by different nucleotides. GEC were treated with 3

mM of ATP, ADP, AMP, or UTP, or left untreated for 1 hour, and analyzed by image J as in (B). The bars show the average values and SD of three independent experiments.

Fig. 2. Involvement of $P2X_4$, $P2X_7$, and pannexin-1 in ATP-mediated ROS generation. (A) Total RNA from immortalized GEC was extracted and reversed transcribed (RT) to cDNA. The cDNA was used to perform PCR with the primers specific for the indicated genes, and the PCR products were finally visualized by EtBr staining. (B) GEC were treated with 100 μM or 3 mM ATP as indicated for 1 hour, and ROS production was measured with DCF staining and visualized by fluorescence microcopy. Quantification of the fluorescence in three independent experiments with SD is shown in (C). (D-E) ROS production was measured by DCF staining in GEC stimulated under different conditions. GEC were left untreated or stimulated with 20 μM nigericin or 3 mM ATP for 1 hour followed by fluorescence microscopy. Diminished ROS generation by different receptor antagonists was examined by pretreating cells with 100 μM oxATP for 30 minutes, 1 mM probenecid for 10 minutes, or 50 μM 5-BDBD or 100 μM PPADS for 15 minutes, followed by 3 mM ATP stimulation for 1 hour.

Fig. 3. Diminished ATP-induced ROS production due to depletion of $P2X_4$ or $P2X_7$ by RNA interference. (A) Immortalized GEC were transduced with lentiviruses carrying the indicated shRNA-expressing plasmid for 1 day and selected with puromycin. After selection, cells were collected and total RNA was analyzed by qPCR to confirm knockdown efficiency. (B) DCF staining of ROS production after 3 mM ATP stimulation for 1 hour in different cell lines. The fluorescence shown in (C) was quantified as in Fig. 1 and normalized to shCtrl, which was transduced with control, non-mammalian shRNA.

Fig. 4. Impaired ATP-stimulated caspase-1 activation due to disruption of the complex containing $P2X_4$, $P2X_7$, and pannexin-1. (A) Immortalized GEC that had been depleted of $P2X_4$ or $P2X_7$ using lentiviral particles were treated with 100 μM or 3 mM ATP for 3 hours, and supernatants were collected for caspase-1 activity measurement. Caspase-1 activity was measured by ELISA as described in Material and Methods. (B) Total proteins isolated from GEC were subjected to immunoprecipitation (IP) by a polyclonal anti-$P2X_4$ antibody or Dynabeads as a control. Precipitates or total protein extract (as input) were resolved on SDS-PAGE and analyzed on immunoblots with anti-$P2X_7$ (top), anti-pannexin-1 (middle), or anti-$P2X_4$ (bottom) antibodies.

Fig. 5. Abrogation of ATP-induced IL-1β secretion in *P. gingivalis*-infected GEC by inhibition of $P2X_4$, $P2X_7$, or pannexin-1. Primary GEC (C and D) and immortalized GEC (A and B) were infected with or without *P. gingivalis* (*P.g.*) at an M.O.I. of 100 for 6 hours, followed by treatment with different pharmaceutical agents. Infected cells were treated with 100 μM ATP, 3 mM ATP, 3 mM ADP, 3 mM AMP, or 3 mM UTP individually for 1 hour (A and C). Alternatively, infected cells were pre-treated with 50 μM 5-BDBD for 15 minutes, 100 μM PPADS for 15 minutes, 100 μM oxATP for 30 minutes, or 1 mM probenecid for 10 minutes, followed by treatment with 3 mM ATP for 1 hour (B and D). The supernatants were collected and subjected to ELISA to measure IL-1β secretion. (E) Primary GEC were transfected with siRNA sequences against $P2X_4$ or $P2X_7$ for one day, and mRNA levels were detected by qPCR.

(F) Primary GEC depleted of $P2X_4$ or $P2X_7$ were infected with *P. gingivalis* (*P.g.*) and treated with probenecid and 3 mM ATP as shown in (B). IL-1β secretion in the supernatants was analyzed by ELISA. The values showed averages and SD from duplicate samples, which were obtained from three separate experiments.

Fig. 6. Model showing the role of $P2X_4$ and $P2X_7$ in ROS production and inflammasome activation in GEC stimulated with extracellular ATP.

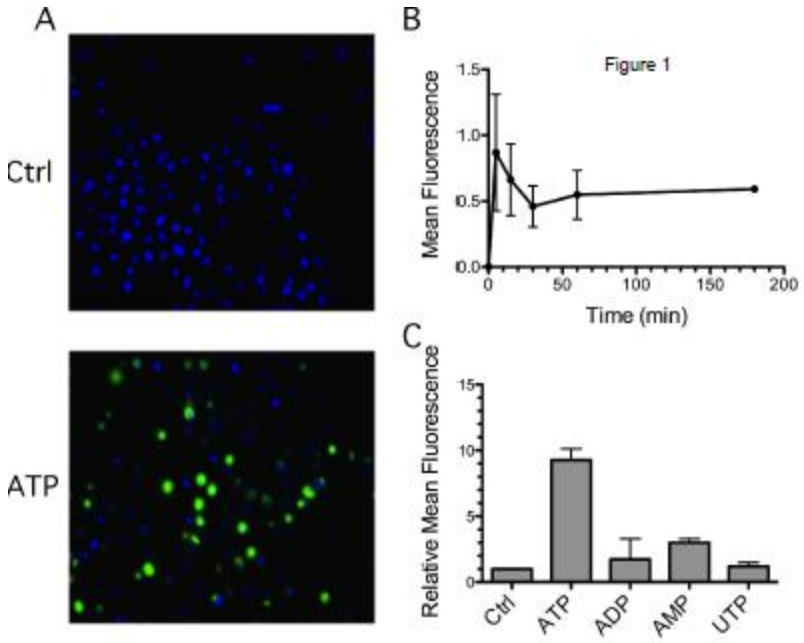
A
Ctrl
ATP
B
Figure 1
Mean Fluorescence
1.5
1.0
0.5
0.0
0
50
100
150
200
Time (min)
C
Relative Mean Fluorescence
15
10
5
0
Ctrl
ATP
ADP
AMP
UTP

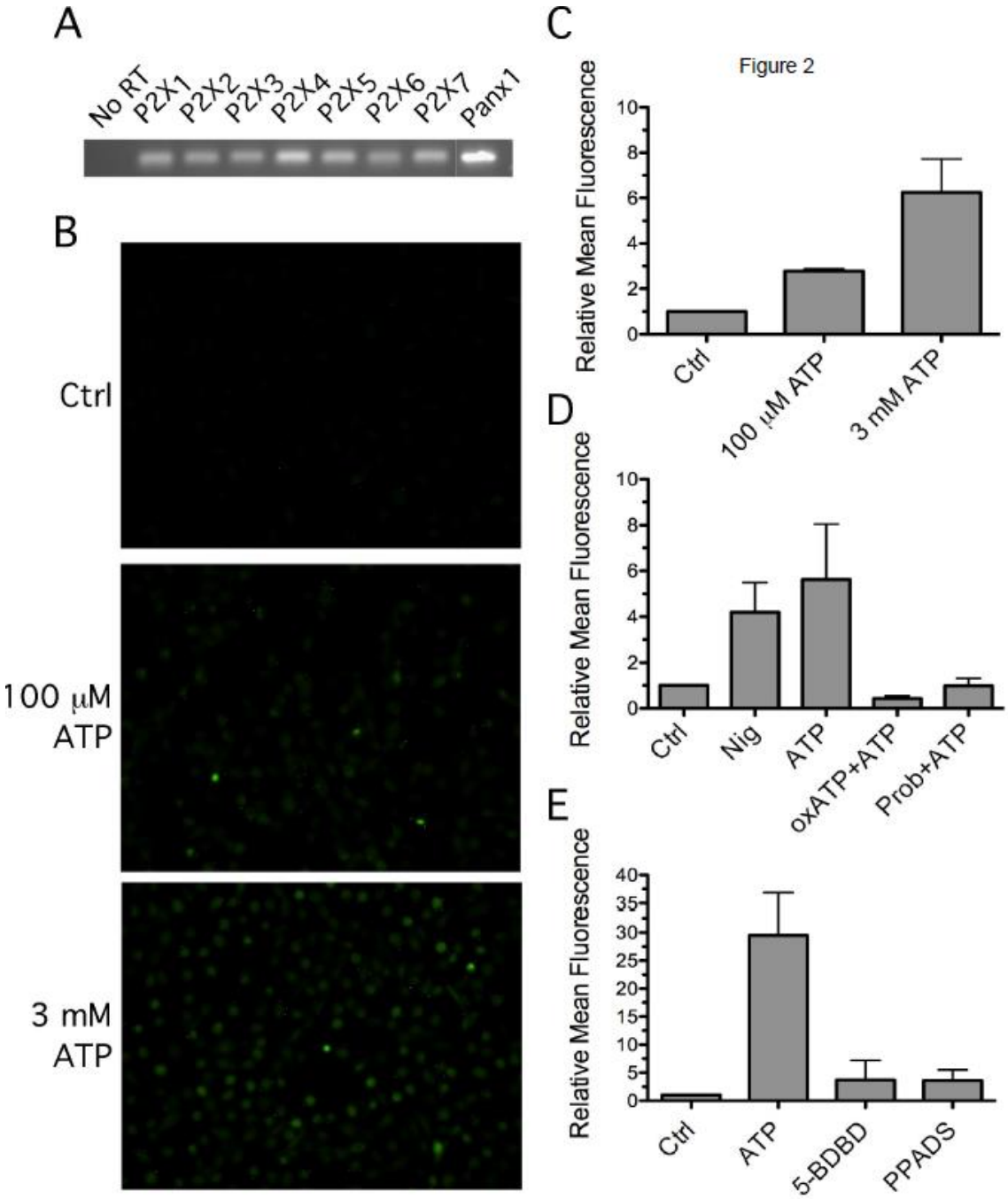
A
No RT
P2X1
P2X2
P2X3
P2X4
P2X5
P2X6
P2X7
Panx1
B
Ctrl
100 μM ATP
3 mM ATP
C
Figure 2
Relative Mean Fluorescence
Ctrl
100 μM ATP
3 mM ATP
D
Relative Mean Fluorescence
Ctrl
Nig
ATP
oxATP+ATP
Prob+ATP
E
Relative Mean Fluorescence
Ctrl
ATP
5-BDBD
PPADS

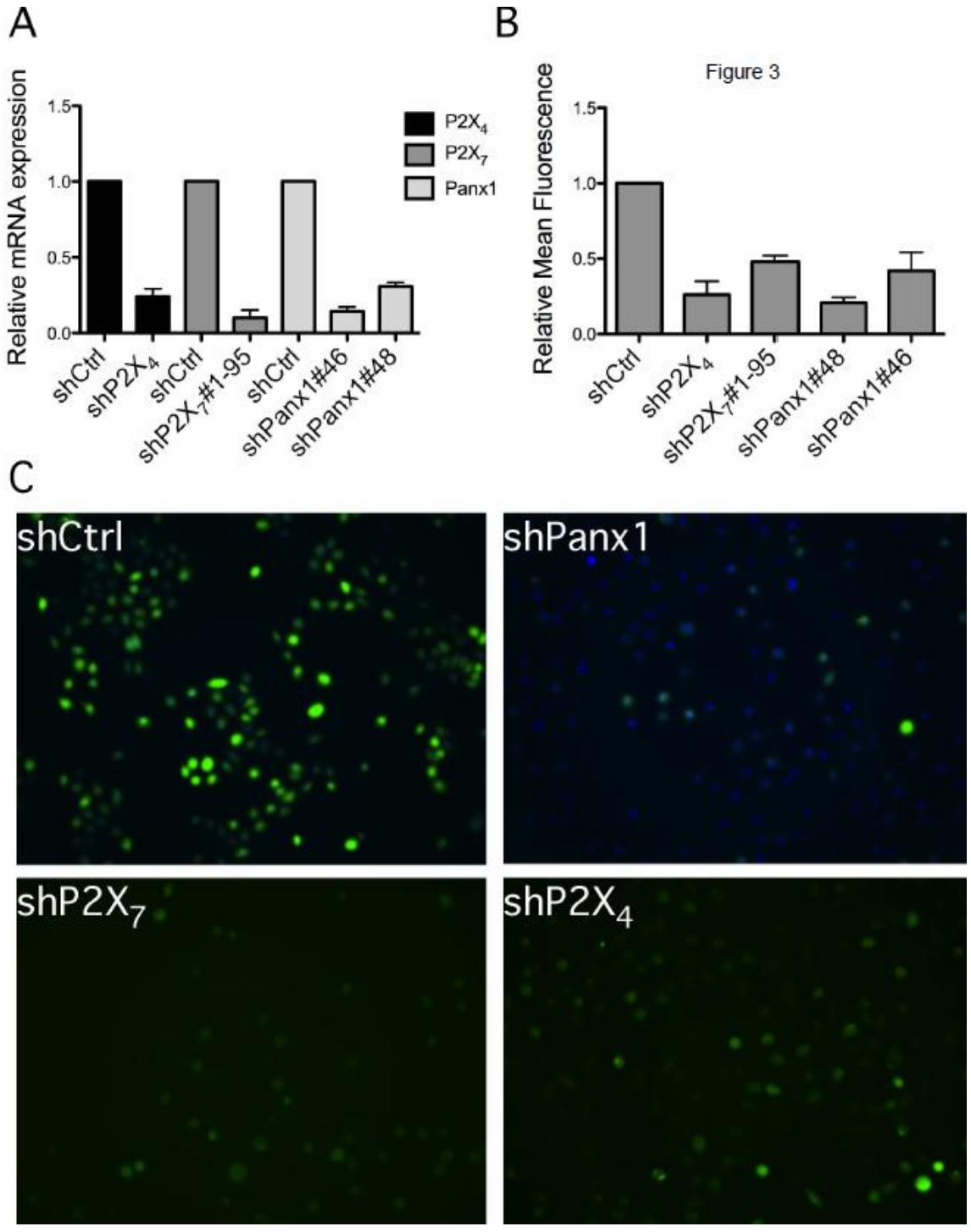
A
Relative mRNA expression
1.5
1.0
0.5
0.0
P2X4
P2X7
Panx1
shCtrl
shP2X4
shCtrl
shP2X7#1-95
shCtrl
shPanx1#46
shPanx1#48
B
Figure 3
Relative Mean Fluorescence
1.5
1.0
0.5
0.0
shCtrl
shP2X4
shP2X7#1-95
shPanx1#48
shPanx1#46
C
shCtrl
shPanx1
shP2X7
shP2X4

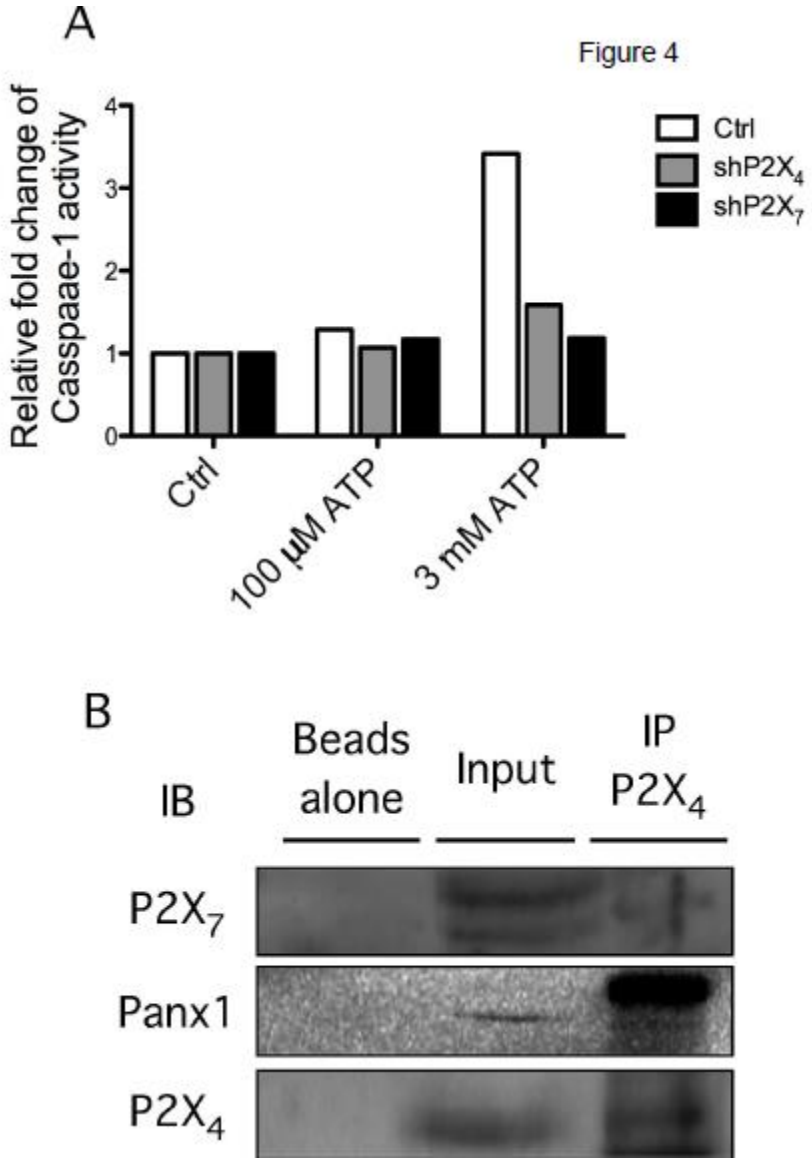
A
Figure 4
Relative fold change of Casspaae-1 activity
0
1
2
3
4
Ctrl
shP2X4
shP2X7
Ctrl
100 μM ATP
3 mM ATP
B
IB
Beads alone
Input
IP P2X4
P2X7
Panx1
P2X4

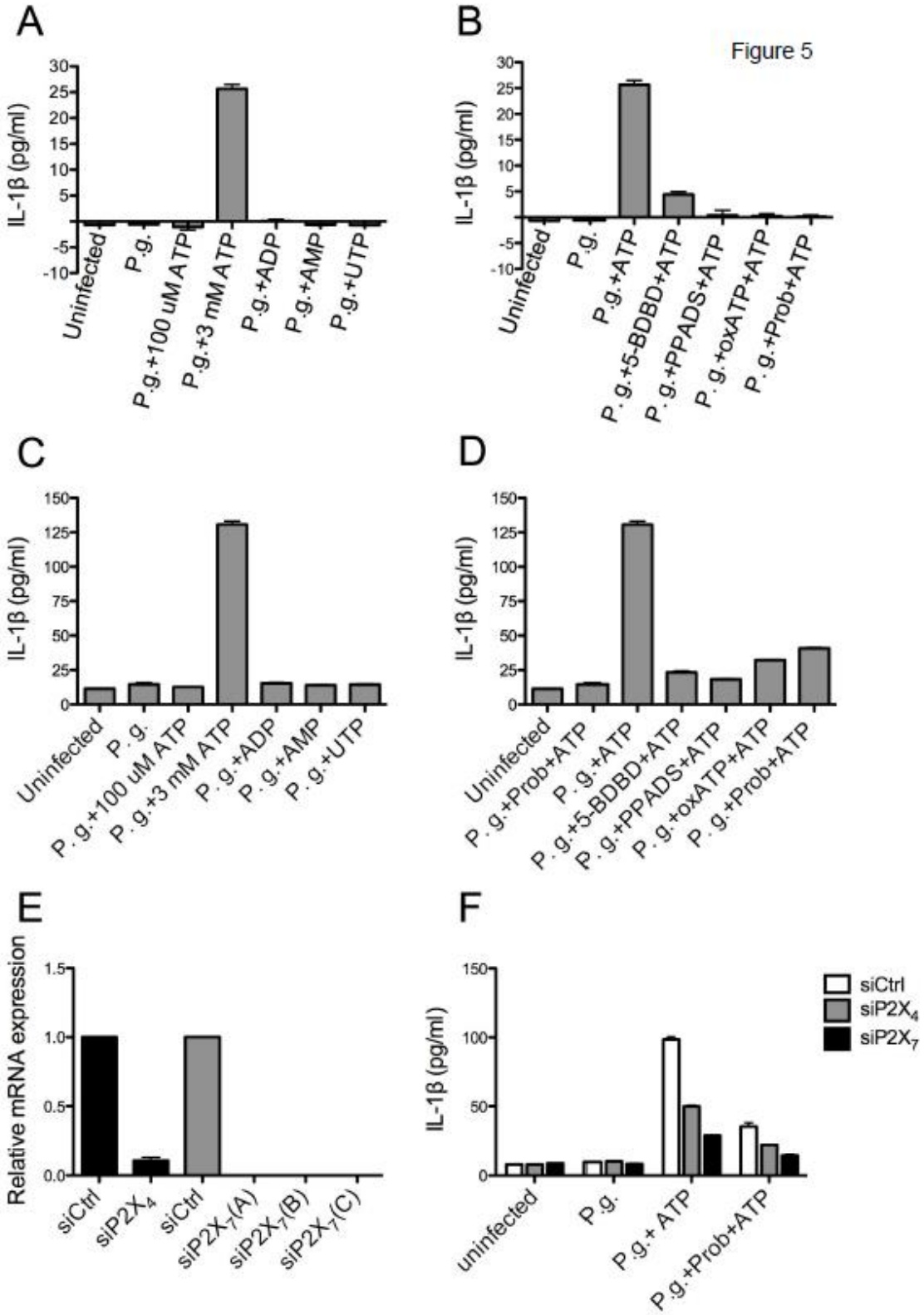
A
IL-1β (pg/ml)
30
25
20
15
10
5
-5
-10
Uninfected
P.g.
P.g.+100 uM ATP
P.g.+3 mM ATP
P.g.+ADP
P.g.+AMP
P.g.+UTP
B
Figure 5
IL-1β (pg/ml)
Uninfected
P.g.
P.g.+ATP
P.g.+5-BDBD+ATP
P.g.+PPADS+ATP
P.g.+oxATP+ATP
P.g.+Prob+ATP
C
IL-1β (pg/ml)
150
125
100
75
50
25
0
Uninfected
P.g.
P.g.+100 uM ATP
P.g.+3 mM ATP
P.g.+ADP
P.g.+AMP
P.g.+UTP
D
IL-1β (pg/ml)
Uninfected
P.g.+Prob+ATP
P.g.+ATP
P.g.+5-BDBD+ATP
P.g.+PPADS+ATP
P.g.+oxATP+ATP
P.g.+Prob+ATP
E
Relative mRNA expression
1.5
1.0
0.5
0.0
siCtrl
siP2X4
siCtrl
siP2X7(A)
siP2X7(B)
siP2X7(C)
F
IL-1β (pg/ml)
150
100
50
0
uninfected
P.g.
P.g.+ ATP
P.g.+Prob+ATP
siCtrl
siP2X4
siP2X7

Figure 6

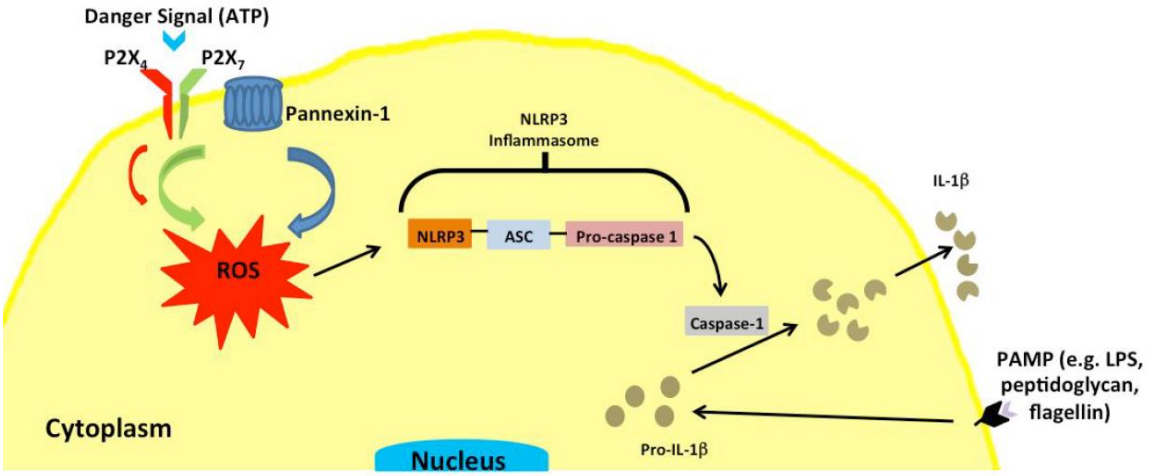
Danger Signal (ATP)
P2X4
P2X7
Pannexin-1
NLRP3
Inflammasome
IL-1β
NLRP3
ASC
Pro-caspase 1
ROS
Caspase-1
PAMP (e.g. LPS,
peptidoglycan,
flagellin)
Cytoplasm
Nucleus
Pro-IL-1β

Chapter 3: *Porphyromonas gingivalis*

3.1 Introduction

P. gingivalis is a Gram-negative human opportunistic pathogen that is highly adapted to colonize the oral epithelial tissues and plays a major role in the etiology of severe and chronic forms of periodontal diseases [77]. The organism has been associated with a variety of other chronic and inflammatory conditions including orodigestive cancers, rheumatoid arthritis, liver disease, and diabetes. Gingival epithelial cells (GECs) that line the gingival mucosa are among the first cells in the oral cavity encountering and invaded by the microorganisms. We aimed to study the mechanisms that allow *P. gingivalis* to survive and evade the host immune system in GECs.

P. gingivalis has evolved to survive and evade host immune recognition as an intracellular pathogen. Many intracellular bacteria such as *Streptococcus pyogenes*, *Listeria Monocytogenes*, and *Chlamydia trachomatis* take control of host cells through autophagy pathways [78-80]. After internalization into a cell, *P. gingivalis* migrate into the cytosol and localize in the perinuclear region [81]. The vacuoles provide not only a protective barrier from lysosomes and degradation, but also an environment of nutrients rerouted to the autophagosomes [82]. Survival of *P. gingivalis* is contributed by nucleoside-diphosphate kinase (NDK) release during infection to disrupt extracellular danger signaling. Extracellular nucleotides, such as ATP, originate from infected cells released as a danger signal [83]. ATP is rapidly degraded in the extracellular medium, so activation of receptors is through autocrine or paracrine signaling. The binding of ATP to a purinoceptors, like $P2X_7$, can lead to secretion of pro-inflammatory cytokines as an inflammatory response to intracellular pathogen infection [84]. By inhibiting ATP binding to its danger-associated molecular pattern receptor, $P2X_7$, it suppresses reactive oxygen species generation, which is a contributor to inflammasome activation [59, 85].

It is still unclear of the significant role of NDK and inflammasome activation. The hypothesis is wild-type infection will inhibit ATP-induced inflammasome activation by secretion of NDK. Therefore, *ndk*-deficient *P. gingivalis* infection is speculated to not as effectively inhibit ATP-induced inflammasome activation. Cytokine secretion and downstream of inflammasome activation are also not well characterized. Cells infected with *P. gingivalis* has been shown to express IL-8 mRNA, but its secretion is degraded by the bacteria [86]. As IL-8 is important as a chemoattractant for neutrophil migration, we aim to evaluate other pro-inflammatory cytokines such as IL-1β and HMGB1, which have not been tested in GECs.

There is still very little knowledge on how different microorganisms or their components regulate the expression and secretion of HMGB1. Since we predict *P. gingivalis* will inhibit inflammasome activation by secretion of NDK, we expected to observe a decrease in IL-1β secretion for cells infected with the wild-type *P. gingivalis*. As for infected cells with *ndk*-deficient *P. gingivalis*, we suspected cytokine secretion to be elevated compared to wild-type *P. gingivalis*. This effect should have also mimic HMGB1 release. Uninfected cells more likely wouldn't secrete IL-1β because there is no PAMP signal to express the pro-inflammatory cytokine. However, it is uncertain of effects on HMGB1 release in uninfected treated with ATP. This study focused on NDK to regulate inflammasome activation and cytokine secretion adds to the understanding of the one mechanisms *P. gingivalis* evades the immune system.

We published our findings in *Microbes and Infection* showing that *P. gingivalis* attenuates ATP-mediated inflammasome activation and HMGB1 release because of its production of NDK. It was surprising to find *P. gingivalis* infection without ATP stimulation induced translocation of HMGB1 from the nucleus to the cytosol. Wild-type *P. gingivalis* also reduced ATP-dependent IL-1β secretion through release of NDK. Taken together, *P. gingivalis* NDK contributes to dampening pro-inflammatory response in GECs.

3.2 *Porphyromonas gingivalis* attenuates ATP-mediated inflammasome activation and HMGB1 release through expression of a nucleoside-diphosphate kinase

ELSEVIER

Institut Pasteur

Microbes and Infection 17 (2015) 369–377

www.elsevier.com/locate/micinf

Original article

Porphyromonas gingivalis attenuates ATP-mediated inflammasome activation and HMGB1 release through expression of a nucleoside-diphosphate kinase

Larry Johnson [a,b,1], Kalina R. Atanasova [c,d,1], Phuong Q. Bui [a,b], Jungnam Lee [c,d], Shu-Chen Hung [a,b], Özlem Yilmaz [c,d,**], David M. Ojcius [a,b,*]

[a] *Department of Molecular Cell Biology, University of California, Merced, CA 95343, USA*
[b] *Health Sciences Research Institute, University of California, Merced, CA 95343, USA*
[c] *Department of Periodontology, University of Florida, Gainesville, FL 32610, USA*
[d] *Emerging Pathogens Institute, University of Florida, Gainesville, FL 32610, USA*

Received 19 March 2015; accepted 19 March 2015
Available online 27 March 2015

Abstract

Many intracellular pathogens evade the innate immune response in order to survive and proliferate within infected cells. We show that *Porphyromonas gingivalis*, an intracellular opportunistic pathogen, uses a nucleoside-diphosphate kinase (NDK) homolog to inhibit innate immune responses due to stimulation by extracellular ATP, which acts as a danger signal that binds to $P2X_7$ receptors and induces activation of an inflammasome and caspase-1. Thus, infection of gingival epithelial cells (GECs) with wild-type *P. gingivalis* results in inhibition of ATP-induced caspase-1 activation. However, *ndk*-deficient *P. gingivalis* is less effective than wild-type *P. gingivalis* in reducing ATP-mediated caspase-1 activation and secretion of the pro-inflammatory cytokine, IL-1β, from infected GECs. Furthermore, *P. gingivalis* NDK modulates release of high-mobility group protein B1 (HMGB1), a pro-inflammatory danger signal, which remains associated with chromatin in healthy cells. Unexpectedly, infection with either wild-type or *ndk*-deficient *P. gingivalis* causes release of HMGB1 from the nucleus to the cytosol. But HMGB1 is released to the extracellular space when uninfected GECs are further stimulated with ATP, and there is more HMGB1 released from the cells when ATP-treated cells are infected with *ndk*-deficient mutant than wild-type *P. gingivalis*. Our results reveal that NDK plays a significant role in inhibiting $P2X_7$-dependent inflammasome activation and HMGB1 release from infected GECs.

Keywords: Innate immunity; Purinergic receptor; *Porphyromonas gingivalis*; Interleukins; Inflammation

1. Introduction

Porphyromonas gingivalis is a Gram-negative opportunistic pathogen that colonizes the human oral epithelial tissues and plays a major role in the etiology of severe and chronic forms of periodontal disease [1]. The organism has been associated recently with a variety of other chronic and inflammatory conditions including orodigestive cancer, rheumatoid arthritis, liver disease, and diabetes [2,3]. Gingival epithelial cells (GECs) are among the first cells in the oral cavity that are encountered and invaded by *P. gingivalis*, and they play an important barrier role while also sensing and responding to microbial colonizers [1,2,4].

Immune recognition of cellular damage and invading pathogens is carried out through pattern recognition receptors such as Toll-like receptors (TLRs) and purinergic P_2X receptors

* Corresponding author. Department of Molecular Cell Biology, University of California, 5200 North Lake Road, Merced, CA 95343, USA. Tel.: +1 209 228 2948.
** Corresponding author. Department of Periodontology, University of Florida, Gainesville, FL 32610, USA. Tel.: +1 352 273 8003.
E-mail addresses: oyilmaz@ufl.edu (Ö. Yilmaz), david.ojcius@gmail.com (D.M. Ojcius).
[1] Both authors contributed equally to this work.

http://dx.doi.org/10.1016/j.micinf.2015.03.010
1286-4579/

situated on the plasma membrane, and nucleotide-binding oligomerization domain (NOD)-like receptors (NLRs) in the cytoplasm [5–7]. Ligation of the purinergic receptor, $P2X_7$, typically leads to assembly of a complex of proteins, called the inflammasome, which results in activation of caspase-1 and subsequent processing and secretion of the pro-inflammatory cytokines, IL-1β and IL-18. The most widely studied inflammasome contains the NLR member, NLRP3, the adaptor protein, apoptosis-associated speck-like protein containing a CARD (ASC), and the protease, caspase-1 [7,8]. The NLRP3 inflammasome can be activated by multiple stimuli, including the "danger signal," extracellular ATP, which is released by damaged, stressed, or infected cells [7,9]. GECs express functional $P2X_7$, whose ligation by ATP leads to production of reactive oxygen species (ROS) and assembly and activation of the NLRP3 inflammasome [7,10–13].

Another danger signal molecule, high mobility group box 1 protein (HMGB1), can be secreted after inflammasome activation [14,15]. In healthy cells, HMGB1 is associated with chromatin and enhances the binding of regulatory proteins to a variety of genes [14]. Outside the cell, HMGB1 has potent and diverse immunomodulatory functions after binding to its receptor, RAGE, TLR2 or TLR4 [16]. Extracellular HMGB1 has been linked with different inflammatory conditions, from endotoxemia, ischemia and liver injury to squamous cell carcinoma [17–19]. Increased HMGB1 release and RAGE expression is also described to possibly play a role in diabetes-associated periodontitis [20]. Recently, HMGB1 release has been shown to be regulated by inflammasomes [21–23]. However, there is still little known on how different microorganisms or their components regulate the expression and secretion of HMGB1.

As a successful facultative intracellular organism, *P. gingivalis* has evolved an array of virulence factors and associated mechanisms that allow the organism's survival and spread in the gingival epithelium, and evasion of recognition by the host immune system [1]. Prominent virulence factors include gingipains and a secreted homologue of nucleoside-diphosphate kinases (NDKs) [24–27].

NDKs catalyze the transfer of orthophosphates from nucleoside triphosphates, such as ATP, to nucleoside diphosphates, thus enabling it to control nucleotide pools inside the cells [24]. Additionally, secreted NDKs can be used by intracellular persistent bacteria, such as *Mycobacterium tuberculosis* and *P. gingivalis*, to mask their presence from the host immune system by scavenging extracellular ATP [9,28–30]. Unlike many other infectious bacteria, *P. gingivalis* can stimulate the production of biologically inactive pro-IL-1β in infected GECs, but does not induce significant release of the secreted active form of IL-1β [12]. Active IL-1β secretion in *P. gingivalis*-infected GECs only occurs after stimulation with extracellular ATP [12]. Our previous studies have shown that *P. gingivalis* NDK secretion is important for maximal inhibition of ATP-triggered $P2X_7$-mediated apoptosis in infected GECs as well as ATP-induced generation of cellular ROS [13,31,32]. These studies imply a potentially critical role for *P. gingivalis* NDK in the modulation of the inflammasome-mediated host response and IL-1β secretion. The current knowledge on the mechanisms of inflammasome activation has been predominantly derived from cells of the myeloid lineage [33]. Epithelial cells in general, including GECs, have attracted less attention. Additionally the mechanisms of regulation of other inflammasome-dependent danger-signals, such as HMGB1, are widely unexplored. Therefore, we aimed to examine the potential role of the effector molecule NDK on ATP-mediated inflammasome activation and pro-inflammatory cytokine release. We hypothesize that the release of NDK inhibits caspase-1 activation and secretion of pro-inflammatory cytokines and HMGB1 in *P. gingivalis*-infected GECs.

2. Materials and methods

2.1. Primary and immortalized GECs

Healthy gingival tissue was obtained by oral surgery to produce primary GECs cultures as previously described [34]. No subject recruitment per se was done. Adult patients were selected at random and anonymously from those presenting at the University of Florida Dental Clinics for tooth crown lengthening or impacted third molar extraction. Gingival tissue that would otherwise be discarded was collected after informed written consent by the patient. This study is approved by the Institutional Review Board under the University of Florida. Cells were cultured as monolayers in serum-free keratinocyte growth medium (Lonza) at 37 °C in a 5% CO_2 incubator. The human immortalized GEC (HIGK) cell line was obtained as previously described [35]. Cells were cultured in defined keratinocytes serum-free media (K-SFM, Life Technologies) at 37 °C in a 5% CO_2 incubator.

2.2. Porphyromonas gingivalis *culture*

P. gingivalis ATCC 33277 and its isogenic *ndk*-deficient mutant were cultured anaerobically for 24 h at 37 °C in trypticase soy broth supplemented with yeast extract (1 mg/ml), hemin (5 mg/ml), and menadione (1 mg/ml). Erythromycin (10 mg/ml) was added to the media as a selective agent for the growth of the *ndk*-deficient mutant strain, which was previously described (29). Bacteria were grown for 24 h and collected by centrifugation at 6000 × *g* for 10 min at 4 °C. The bacteria were then washed twice and resuspended with Dulbecco's phosphate-buffered saline (PBS) (Life Technologies). Quantification of bacteria was determined using a Klett-Summerson photoelectric colorimeter.

2.3. *Infection of primary and immortalized GECs with* P. gingivalis *and treatment with ATP and inhibitors*

Primary GECs and HIGK cells were seeded onto 6-well plates and upon reaching 75–80% confluence the cells were infected with either wild-type or *ndk*-deficient *P. gingivalis* at a multiplicity of infection (MOI) of 100 which has previously been shown to be biologically relevant [27,36,37]. Cells used for HMGB1 Western blot assays were collected after 9 h of

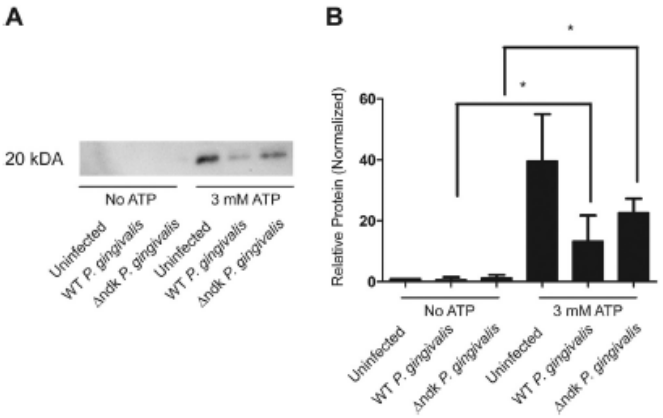

Fig. 1. NDK modulates ATP-induced caspase-1 activation in GECs. Cells were infected or uninfected with wild-type *P. gingivalis* or *ndk*-deficient *P. gingivalis* for 6 h, and then treated with 3 mM ATP for 3 h. (A) Caspase-1 (20 kDa) activation in HIGK cell supernatants was detected by SDS-PAGE Western blot assay. (B) Average of three Western blot experiments, quantified by densitometry. Error bars represent the standard deviations (±SD) of at least two independent experiments ran in at least duplicates (*P < 0.05 Student *t*-test).

infection. For cells treated with the caspase-1 inhibitor, YVAD (z-YVAD-fmk, R&D Systems) [10,38,39], YVAD was added to the media at a final concentration of 50 μM and incubated at 37 °C in a 5% CO_2 incubator. The cells were treated with 3 mM ATP (Sigma) 30 min after addition of YVAD, or 6 h after infection and incubated for additional 3 h. Cell-culture fluids were collected and centrifuged at 100 × *g* to remove cell debris. Protease inhibitors (PhosStop, Roche) were added to all samples to prevent protein degradation.

2.4. Measurement of IL-1β secretion by ELISA

Samples from at least three separate experiments were collected for each infection and treatment condition. Samples were cleared of cellular debris by centrifugation at 800 × *g* for 5 min and cell-free supernatants were used for IL-1β ELISA assay. IL-1β secretion levels were measured using Human IL-1β ELISA kit II (BD Biosciences). ELISAs were performed as per manufacturer's instructions. Briefly, samples, controls, and standards were diluted with assay diluent, loaded onto a 96-well plate, and incubated for 2 h at room temperature. Wells were washed and incubated with the detection antibody for 1 h at room temperature. After washing, substrate was added to all wells. The reactions were stopped with stop solution and optical densities were read at an absorbance of 450 nm using a Synergy MX plate reader (BioTek Instruments). P-values were calculated using two-tailed Student's *t*-test.

2.5. Western blot

Proteins from cell-free culture fluids were concentrated using trichloroacetic acid (TCA) [40]. TCA at 100% was added to supernatants for a final concentration of 20% TCA. Samples were vortexed and incubated on ice. After incubation, samples were centrifuged and supernatants were discarded. The pellets were washed twice with cold acetone and allowed to air-dry. Pellets were resuspended with sample buffer (Thermo Scientific) and boiled. Protein concentration in samples was measured using the BioRad protein assay. Samples were loaded at equal final protein concentrations and run on SDS-PAGE gels, followed by transfer onto PVDF

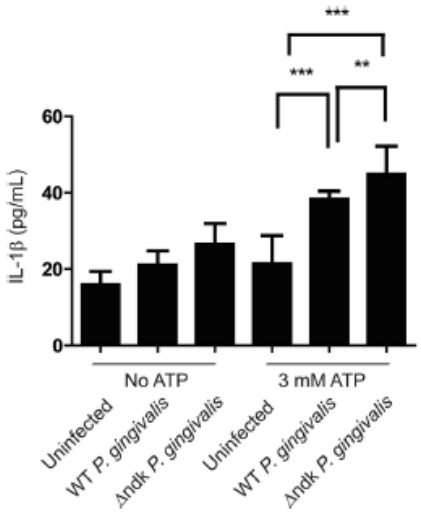

Fig. 2. NDK hydrolysis of ATP inhibits secretion of IL-1β in ATP-induced GECs. Cells were infected or uninfected with wild-type *P. gingivalis* or *ndk*-deficient *P. gingivalis* for 6 h, and then treated with 3 mM ATP for 3 h. ELISA of IL-1β secretion was measured in supernatants of *P. gingivalis*-infected primary GECs treated with ATP. Error bars represent the standard deviations (±SD) of at least two independent experiments ran in at least duplicates (**P < 0.001 and ***P < 0.0001 Student *t*-test).

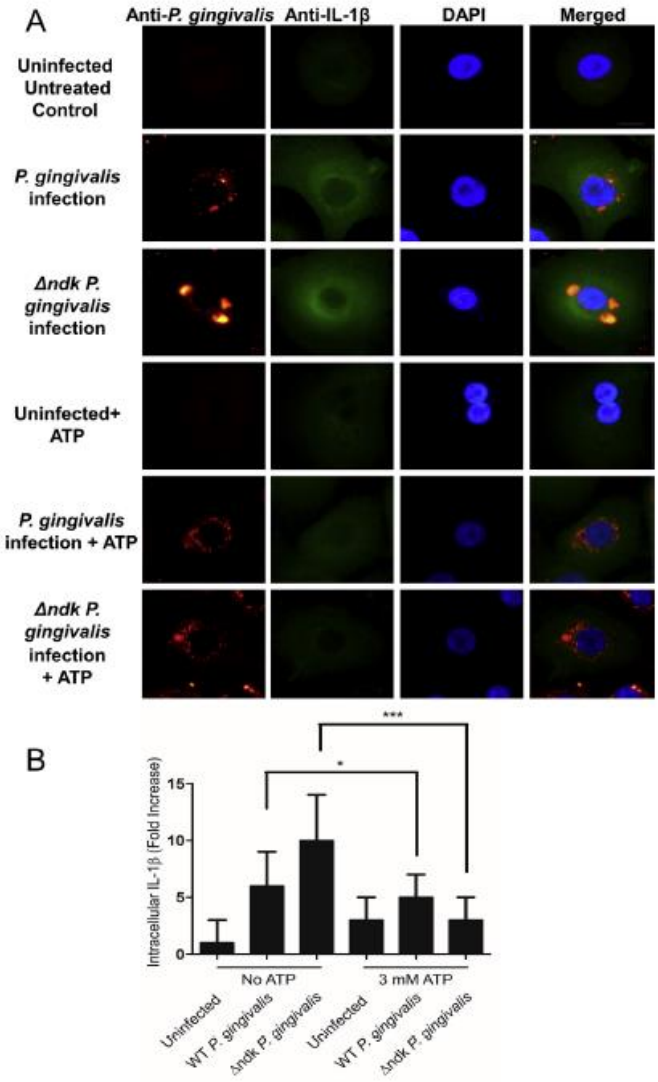

Fig. 3. NDK affects intracellular IL-1β accumulation and ATP-dependent release in primary GECs. GECs were infected or uninfected with wild-type *P. gingivalis* or *ndk*-deficient *P. gingivalis* for 6 h, and then treated with 3 mM ATP for 3 h. (A) Immunofluorescence staining of DAPI-labeled nuclei (blue), Alexa-Fluor-594-labeled *P. gingivalis* (red), and fluorescein-isothiocyanate (FITC)-labeled IL-1β (green). Images were taken at 40X magnification, and scale bars represent10 μm. (B) Quantification analysis for mean fluorescence intensity was performed using NIH-ImageJ. Error bars represent the standard deviations (±SD) of at least 25 independent cells (*$P < 0.05$ and ***$P < 0.0001$ Student *t*-test).

membranes. Membranes were blocked with 5% BSA for 1 h at RT, and then incubated with primary antibodies against caspase-1 (Cell Signaling) or HMGB1 (Cell Signaling). After 1 h, blots were washed and incubated with secondary anti-rabbit HRP (Millipore) for another hour. Finally, membranes were washed and exposed to Luminata Forte (Millipore) substrate. Images were acquired using ChemiDoc XRS + system (Bio-Rad) and analyzed using NIH-ImageJ.

2.6. Immunofluorescence examination of intracellular IL-1β and HMGB1

Primary GECs were cultured in 4-well culture plates (Nunc) containing round glass inserts. Cells were infected at a confluence of 75–80% with either wild-type *P. gingivalis* or the *ndk*-deficient mutant strain at an MOI of 100. Six hours later, cells were treated with ATP at a final concentration of 3 mM for an additional 3 h. Cells were washed three times with PBS and fixed with 4% paraformaldehyde for 15 min. Cells were permeabilized using 0.01% Triton X-100 solution in PBS and incubated with the primary antibodies. IL-1β was detected using an FITC-conjugated mouse monoclonal antibody (R&D Systems). HMGB1 was detected using a rabbit polyclonal anti-human HMGB1 antibody (Cell Signaling). *P. gingivalis* infection was detected using anti-*P. gingivalis* rabbit polyclonal antibody, coupled with a secondary goat-anti-rabbit polyclonal antibody (Invitrogen), and all inserts were mounted onto glass slides using VectaShield mounting medium (Fisher) containing DAPI stain. The intensity of IL-1β and HMGB1 staining was measured using NIH-ImageJ, and measurements of at least 25 cells, originating from at least three separate replicate experiments, were averaged.

2.7. Statistical analysis

Data are reported as mean ± standard deviation (SD). Statistical significance was calculated by two-tailed Student's *t*-test and was considered significant at $P < 0.05$.

3. Results

3.1. NDK inhibits Caspase-1 activation

We previously showed that ATP stimulation of $P2X_7$ resulted in assembly with $P2X_4$ and pannexin-1 and generation of reactive oxygen species (ROS) [10]. Stimulation with ATP alone could induce caspase-1 activation in GECs, but *P. gingivalis* infection diminished the effect of ATP [12], likely through hydrolysis of extracellular ATP by secretion of the NDK homologue [31]. Therefore, we aimed here to evaluate the effects of *P. gingivalis* NDK on ATP-mediated inflammasome activation during infection of GECs. As shown in Fig. 1A and B, HIGKs infected with wild-type *P. gingivalis* showed reduced ATP-induced caspase-1 activation, whereas cells infected with *ndk*-deficient *P. gingivalis* resembled uninfected cells, with higher levels of secreted (activated) caspase-1. This suggests that the NDK homologue of *P. gingivalis* regulates caspase-1 activation and may therefore influence secretion of pro-inflammatory cytokines.

3.2. NDK inhibits IL-1β secretion

Our previous studies have shown that *P. gingivalis*-infected or LPS-primed GECs require stimulation with a second danger signal, such as ATP, in order to release active IL-1β [12]. In order to evaluate the role of NDK in inhibiting signaling by ATP, we infected primary GECs with *P. gingivalis* followed by stimulation with ATP, and examined the supernatant for IL-1β by ELISA. The results demonstrated significantly lower ATP-induced IL-1β secretion in wild-type *P. gingivalis*-infected GECs, compared to *ndk*-deficient *P. gingivalis*-infected GECs or uninfected cells (Fig. 2).

Immunofluorescence staining for IL-1β showed that *ndk*-deficient *P. gingivalis* induces higher levels of IL-1β accumulation within primary GECs (Fig. 3A) and there is a significant decrease in fluorescence intensity upon stimulation with ATP. In contrast, GECs infected with wild-type *P. gingivalis* showed reduced IL-1β release and relatively higher intracellular staining after ATP treatment, compared with cells infected with *ndk*-deficient *P. gingivalis* (Fig. 3B), suggesting that NDK produced by wild-type *P. gingivalis* inhibits ATP-mediated IL-1β secretion.

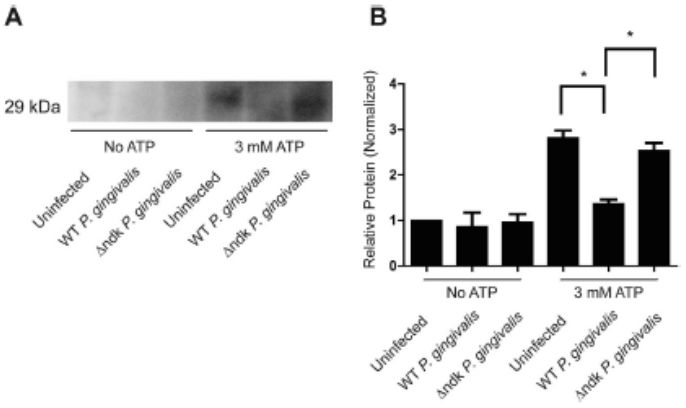

Fig. 4. NDK affects release of HMGB1 in GECs. Cells were infected or uninfected with wild-type *P. gingivalis* or *ndk*-deficient *P. gingivalis* for 6 h, and then treated with 3 mM ATP for 3 h (A) HMGB1 secretion in GEC cell supernatants was imaged by SDS-PAGE Western blot assay. (B) Average of two Western blot experiments, quantified by densitometry. Error bars represent the standard deviations (±SD) (*$P < 0.05$ Student t-test).

3.3. NDK modulates the release of HMGB1

We next evaluated whether *P. gingivalis* NDK affects release of another danger signaling molecule, HMGB1. Under normal conditions, HMGB1 is found within the nucleus of eukaryotic cells and is associated with DNA, where it functions as a regulator of gene expression [17]. However, HMGB1 can act as a danger signaling molecule when released by stressed cells or cells undergoing necrosis [17]. In a previous study using *Salmonella*-infected macrophages, it was shown that HMGB1 release is caspase-1 activation-dependent [22]. We therefore hypothesized that NDK may inhibit HMGB1 release due to its ability to inhibit ATP-mediated caspase-1 activation. To study this possibility, we examined the release of HMGB1 by Western blot analysis. Our results showed that ATP treatment induces HMGB1 release from uninfected GECs, and that wild-type *P. gingivalis* infection is more effective than infection with *ndk*-deficient *P. gingivalis* in inhibiting ATP-induced HMGB1 release (Fig. 4A and B).

Due to the localization of HMGB1 in the nucleus under quiescent conditions, we hypothesized that HMGB1-release may require relocalization from the nucleus through the cytosol and to the extracellular space. We therefore performed immunofluorescence staining against HMGB1 and confirmed the expected nuclear localization of HMGB1 in uninfected untreated primary GECs (Fig. 5A). However, when uninfected cells were treated with ATP, we observed a relocation of HMGB1 from the nucleus to the extracellular space, which was attenuated in cells treated with the caspase-1 inhibitor. Moreover, there was relocation of HMGB1 from the nucleus to the cytosol in GECs infected with either the wild-type or *ndk*-deficient *P. gingivalis* strain. Upon ATP stimulation, the intensity of HMGB1 in the cytosol was significantly decreased in the cells infected with *ndk*-deficient *P. gingivalis*, consistent with the release of HMGB1 from the cell demonstrated in the Western blot assay (Fig. 5A and B). The cells infected with the wild-type *P. gingivalis* showed a substantially higher intensity of HMGB1 in the cytosol after ATP stimulation, compared to cells infected with the *ndk*-deficient *P. gingivalis*, supporting the proposed role of *P. gingivalis* NDK in inhibiting ATP-mediated HMGB1 release.

4. Discussion

The healthy human oral mucosa is colonized by a diversity of organisms, including high numbers of different bacterial species in addition to fungi and protozoa [41]. These microbes can reside within pockets between the teeth and epithelium to form biofilms and carry on as commensals or potential pathogenic colonizers [42]. Some of these microorganisms have evolved elaborate virulence factors to ensure their survival within the oral mucosa without eliciting an immediate destructive host immune response [1]. Among these organisms, *P. gingivalis* uses its major fimbriae to adhere to the

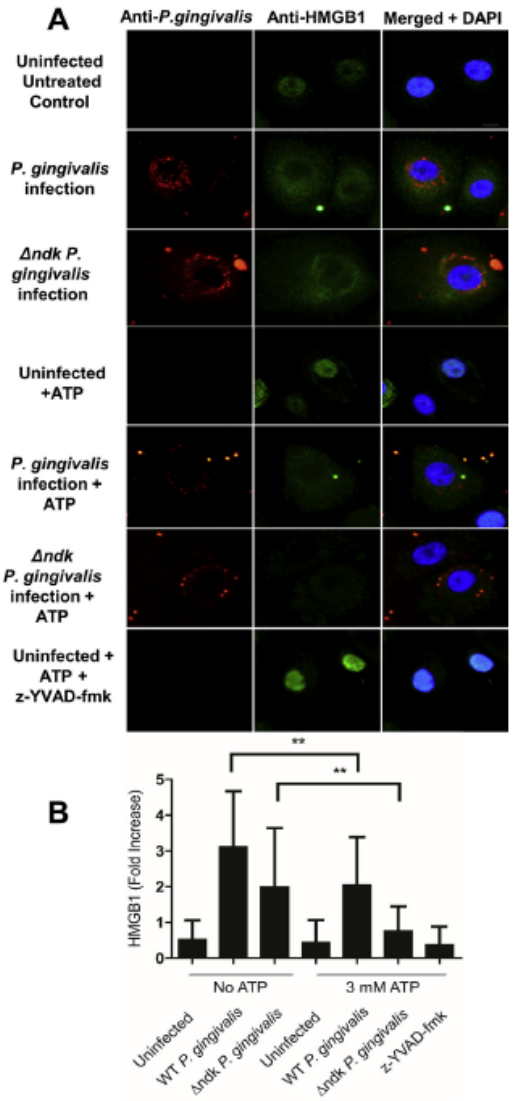

Fig. 5. NDK or *P. gingivalis* infection affects intracellular HMGB1 localization in primary GECs or ATP-mediated HMGB1 secretion. Cells were infected or uninfected with wild-type *P. gingivalis* or *ndk*-deficient *P. gingivalis* for 6 h, and then treated with 3 mM ATP for 3 h. YVAD inhibitor was administered at a final concentration of 50 μM prior to ATP stimulation. (A) Immunofluorescence staining representing DAPI-labeled nuclei (blue), Alexa-Fluor-594-labeled *P. gingivalis* (red), and Alexa-Fluor-488-labeled HMGB1 (green). Images were taken at 40X magnification, and scale bars represent 10 μm. (B) Quantification analysis for mean fluorescence intensity was performed using NIH-ImageJ. Error bars represent the standard deviations (±SD) of at least 25 independent cells (**$P < 0.001$ Student *t*-test).

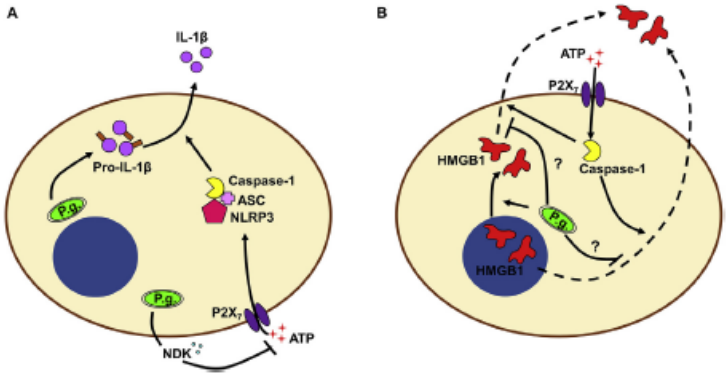

Fig. 6. Proposed model for the role of NDK in HMGB1 localization during *P. gingivalis* infection. (A) *P. gingivalis* inhibits ATP-mediated caspase-1 activation and maturation of IL-1β by NDK hydrolysis of ATP. (B) *P. gingivalis* modulates caspase-1 dependent HMGB1 release from the host cell [12,13].

host-cell membrane and quickly localize to the endoplasmic reticulum rich perinuclear region [13,27,43]. *P. gingivalis* infection can also inhibit the host apoptotic response in GECs by activating the PI3K/Akt pathway and modulating expression of Bcl-2 family proteins [1,44]. Finally, *P. gingivalis* secretes an enzyme homologue of the evolutionarily conserved NDKs [13,31], which is critical for suppression of cellular ROS production and ATP-induced host cell death [13,31]. In the present study, we show that the lack of NDK significantly reduces the inhibition of ATP-dependent inflammasome activation and subsequent release of pro-inflammatory cytokines by GECs. Our previous studies have elucidated the role of this effector of *P. gingivalis* as an important modulator of cellular ROS generation, as well as demonstrated that the *ndk*-deficient strain has significantly less intracellular survival ability compared to its isogenic wild strain upon ATP-stimulation in primary GECs [12,13,31]. Further, there was a significant intracellular recovery of the *ndk*-deficient strain after treatment with the potent ROS-inhibitor N-acetyl-cysteine (NAC) and complementation of the *ndk* gene restored the observed phenotype [13]. Since ROS generation contributes to inflammasome activation [45], our results showing a suppression of caspase-1 activation by wild-type *P. gingivalis* infection was expected. Our previous studies have extensively demonstrated that *P. gingivalis* is a facultative intracellular bacterium and in the GECs, the majority of bacteria rapidly enters and resides in the GECs [1,36,46]. Further, our previous studies displayed that GECs that are infected with *P. gingivalis* had intact membranes while their supernatant showed a time-dependent release of the small NDK molecule [13]. Altogether, this evidence points that the majority of the NDK in supernatants are derived from the intracellular bacteria, rather than incidental extracellular *P. gingivalis*.

Previous studies have shown that IL-1β secretion requires two signals. Recognition of a pathogen-associated molecular pattern by a pattern recognition receptor such as TLR provides the first signal and stimulates pro-IL-1β production [47]. A second signal, from a danger signal such as ATP, activates the inflammasome and caspase-1, resulting in processing of pro-IL-1β and secretion of the mature cytokine, IL-1β [47]. We hypothesized that ATP-dependent IL-1β secretion would be reduced by infection with wild-type *P. gingivalis* due to its ability to produce NDK, which should scavenge extracellular ATP. The findings in this study confirm the anti-inflammatory role of NDK in infected GECs.

We also investigated whether *P. gingivalis* infection could affect the release by GECs of another danger signal, HMGB1 [48,49]. Unexpectedly, our studies also revealed that *P. gingivalis* induces translocation of HMGB1 from the nucleus to the cytosol. However, similarly to IL-1β secretion, ATP was required as a secondary stimulus to release HMGB1 from the cell (Fig. 6). Furthermore, *ndk*-deficient *P. gingivalis* infection was less effective than infection with wild-type *P. gingivalis* in inhibiting HMGB1 release from infected GECs, which also required caspase-1 activation.

NDKs have recently attracted attention due to their involvement in a variety of chronic inflammatory diseases, and increased expression of human NDK was recently described in affected tissues of oral squamous cell carcinoma patients [50]. In addition, *P. gingivalis* is associated with oral squamous cell carcinomas and other chronic diseases [3,51]. Our findings also support studies showing that HMGB1 is another possible candidate for an early inflammatory disease marker [52,53]. Collectively, these results suggest that *P. gingivalis* NDK dampens the host-immune response by decreasing release of pro-inflammatory cytokine, IL-1β, and the pro-inflammatory danger signal, HMGB1, from infected GECs. Identification of NDK as a key mediator used by *P. gingivalis* to modulate inflammation suggests that therapeutic strategies against periodontitis could also target this effector.

Conflict of interest

The authors declare no conflict of interest.

Acknowledgments

This study was supported by the NIDCR grants R01DE016593 and R01DE019444, and a University of California Presidential Chair. We would like to thank the Stem Cell Instrumentation Foundry (SCIF), UC Merced, for instrument support.

References

[1] Yilmaz O. The chronicles of *Porphyromonas gingivalis*: the microbium, the human oral epithelium and their interplay. Microbiology 2008;154:2897–903.
[2] Darveau RP. Periodontitis: a polymicrobial disruption of host homeostasis. Nat Rev Microbiol 2010;8:481–90.
[3] Atanasova KR, Yilmaz O. Looking in the *Porphyromonas gingivalis* cabinet of curiosities: the microbium, the host and cancer association. Mol Oral Microbiol 2014;29:55–66.
[4] Krisanaprakornkit S, Kimball JR, Weinberg A, Darveau RP, Bainbridge BW, Dale BA. Inducible expression of human beta-defensin 2 by *Fusobacterium nucleatum* in oral epithelial cells: multiple signaling pathways and role of commensal bacteria in innate immunity and the epithelial barrier. Infect Immun 2000;68:2907–15.
[5] Martinon F, Mayor A, Tschopp J. The inflammasomes: guardians of the body. Annu Rev Immunol 2009;27:229–65.
[6] Lotze MT, Zeh HJ, Rubartelli A, Sparvero LJ, Amoscato AA, Washburn NR, et al. The grateful dead: damage-associated molecular pattern molecules and reduction/oxidation regulate immunity. Immunol Rev 2007;220:60–81.
[7] Said-Sadier N, Ojcius DM. Alarmins, inflammasomes and immunity. Biomed J 2012;35:437–49.
[8] Martinon F, Gaide O, Petrilli V, Mayor A, Tschopp J. NALP inflammasomes: a central role in innate immunity. Semin Immunopathol 2007;29:213–29.
[9] Coutinho-Silva R, Ojcius DM. Role of extracellular nucleotides in the immune response against intracellular bacteria and protozoan parasites. Microbes Infect 2012;14:1271–7.
[10] Hung SC, Choi CH, Said-Sadier N, Johnson L, Atanasova KR, Sellami H, et al. P2X4 assembles with P2X7 and pannexin-1 in gingival epithelial cells and modulates ATP-induced reactive oxygen species production and inflammasome activation. PLoS One 2013;8:e70210.
[11] Schwiebert EM, Zsembery A. Extracellular ATP as a signaling molecule for epithelial cells. Biochim Biophys Acta 2003;1615:7–32.
[12] Yilmaz O, Sater AA, Yao L, Koutouzis T, Pettengill M, Ojcius DM. ATP-dependent activation of an inflammasome in primary gingival epithelial cells infected by *Porphyromonas gingivalis*. Cell Microbiol 2010;12:188–98.
[13] Choi CH, Spooner R, DeGuzman J, Koutouzis T, Ojcius DM, Yilmaz O. *Porphyromonas gingivalis*-nucleoside-diphosphate-kinase inhibits ATP-induced reactive-oxygen-species via P2X7 receptor/NADPH-oxidase signalling and contributes to persistence. Cell Microbiol 2013;15:961–76.
[14] Keyel PA. How is inflammation initiated? individual influences of IL-1, IL-18 and HMGB1. Cytokine 2014;69:136–45.
[15] Vande Walle L, Kanneganti TD, Lamkanfi M. HMGB1 release by inflammasomes. Virulence 2011;2:162–5.
[16] Wang H, Bloom O, Zhang M, Vishnubhakat JM, Ombrellino M, Che J, et al. HMG-1 as a late mediator of endotoxin lethality in mice. Science 1999;285:248–51.
[17] Klune JR, Dhupar R, Cardinal J, Billiar TR, Tsung A. HMGB1: endogenous danger signaling. Mol Med 2008;14:476–84.
[18] Kamo N, Ke B, Ghaffari AA, Shen XD, Busuttil RW, Cheng G, et al. ASC/caspase-1/IL-1beta signaling triggers inflammatory responses by promoting HMGB1 induction in liver ischemia/reperfusion injury. Hepatology 2013;58:351–62.
[19] Pang X, Zhang Y, Wei H, Zhang J, Luo Q, Huang C, et al. Expression and effects of high-mobility group box 1 in cervical cancer. Int J Mol Sci 2014;15:8699–712.
[20] Morimoto-Yamashita Y, Ito T, Kawahara K, Kikuchi K, Tatsuyama-Nagayama S, Kawakami-Morizono Y, et al. Periodontal disease and type 2 diabetes mellitus: is the HMGB1-RAGE axis the missing link? Med Hypotheses 2012;79:452–5.
[21] Lu B, Wang H, Andersson U, Tracey KJ. Regulation of HMGB1 release by inflammasomes. Protein Cell 2013;4:163–7.
[22] Lamkanfi M, Sarkar A, Vande Walle L, Vitari AC, Amer AO, Wewers MD, et al. Inflammasome-dependent release of the alarmin HMGB1 in endotoxemia. J Immunol 2010;185:4385–92.
[23] Willingham SB, Allen IC, Bergstralh DT, Brickey WJ, Huang MT, Taxman DJ, et al. NLRP3 (NALP3, Cryopyrin) facilitates in vivo caspase-1 activation, necrosis, and HMGB1 release via inflammasome-dependent and -independent pathways. J Immunol 2009;183:2008–15.
[24] Spooner R, Yilmaz O. Nucleoside-diphosphate-kinase: a pleiotropic effector in microbial colonization under interdisciplinary characterization. Microbes Infect 2012;14:228–37.
[25] Grenier D, Imbeault S, Plamondon P, Grenier G, Nakayama K, Mayrand D. Role of gingipains in growth of *Porphyromonas gingivalis* in the presence of human serum albumin. Infect Immun 2001;69:5166–72.
[26] Into T, Inomata M, Kanno Y, Matsuyama T, Machigashira M, Izumi Y, et al. Arginine-specific gingipains from *Porphyromonas gingivalis* deprive protective functions of secretory leucocyte protease inhibitor in periodontal tissue. Clin Exp Immunol 2006;145:545–54.
[27] Yilmaz O, Young PA, Lamont RJ, Kenny GE. Gingival epithelial cell signalling and cytoskeletal responses to *Porphyromonas gingivalis* invasion. Microbiology 2003;149:2417–26.
[28] Sansom FM, Robson SC, Hartland EL. Possible effects of microbial ecto-nucleoside triphosphate diphosphohydrolases on host-pathogen interactions. Microbiol Mol Biol Rev 2008;72:765–81.
[29] Galgiani JN, Ampel NM, Blair JE, Catanzaro A, Johnson RH, Stevens DA, et al. Coccidioidomycosis. Clin Infect Dis 2005;41:1217–23.
[30] Zaborina O, Li X, Cheng G, Kapatral V, Chakrabarty AM. Secretion of ATP-utilizing enzymes, nucleoside diphosphate kinase and ATPase, by *Mycobacterium bovis* BCG: sequestration of ATP from macrophage P2Z receptors? Mol Microbiol 1999;31:1333–43.
[31] Yilmaz O, Yao L, Maeda K, Rose TM, Lewis EL, Duman M, et al. ATP scavenging by the intracellular pathogen *Porphyromonas gingivalis* inhibits P2X7-mediated host-cell apoptosis. Cell Microbiol 2008;10:863–75.
[32] Spooner R, Yilmaz O. The role of reactive-oxygen-species in microbial persistence and inflammation. Int J Mol Sci 2011;12:334–52.
[33] Yazdi AS, Drexler SK, Tschopp J. The role of the inflammasome in nonmyeloid cells. J Clin Immunol 2010;30:623–7.
[34] Yilmaz O, Jungas T, Verbeke P, Ojcius DM. Activation of the phosphatidylinositol 3-kinase/Akt pathway contributes to survival of primary epithelial cells infected with the periodontal pathogen *Porphyromonas gingivalis*. Infect Immun 2004;72:3743–51.
[35] Oda D, Bigler L, Lee P, Blanton R. HPV immortalization of human oral epithelial cells: a model for carcinogenesis. Exp Cell Res 1996;226:164–9.
[36] Choi CH, DeGuzman JV, Lamont RJ, Yilmaz O. Genetic transformation of an obligate anaerobe, *P. gingivalis* for FMN-green fluorescent protein expression in studying host-microbe interaction. PLoS One 2011;6:e18499.
[37] Dawes C. Estimates, from salivary analyses, of the turnover time of the oral mucosal epithelium in humans and the number of bacteria in an edentulous mouth. Arch Oral Biol 2003;48:329–36.
[38] Bian ZM, Elner SG, Elner VM. Dual involvement of caspase-4 in inflammatory and ER stress-induced apoptotic responses in human retinal pigment epithelial cells. Invest Ophthalmol Vis Sci 2009;50:6006–14.
[39] Chen CC, Tsai SH, Lu CC, Hu ST, Wu TS, Huang TT, et al. Activation of an NLRP3 inflammasome restricts *Mycobacterium kansasii* infection. PLoS One 2012;7:e36292.

[40] Koontz L. Chapter one - TCA precipitation. In: Jon L, editor. Methods enzymol. Academic Press; 2014. p. 3–10.
[41] Zaura E, Nicu EA, Krom BP, Keijser BJ. Acquiring and maintaining a normal oral microbiome: current perspective. Front Cell Infect Microbiol 2014;4:85.
[42] Avila M, Ojcius DM, Yilmaz O. The oral microbiota: living with a permanent guest. DNA Cell Biol 2009;28:405–11.
[43] Yilmaz O, Watanabe K, Lamont RJ. Involvement of integrins in fimbriae-mediated binding and invasion by *Porphyromonas gingivalis*. Cell Microbiol 2002;4:305–14.
[44] Yao L, Jermanus C, Barbetta B, Choi C, Verbeke P, Ojcius DM, et al. *Porphyromonas gingivalis* infection sequesters pro-apoptotic bad through Akt in primary gingival epithelial cells. Mol Oral Microbiol 2010;25:89–101.
[45] Tschopp J, Schroder K. NLRP3 inflammasome activation: the convergence of multiple signalling pathways on ROS production? Nat Rev Immunol 2010;10:210–5.
[46] Yilmaz O, Verbeke P, Lamont RJ, Ojcius DM. Intercellular spreading of *Porphyromonas gingivalis* infection in primary gingival epithelial cells. Infect Immun 2006;74:703–10.
[47] Lopez-Castejon G, Brough D. Understanding the mechanism of IL-1beta secretion. Cytokine Growth Factor Rev 2011;22:189–95.
[48] Eskan MA, Benakanakere MR, Rose BG, Zhang P, Zhao J, Stathopoulou P, et al. Interleukin-1beta modulates proinflammatory cytokine production in human epithelial cells. Infect Immun 2008;76:2080–9.
[49] Erlandsson Harris H, Andersson U. Mini-review: the nuclear protein HMGB1 as a proinflammatory mediator. Eur J Immunol 2004;34:1503–12.
[50] Turhani D, Krapfenbauer K, Thumher D, Langen H, Fountoulakis M. Identification of differentially expressed, tumor-associated proteins in oral squamous cell carcinoma by proteomic analysis. Electrophoresis 2006;27:1417–23.
[51] Atanasova KR, Yilmaz O. Prelude to oral microbes and chronic diseases: past, present and future. Microbes Infect 2015 Mar 23. http://dx.doi.org/10.1016/j.micinf.2015.03.007 [in press]. pii: S1286-4579(15)00050-7.
[52] Nogueira AV, de Souza JA, de Molon RS, Pereira Eda S, de Aquino SG, Giannobile WV, et al. HMGB1 localization during experimental periodontitis. Mediat Inflamm 2014;2014:816320.
[53] Luo L, Xie P, Gong P, Tang XH, Ding Y, Deng LX. Expression of HMGB1 and HMGN2 in gingival tissues, GCF and PICF of periodontitis patients and peri-implantitis. Arch Oral Biol 2011;56:1106–11.

Chapter 4: *Fusobacterium nucleatum*

4.1 Introduction

Fusobacterium nucleatum, a Gram-negative anaerobic bacteria, is found in high frequencies of people affected by periodontitis [87]. The organism has been isolated from other infections outside the oral cavity, including the blood, brain chest, lung, liver, joint, abdominal, obstetrical and gynecological infections and abscesses [87].

F. nucleatum is one of the first species to become established in plaque biofilm and adhere to teeth [88]. It has been shown *F. nucleatum* is the predominant organism after a week of cultivation on bovine enamel and high in frequency within older and denser biofilms, which may arise from a depletion of oxygen in the biofilms [89]. As the bacteria proliferate in the biofilm, its growth in close proximity to GECs provides opportunity to adhere and invade these cells. During co-infections with *P. gingivalis* and *F. nucleatum* in bone marrow-derived macrophages it has been shown that inflammasome activation can be suppressed due to *P. gingivalis* infection [90]. However, when we began these studies, it was not understood the influence of *F. nucleatum* infection on inflammasome activation in GECs. An *in vivo* model of *F. nucleatum* oral infection had not been previously characterized.

We aimed to study the host recognition and inflammatory response, focusing on the inflammasome, in *F. nucleatum* infected GECs. Our findings were published in *Cellular Microbiology*, where we found *F. nucleatum* can activate NF-κB and induce generation of pro-IL-1β. The NLRP3 inflammasome is also activated during infection and contributed to release of IL-1β, ASC, and HMGB1 in a time dependent manner. Collectively, we showed *F. nucleatum* induces caspase-1 activation leading to release of danger signals ASC and HMGB1.

We continued our studies with *F. nucleatum* by exploring oral infection *in vivo*. Our BALB/c results indicated gene expression of pro-inflammatory cytokines day 1 post-infection. Pro-inflammatory cytokine production was observed at 4 day post-infection. This correlated with a heightened immune cell response compared to uninfected mice, specifically macrophage activation, which led to osteoclast activation and bone resorption. Both *in vitro* and *in vivo* results emphasize the significance of *F. nucleatum* as an inducer of inflammasome activation and cytokine production.

Using a C57BL/6 background for *F. nucleatum* oral infection, we obtained preliminary data showing an increase in pro-inflammatory cytokine production over a 7 day period post-infection in wild-type C57BL/6 mice. However, no statistical significance was observed in our experiments comparing wild-type and caspase-1 KO mice. This significance may improve with collection of samples at a later time point. A proposal would be to evaluate samples at day 7 and not day 1 post-infection as we observed significant increase in IL-1β production at day 7. The findings from the BALB/c and C57BL/6 experiments supports *F. nucleatum* can induce a pro-inflammatory response.

4.2 *Fusobacterium nucleatum* infection of gingival epithelial cells leads to NLRP3 inflammasome-dependent secretion of IL-1β and the danger signals ASC and HMGB1

Cellular Microbiology (2016) doi:10.1111/cmi.12560

Fusobacterium nucleatum infection of gingival epithelial cells leads to NLRP3 inflammasome-dependent secretion of IL-1β and the danger signals ASC and HMGB1

Fiona Q. Bui,[1] Larry Johnson,[1,2] JoAnn Roberts,[3,†] Shu-Chen Hung,[1] Jungnam Lee,[3] Kalina Rosenova Atanasova,[3] Pei-Rong Huang,[4] Özlem Yilmaz[3,†] and David M. Ojcius[1*]

[1] *Department of Biomedical Sciences, University of the Pacific, Arthur Dugoni School of Dentistry, San Francisco, CA, 95343, USA.*

[2] *Immunobiology Program, Instituto de Biofísica Carlos Chagas Filho, Federal University of Rio de Janeiro, Rio de Janeiro 21941, Brazil.*

[3] *Department of Periodontology and Emerging Pathogens Institute, University of Florida, Gainesville, FL, 32610, USA.*

[4] *Center for Molecular and Clinical Immunology, Chang Gung University, Gueishan, Taoyuan 333, Taiwan.*

Summary

Fusobacterium nucleatum **is an invasive anaerobic bacterium that is associated with periodontal disease. Previous studies have focused on virulence factors produced by *F. nucleatum*, but early recognition of the pathogen by the immune system remains poorly understood. Although an inflammasome in gingival epithelial cells (GECs) can be stimulated by danger-associated molecular patterns (DAMPs) (also known as danger signals) such as ATP, inflammasome activation by this periodontal pathogen has yet to be described in these cells. This study therefore examines the effects of *F. nucleatum* infection on pro-inflammatory cytokine expression and inflammasome activation in GECs. Our results indicate that infection induces translocation of NF-κB into the nucleus, resulting in cytokine gene expression. In addition, infection activates the NLRP3 inflammasome, which in turn activates caspase-1 and stimulates secretion of mature IL-1β. Unlike other pathogens studied until now, *F. nucleatum* activates the inflammasome in GECs in the absence of exogenous DAMPs such as ATP. Finally, infection promotes release of other DAMPs that mediate inflammation, such as high-mobility group box 1 protein and apoptosis-associated speck-like protein, with a similar time-course as caspase-1 activation. Thus, *F. nucleatum* expresses the pathogen-associated molecular patterns necessary to activate NF-κB and also provides an endogenous DAMP to stimulate the inflammasome and further amplify inflammation through secretion of secondary DAMPs.**

Received 16 August, 2015; revised 13 December, 2015; accepted 15 December, 2015. *For correspondence. E-mail dojcius@pacific.edu; Tel. (415) 780-2095; Fax (415) 780-2083.
†Present address: Medical University of South Carolina, College of Dental Medicine, Charleston, SC, 29425, USA.

Introduction

Oral inflammatory diseases represent the most common chronic diseases in the world, affecting over half of the adult population. In 2010, oral conditions affected approximately 3.9 billion people worldwide, with the prevalence of periodontitis being 35% (Richards, 2013) and severe periodontitis, 11 % (Oliver *et al.*, 1998). An estimated 47.2% of American adults have periodontitis, ranging from mild to severe forms (Richards, 2014). Furthermore, periodontitis is more prevalent and severe in developing countries because of poorer oral hygiene and greater plaque retention (Pilot, 1998; Pihlstrom *et al.*, 2005). Untreated periodontitis can lead to damage of the gum tissue surrounding the tooth and alveolar bone damage, resulting in tooth loss (Han *et al.*, 2000; Saini *et al.*, 2009; Atanasova and Yilmaz, 2015).

One of the first barriers to oral disease is represented by the gingival epithelium, which not only forms attachments to the surface of teeth and but also acts as a physical and chemical shield against infection (Ji *et al.*, 2009; Signat *et al.*, 2011). Gingival epithelial cells (GECs) release antimicrobial peptides such as human β-defensins (hBDs) as a mechanism of defence to prevent biofilm formation (Dommisch *et al.*, 2007; Yin and Chung, 2011; Signat *et al.*, 2011). hBDs have a broad spectrum of activity against Gram-negative and Gram-positive bacteria, and they also stimulate adaptive and innate immune responses, resulting in a coordinated defence of the epithelia against

invading bacteria. The production of hBDs in GECs is pathogen-specific and is regulated by epigenetic changes in various genes (Yin and Chung, 2011).

The innate immune system consists of cells of hematopoietic origin such as macrophages and neutrophils, which can become activated at early times of infection. While epithelial cells are not typically considered to be specialized innate immune cells, they can also recognize infection and respond by secreting chemokines and cytokines such as IL-8 and IL-1β, as in the case of GECs (Yilmaz *et al.*, 2010; Hung *et al.*, 2013; Johnson *et al.*, 2015) and other epithelial cells (Santana *et al.*, 2015). Receptors on both immune cells and epithelial cells recognize microbial products such as lipopolysaccharide and peptidoglycan, also known as pathogen-associated molecular patterns (PAMPs), through pattern recognition receptors such as toll-like receptors, which stimulate expression of antimicrobial genes, and inflammatory cytokines and chemokines (Janeway and Medzhitov, 2002; Takeda and Akira, 2005; Cassel *et al.*, 2009; Said-Sadier and Ojcius, 2012). At the same time, cells that are dying or stressed because of infection can release host-derived molecules, such as ATP, that are called alarmins, danger signals or danger-associated molecular patterns (DAMPs) (Said-Sadier and Ojcius, 2012; Santana *et al.*, 2015). For the cytokines IL-1β and IL-18, ligation of pattern recognition receptors by PAMPs leads to intracellular production of pro-IL-1β and pro-IL-18, but not their secretion. Simultaneous ligation of receptors for DAMPs, such as the ATP receptor P2X7, leads to assembly of the NLRP3 inflammasome and auto-cleavage of pro-caspase-1 to its activated form, caspase-1 (Cassel *et al.*, 2009; Tschopp and Schroder, 2010; Said-Sadier and Ojcius, 2012; Kim and Jo, 2013; Harijith *et al.*, 2014). Activated caspase-1 can then cleave pro-IL-1β and pro-IL-18 to their mature and secreted form, IL-1β and IL-18 (Srinivasula *et al.*, 2002).

Fusobacterium nucleatum, a Gram-negative anaerobic bacterium, stimulates inflammation in the human oral cavity and gut mucosa (Strauss *et al.*, 2011) and has been identified in high frequencies in adults afflicted with mild to acute periodontitis (Signat *et al.*, 2011). *F. nucleatum* can also invade host tissues and obstruct healing of damaged oral tissues (Bartold *et al.*, 1991; Jeng *et al.*, 1999). Infection of murine macrophages with *F. nucleatum* has been shown to result in NLPR3 inflammasome activation and IL-1β secretion (Taxman *et al.*, 2012); however, the mechanism was not characterized, and infection of the preferred host cells of the bacteria, GECs, has not been previously examined.

Studies have shown a significantly high level of IL-1β expression in gingival crevicular fluid at sites of recent bone and attachment loss in periodontitis patients (Lee *et al.*, 1995). Furthermore, IL-1β deficient mice demonstrated less *Porphyromonas gingivalis* lipopolysaccharide-induced periodontium destruction compared with wild-type mice undergoing the same treatment (Chiang *et al.*, 1999), suggesting a strong association between severity of periodontitis and elevated levels of IL-1β (Hodge and Michalowicz, 2001), which may directly or indirectly stimulate osteoclast formation (Chiang *et al.*, 1999). IL-1β also plays a prominent role in promoting tissue pathology and inflammatory responses in periodontal lesions and stimulating the loss of connective tissue and bone (Chiang *et al.*, 1999).

High-mobility group box 1 (HMGB1) is normally associated with chromatin but mediates the response to injury, infection and inflammation when secreted into the cytosol (Lotze and Tracey, 2005; Lu *et al.*, 2012). In the extracellular space, it has been proposed that HMGB1 behaves as a DAMP (Said-Sadier and Ojcius, 2012). Moreover, the secretion of HMGB1 from the nucleus to the extracellular space during inflammation and infection is thought to require the inflammasome and caspase-1 activation (Qin *et al.*, 2006; Willingham *et al.*, 2009; Lamkanfi *et al.*, 2010; Andersson and Tracey, 2011). Similarly to HMGB1, it has recently been shown that the protein ASC (apoptosis-associated speck-like protein containing a carboxy-terminal CARD), which functions as an adaptor in assembly of the NLPR3 inflammasome, can be secreted from macrophages during inflammasome activation and can function as a DAMP (Baroja-Mazo *et al.*, 2014; Franklin *et al.*, 2014).

This study aims to determine whether *F. nucleatum* infection can activate the NLRP3 inflammasome in GECs, which represents the first barrier to infection in the oral cavity. Additionally, we examined potential mechanisms that could lead to NLRP3 inflammasome and evaluated whether inflammasome activation in GECs could be amplified further through secretion of additional danger signals, which has not been previously examined in GECs.

Results

F. nucleatum *infection induces caspase-1 activation and NF-κB translocation*

F. nucleatum infection of GECs was confirmed by immunofluorescence imaging, which showed intracellular *F. nucleatum* aggregation at 1 h after the start of infection (Fig. 1). Despite the *F. nucleatum* infection at an MOI of 100, GECs remained healthy and showed no significant cell death at 8 h post-infection. Cell viability assays via TB staining also showed normal cell morphology (data not shown) and no significant cell death after 0, 2, 4, 6 and 8 h in Opti-MEM media (Fig. 1).

To assess host cell responses to *F. nucleatum* infection, supernatants from *F. nucleatum*-infected cells were collected and caspase-1 activation was measured by Western blot at different infection time points and MOIs. The level of caspase-1 secretion (a reflection of caspase-1

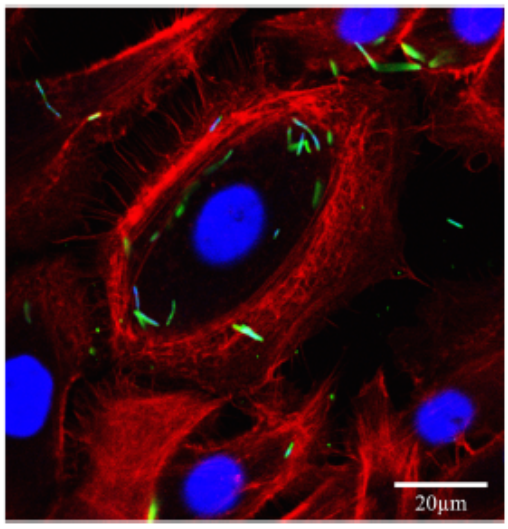

Fig. 1. Intracellular localization of *Fusobacterium nucleatum* in GECs. Immunofluorescence confocal micrograph GECs infected with *F. nucleatum* (MOI of 100) for 1 h. The single optical section through the middle of the host cell confirms the intracellular localization of the bacteria. Fixed GECs were stained with phalloidin–tetramethylrhodamine B isothiocyanate (red) to show actin filaments, and anti-*F. nucleatum* antibody (green). Bar represents 20 μm.

activation) measured by Western blot showed a significant increase as a function of the MOI, being highest at an MOI of 100 (Fig. 2A). Furthermore, caspase-1 activation was observed within 2 h of infection and was significant after 6 h of infection, compared with control samples (Fig. 2B).

NF-κB confocal microscopy was used to visualize NF-κB translocation to the nucleus in uninfected and *F. nucleatum*-infected cells, which reflects NF-κB activation in the cells. A high level of NF-κB translocation was in fact observed when cells were infected at an MOI of 100 for 1 h (Fig. 3A). The time-course of nuclear translocation was followed by acquiring immunofluorescence images after 30 min, 1 and 2 h of infection (Fig. 2). Analysis of the images showed that was a significant increase in NF-κB staining in the nucleus in GECs infected with *F. nucleatum* at an MOI of 100 for 30 min, with highest levels of NF-κB activation observed after 1 h of infection and decreasing afterwards (Fig. 3B). NF-κB activation after 6 h of infection remained above basal levels (Fig. 3B).

F. nucleatum *infection leads to IL-1β gene expression and IL-1β protein secretion, in the absence of exogenous danger signal*

We examined whether inflammasomes may play a role during *F. nucleatum* infection by measuring IL-1β processing and secretion in collected supernatants from *F. nucleatum*-infected GECs with different MOI and times of infection by Western blot. As expected, *F. nucleatum* infection induced IL-1β secretion as a function of the MOI, with the highest levels observed at an MOI of 100 (Fig. 4A). Furthermore, IL-1β secretion was measurable at 4 h and was most intense at 8 h post-infection (Fig. 4B). As a confirmation of the Western blot analysis, ELISA was used to measure the time-course of IL-1β secretion after 2, 4 and 8 h of infection (Fig. 4C). A significantly high level of IL-1β secretion was detected by 4 h post-infection and became dramatically higher by 8 h post-infection (Fig. 4C).

Gene expression of *IL1B* was measured by qPCR, RT-PCR, showing a high level of *IL1B* gene expression at 1 h and 2 h post-infection (Fig. 4D), which, as expected, preceded the secretion of IL-1β protein (Fig. 4B). The *IL1B* gene expression level decreased after 2 h of infection and remained at a plateau above basal levels after 4 h of infection (Fig. 4D). The results are therefore consistent with the interpretation that NF-κB activation, which is maximal at 1 h post-infection (Fig. 3B), precedes *IL1B* gene expression, which in turn results in pro-IL-1β protein synthesis.

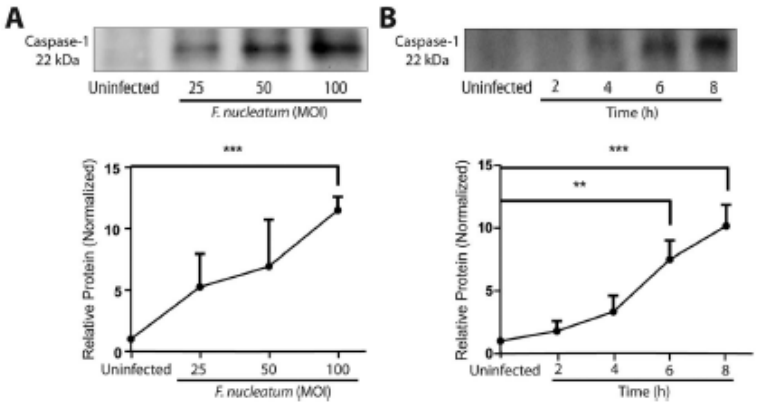

Fig. 2. *F. nucleatum* infection activates caspase-1 in GECs Western blot analysis of supernatants from GECs infected with *F. nucleatum*
A. at MOI of 25, 50 and 100 for 8 h or B. MOI of 100 for 2, 4, 6 or 8 h. Caspase-1 (22 kDa) activation was detected by Western blot, showing the small (22 kDa) fragment of activated caspase-1 in the supernatant. Uninfected samples were collected and processed after 8 h incubation. Results represent an average of three independent experiments, quantified by densitometry. Error bars represent mean ± standard deviations (SD). Asterisks designate statistically significant differences compared with control (** $p < 0.01$ and *** $p < 0.001$, Student's *t*-test).

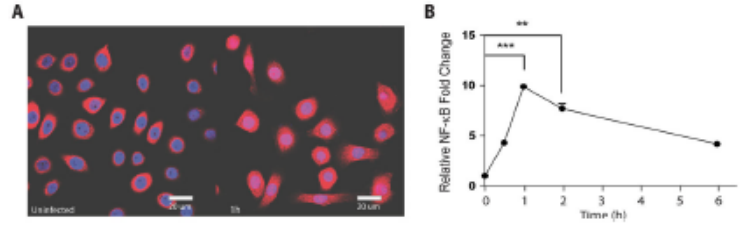

Fig. 3. NF-κB translocation to the nucleus during *F. nucleatum* infection. Cells infected with *F. nucleatum* (MOI of 100) were analysed by confocal microscopy at multiple time points.
A. Image shows cells at 1 h post-infection stained with anti-NF-κB antibodies (red) and DAPI (blue) to visualize the nucleus.
B. Quantification of NF-κB because of fluorescence intensity of staining relative to control at 30 min, 1, 2 and 6 h. Uninfected controls were collected at after 6 h of incubation. Data are representative of two independent experiments ran in duplicates with at least 100 cells counted per time point. Bar represents 20 μm. Asterisks designate statistically significant difference compared with control (**$p < 0.01$ and ***$p < 0.001$, Student's *t*-test).

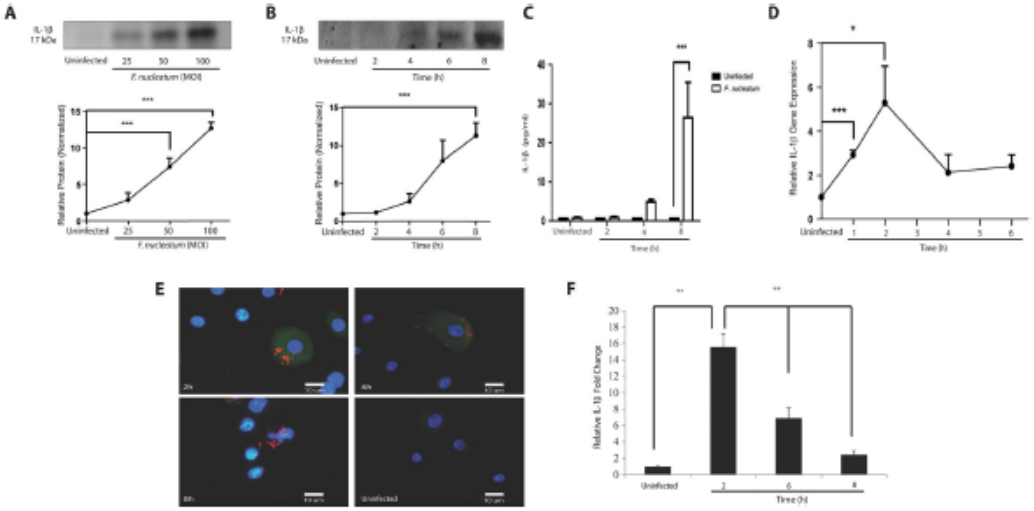

Fig. 4. *F. nucleatum* infection stimulates *IL1B* gene transcription and processing of IL-1β in GECs. Secretion of IL-1β (17 kDa) was measured in cell supernatants by SDS-PAGE Western blot assay. GECs were infected with *F. nucleatum*
A. at an MOI of 25, 50 and 100 for 8 h, or
B. at an MOI of 100 for 2, 4, 6 and 8 h. Western blots were quantified by densitometry.
C. IL-1β protein secretion in GECs was confirmed by ELISA after 2, 4 and 8 h of *F. nucleatum* infection.
D. Relative IL-1β mRNA expression compared with control was evaluated by real-time PCR of GECs infected with *F. nucleatum* (MOI of 100) for 1, 2, 4 and 6 h.
E. Immunofluorescence staining images to evaluate IL-1β protein expression during *F. nucleatum* infection (MOI of 100) for 2, 6 and 8 h. Immunofluorescence intensity levels were measured using NIH-ImageJ and the values of at least 2 standard deviations above the average intensity values of the control group were considered significant. GECs were stained with FITC-conjugated antibody against IL-1β and the nuclear stain DAPI, as indicated in the Materials and methods section. Bar represents 10 μm.
F. Quantification of immunofluorescence intensity measured relative to controls at 2, 6 and 8 h. Results represent an average of three independent experiments performed in duplicates. Error bars represent the mean ± SD. Asterisks designate statistically significant difference compared with control (*$p < 0.05$, **$p < 0.01$ and ***$p < 0.001$, Student's *t*-test).

IL-1β protein secretion requires cleavage of pro-IL-1β by caspase-1, which is activated within 2 h of infection (Fig. 2B). We therefore used immunofluorescence staining to examine the time course for pro-IL-1β accumulation in *F. nucleatum*-infected primary GECs. The results showed a high level of pro-IL-1β accumulation within

F. nucleatum infected GECs at 2 h post-infection, which subsequently dropped by approximately half at 6 h post-infection and continued decreasing at 8 h post-infection (Fig. 4E and 4F). These results are consistent with the appearance of mature, processed IL-1β in the supernatant after 4 h of infection (Fig. 4B). Pro-IL-1β levels in cell lysates were measured using Western blot analysis, showing that pro-IL-1β accumulation starts at 4 h post-infection and reaches a plateau at 6 h and 8 h, which is presumably because of IL-1β secretion (Fig. 3).

Together, the different assays confirmed that NF-κB is activated by *F. nucleatum* infection of GECs, which causes expression of *IL1B* and subsequent production of pro-IL-1β protein. Activation of caspase-1 within 2 h of infection is consistent with secretion of IL-1β protein after 4 h of infection. Finally, these results demonstrate that *F. nucleatum* infection, on its own, is sufficient to provide the PAMPs needed for NF-κB activation and the danger or stress signal required for caspase-1 activation.

F. nucleatum *infection stimulates secretion of the danger signals ASC and HMGB1*

The adapter protein ASC is involved in most cases of NLRP3 inflammasome activation in response to different stimuli (Tschopp and Schroder, 2010; Gomes *et al.*, 2013; Lamkanfi and Dixit, 2014). Furthermore, recent studies showed that ASC can be secreted by cells into the extracellular medium, where ASC can behave as a danger signal (Baroja-Mazo *et al.*, 2014; Franklin *et al.*, 2014). Western blot analysis of supernatant was therefore used to measure the time-course of ASC secretion from *F. nucleatum*-infected GECs. The highest level of ASC secretion was observed at an MOI of 100, with the secretion reaching a plateau by an MOI of 50 (Fig. 5A). Little ASC secretion was observed after 2 h of infection, but high levels were measured after 4 h of infection, reaching a plateau by 6 h of infection with an MOI of 100 (Fig. 5B), suggesting that inflammasome and caspase-1 activation take place before or at the same time as ASC secretion.

Inflammasome activation has previously been shown to stimulate release of HMGB1 by some cells (Lu *et al.*, 2012). Furthermore, the enzymatic activity of caspase-1 is required for the secretion of HMGB1 and other proteins (Vande Walle *et al.*, 2011). In the extracellular medium, HMGB1 can act as a danger signal and promote innate immune responses (Qin *et al.*, 2006; Vande Walle *et al.*, 2011). We therefore measured HMGB1 localization in infected GECs by immunofluorescence and the HMGB1 secretion from GECs by Western blot analysis of

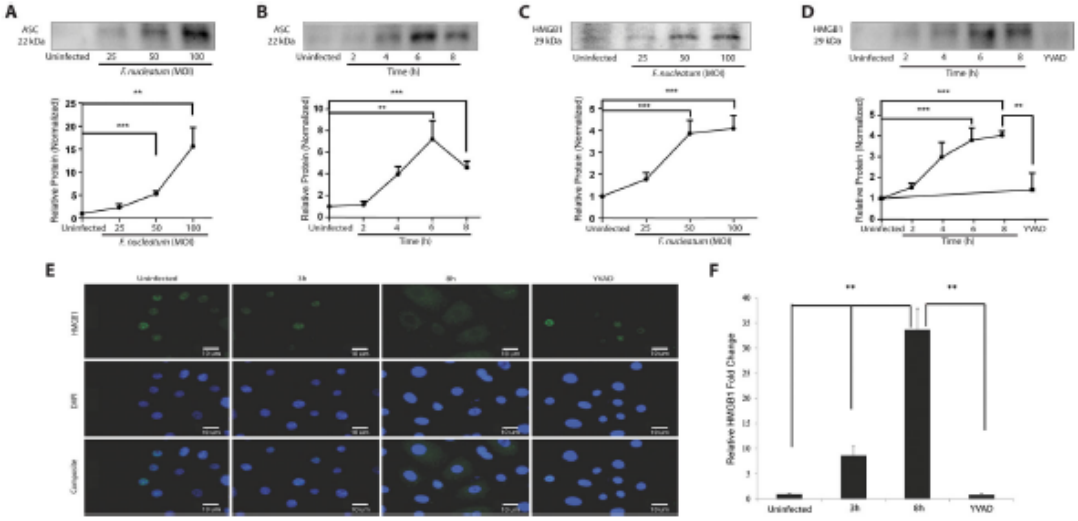

Fig. 5. ASC and HMGB1 release following *F. nucleatum* infection. Release of ASC protein (22 kDa) in cell supernatants was detected using Western blot assay. *F. nucleatum* infected GECs were infected

A. at MOI of 25, 50 and 100 for 8 h, and

B. at MOI of 100 for 2, 4, 6, and 8 h. HMGB1 protein (29 kDa) was measured using Western blot of supernatant from cells infected with *F. nucleatum*

C. at an MOI of 25, 50 and 100 for 8 h an

D. at MOI 100 for 2, 4, 6 and 8 h, or for 8 h in GECs pretreated with 50 mM z-YVAD-fmk for 30 min prior to infection. Western blots were quantified by densitometry.

E. Immunofluorescence images of HMGB1 were captured at 3 and 8 h for infected cells (MOI of 100). Bar represents 10 μm.

F. Quantification of immunofluorescence measured relative to control at 3 and 8 h with or without z-YVAD-fmk pretreatment. Results represent an average of three independent experiments performed in duplicates. Error bars represent the mean ± SD. Asterisks designate statistically significant difference compared with control (**$p < 0.01$, ***$p < 0.001$, Student's *t*-test).

supernatants of GECs, with and without pre-treatment of GECs with the caspase-1 inhibitor, z-YVAD-fmk. Western blot analysis revealed significant levels of HMGB1 release at an MOI of 25, with highest levels and a plateau at an MOI of 50 (Fig. 5C). The time-course of HMGB1 release was also similar to the time course of ASC release, with high levels of HMGB1 release observed after 4 h of infection and a plateau being reached by 6 h of infection (Fig. 5D). Little HMGB1 was found in the supernatant after 8 h of infection if the GECs were pretreated with the caspase-1 inhibitor, z-YVAD-fmk (Fig. 5D), implying that caspase-1 activation is required for HMGB1 secretion.

Redistribution of HMGB1 within GECs was also visualized by immunofluorescence staining, which showed that almost all of the HMGB1 was localized within the nucleus after 3h of infection, but a high level of cytosolic staining was observed after 8 h of infection (Fig. 5E and 5F), suggesting that *F. nucleatum* infection leads to release of HMGB1 from the nucleus to the cytosol. In addition, treatment with the caspase-1 inhibitor, z-YVAD-fmk, decreased almost completely the redistribution of HMGB1 from the nucleus to the cytosol (Fig. 5E and 5F), confirming that caspase-1 is required for release of HMGB1 from the nucleus to the cytosol. The time-course of HMGB1 distribution within the cell was similar to the time-course of release of HMGB1 to the extracellular space (Fig. 5D), consistent with redistribution to the cytosol taking place before or at the same time as secretion from the cell.

The NLRP3 inflammasome is required for caspase-1 activation and IL-1β secretion during F. nucleatum *infection*

Four main types of inflammasomes have been characterized to date, relying on NLRP1, NLRP3, NLRC4 and AIM2 (Tschopp and Schroder, 2010; Said-Sadier and Ojcius, 2012; Lamkanfi and Dixit, 2014). To characterize the importance of NLRP3 in inflammasome activation, we prepared NLRP3-deficient GECs using an RNAi approach with lentiviral particles and evaluated caspase-1 activation and IL-1β secretion after 8 h of infection with *F. nucleatum*. The efficiency of NLRP3 (117 kDa) depletion was first verified by Western blot, which confirmed that NLRP3 protein levels were decreased with an efficiency of 49% in these cells (Fig. 4). As expected, *F. nucleatum*-infected NLRP3-deficient cells showed significantly lower caspase-1 activation in comparison with infected control cells (Fig. 6A). Similarly, there was a significant reduction of IL-1β secretion from NLRP3-depleted cells compared with control cells after 8 h of infection (Fig. 6B). These results imply that the NLRP3 inflammasome is involved in caspase-1 activation and IL-1β secretion during *F. nucleatum* infection of GECs.

Discussion

Periodontal diseases are induced by a complex interaction of periodontal bacteria, composed mainly of gram-negative anaerobes (Han *et al.*, 2000). *F. nucleatum* is one of the first species to become established in plaque biofilms and is distinguished from other oral pathogens because of its highly invasive ability (Han *et al.*, 2000). A recent *in vivo* study found that chronic oral infection is tightly linked with *F. nucleatum* colonization, inducing significant antibody responses along with alveolar bone resorption and intrabony defects (Saini *et al.*, 2009; Velsko *et al.*, 2015). Furthermore, *F. nucleatum* has recently been shown to directly contribute to inflammation of colonic epithelium cells and increase the risk of inflammatory bowel disease, resulting in colorectal tumorigenesis (Strauss *et al.*, 2011; Bashir *et al.*, 2015) and to colonize the mouse placenta and induce placental inflammatory responses (Liu *et al.*, 2007). Given the ability of *F. nucleatum* to induce inflammation, we hypothesized that *F. nucleatum* might also have the ability to activate an

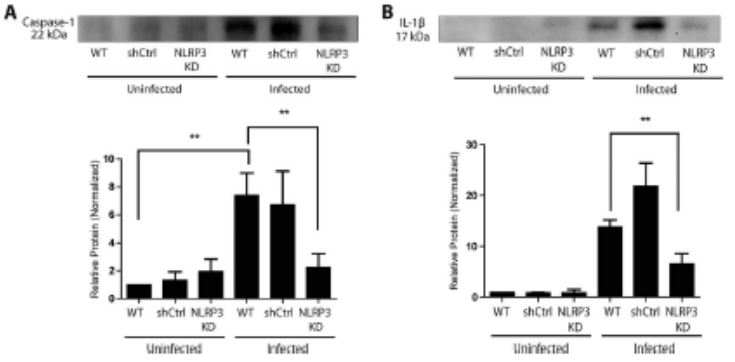

Fig. 6. Depletion of NLRP3 inhibits caspase-1 activation and IL-1β secretion.
A, B. Wildtype and NLRP3-depleted (knockdown, KD) GECs were infected with *F. nucleatum* (MOI of 100) for 8 h. Supernatants were collected and analyzed by Western blot assay for A. caspase-1 activation and B. IL-1β secretion. Results represent three independent experiments. Error bars represent the mean + SD. Asterisks designate statistically significant difference compared with control (** $p < 0.01$).

NLRP3 inflammasome, which can detect different types of cellular stress or damage.

Infection by many types of intracellular bacteria stimulates synthesis of pro-IL-1β, but not its secretion (Tschopp and Schroder, 2010; Said-Sadier and Ojcius, 2012; Lamkanfi and Dixit, 2014). As described for GECs or macrophages infected by *P. gingivalis* (Yilmaz *et al.*, 2010; Taxman *et al.*, 2012), a second signal, due often to a danger signal such as extracellular ATP, activates an inflammasome and caspase-1, which results in processing and secretion of the mature IL-1β protein (Tschopp and Schroder, 2010; Lamkanfi and Dixit, 2014). In the case of *F. nucleatum* infection, we found, instead, that infection can both stimulate expression of the *IL1B* gene and secretion of mature IL-1β protein, implying that *F. nucleatum* infection provides both PAMPs and a danger signal. These results are consistent with a recent report that *F. nucleatum* infection of bone marrow derived macrophages from mice leads to caspase-1 activation and IL-1β secretion (Taxman *et al.*, 2012); although the effect of infection in a physiologically relevant host cell has not been examined.

In our studies, we found that *F. nucleatum* infection in GECs led to early NF-κB activation and translocation into the nucleus, which stimulated expression of *IL1B* and the appearance of intracellular pro-IL-1β. Activation of caspase-1 then led to secretion of IL-1β from the infected cells, through a mechanism requiring the presence of the NLRP3 inflammasome.

Soon after caspase-1 was activated in the infected cells, the danger signal HMGB1 was redistributed from the nucleus to the cytosol, and was secreted to the extracellular space (Fig. 5). HMGB1 is the second most abundant protein in chromatin and is associated with DNA in healthy cells (Lotze and Tracey, 2005) and can be released from damaged cells and is secreted actively by some immune cells (Lamkanfi *et al.*, 2010). In the extracellular medium, HMGB1 can interact with innate immune receptors such as RAGE and toll-like receptors (Sims *et al.*, 2010; Yang *et al.*, 2013; Tsung *et al.*, 2014). It has recently been shown that the NLRP3 inflammasome can promote secretion of HMGB1, and we find that caspase-1 was required for HMGB1 release from the nucleus in *F. nucleatum*-infected GECs.

Similarly, the adaptor protein ASC is involved in NLRP3 inflammasome activation, but recent studies have demonstrated that it can also be secreted from cells during inflammasome activation (Baroja-Mazo *et al.*, 2014; Franklin *et al.*, 2014). In the extracellular space, ASC can amplify inflammatory responses by behaving as a danger signal. We find that infection of cells with *F. nucleatum* also leads to secretion of ASC. We therefore propose that *F. nucleatum* infection by itself is detected by GECs as a danger signal and that caspase-1 dependent secretion of HMGB1 and ASC participate in an auto-amplification loop in order to further enhance inflammation (Fig. 7).

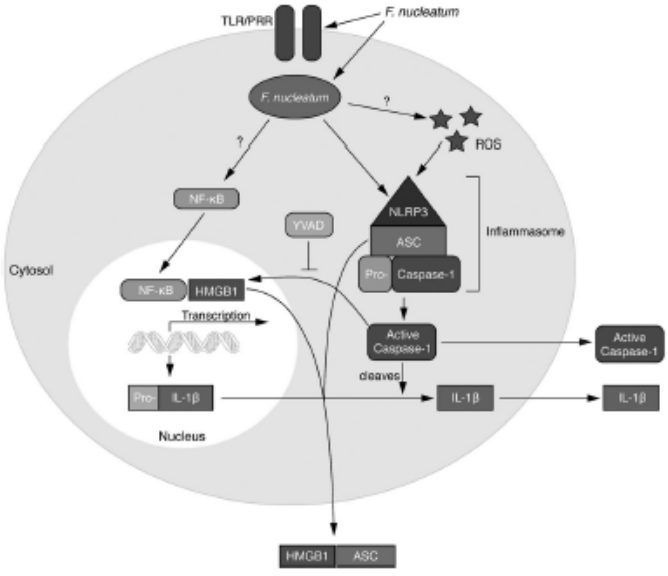

Fig. 7. Model of pro-inflammatory cytokine expression and the inflammasome activation cascade during *F. nucleatum* infection *F. nucleatum* infection activates NF-κB, which translocates to the nucleus, where it stimulates expression of pro-inflammatory genes, including genes encoding pro-IL-1β. In addition, infection activates the NLRP3 inflammasome, which in turns activates caspase-1, resulting in processing and release of IL-1β. Inflammation is magnified further by release of the danger signal ASC, and caspase-1 secretion of HMGB1.

Experimental procedures

Bacterial culture

Fusobacterium nucleatum (ATCC 25586) was cultured under anaerobic condition at 37°C for 24 h in brain–heart infusion broth supplemented with yeast extract (5 mg ml^{-1}), hemin (5 μg ml^{-1}) and menadione (1 mg ml^{-1}). Erythromycin (5 mg ml^{-1}) was added to the media as a selective agent for growth, which was previously described (Zaborina *et al.*, 1999). Bacteria were harvested by centrifugation at 6000 × g for 10 min at 4°C. The bacterial pellets were washed twice and resuspended with Dulbecco's phosphate-buffered saline (PBS) containing calcium and magnesium (Life Technologies). Bacteria were quantified using a Klett-Summerson photoelectric colorimeter.

Primary and immortalized GECs

Healthy gingival tissue was obtained from healthy human subjects by oral surgery to produce primary GEC cultures as previously described (Yilmaz *et al.*, 2004). With the consent of patients, gingival epithelial tissues were collected under the approval of the Institution Review Board of the University of Florida. GECs were cultured as monolayers in serum-free keratinocyte growth medium (Lonza) at 37°C in a 5% CO2 incubator. The human immortalized GEC cell line was obtained as previously described (Oda *et al.*, 1996) and grown in defined keratinocyte serum-free media (Life Technologies) at 37°C in a 5% CO2 incubator. Prior to *F. nucleatum* infection, media was changed to Opti-MEM media (Life Technologies).

Cell viability assay

To measure cell viability of GECs after incubation in Opti-MEM media for 0, 2, 4, 6 and 8 h, we used trypan blue (TB) exclusion staining. GECs were collected at the indicated time points and resuspended with 1× PBS and 0.4% TB solution (Thermo Fisher Scientific) with a 1:1 ratio and mixed thoroughly. The resuspended mixture was then loaded onto a hemocytometer and counted under a light microscope after 5 min of incubation. Approximately 250 cells were counted using cell counter for each time point in duplicate.

Production of NLRP3-deficient GECs

The plasmids pMD.G, pCMVdelR8.91 and pLKO-shNLRP3 (Clone ID: TRCN0000431574) were purchased from National RNAi Core Facility at Academia Sinica of Taiwan. The plasmids pMD.G and pCMVdelR8.91 were used for the packaging of lentiviral particles as described (Huang *et al.*, 2015). The shRNA sequence for NLRP3 was 5′-GAGACTCAGGAGTCGCAATTT-3′. The shRNA sequence 5′-TTGGCAACCGCTTTTTG-3′, which targets firefly luciferase mRNA, was used as the control.

Lentiviral particles were generated as described (Huang *et al.*, 2015). HEK293T cells were cotransfected with lentiviral plasmid (pLKO-shNLRP3) and packaging plasmids (pMD.G and pCMVdelR8.91) by Arrest-In (Open Biosystems) according to manufacturer's instructions. After 16 h of transfection, media containing the transfection reagents were removed and replenished with fresh media. After incubating for another 48 h, the media containing viral particles were centrifuged a 6000× g for 5 min at 4°C, and the supernatants were collected for the infection studies. Infection of cells with lentiviral particles was carried out at 37°C in the presence of polybrene at 8 μg ml^{-1}. Cells that stably express shRNA were obtained by culturing the infected cells in the presence of puromycin at 0.6 μg ml^{-1} for 2 weeks. Prior to *F. nucleatum* infection, media was changed to Opti-MEM media.

Infection of GECs with F. nucleatum

Primary and immortalized GECs were seeded on 6-well plates and grown until 75–80% confluence prior to bacterial infection or the indicated treatments. Cells were infected at a multiplicity of infection (MOI) of 25, 50, or 100. Prior to *F. nucleatum* infection, cells were treated with the inhibitors and incubated in a 5% CO2 incubator at 37°C. Fifty micromolar of caspase-1 inhibitor, YVAD (R&D Systems), was added for at least 15 min before infection (Cruz *et al.*, 2007; Chen *et al.*, 2012; Hung *et al.*, 2013). Supernatant was collected at various time points for experiments described in the succeeding texts.

Western blot

Supernatant sample preparation. An equal number of cells were seeded per sample in order to ensure equal sample loading for all supernatants analysed by Western blot. Thus, 750 000 cells per well were seeded when using 6-well plates, or they were seeded to 75–80% confluence in cell-culture flasks. Proteins from cell-free culture supernatants were concentrated using trichloroacetic acid (TCA) (Koontz, 2014). One hundred percent TCA was added to supernatants for a final concentration of 20%. Samples were vortexed and incubated on ice for 30 min. After incubation, samples were centrifuged at 800 × g and supernatants were discarded. The pellets were washed twice with 100% cold acetone and allowed to air-dry. Pellets were resuspended with Pierce Lane Marker Reducing Sample Buffer (Thermo Scientific) and boiled at 95°C for 5 min. Samples were loaded and run on SDS-PAGE gels and transferred onto PVDF membranes. Membranes were blocked with 5% BSA for 1 h at RT, and then incubated with anti-TMS1 (Abcam), caspase-1 (Nathan), IL-1β (Abcam), anti-NLRP3 (Cell Signaling) or HMGB1 (Nathan) primary antibodies overnight at 4°C. After primary incubation, blots were washed and incubated with secondary goat anti-rabbit HRP (Millipore) for another hour. Finally, membranes were washed and exposed to Luminata Forte (Millipore) substrate. Images

were acquired using ChemiDoc XRS+ system and analysed using NIH-ImageJ.

Cell lysate sample preparation. After removing supernatant, cells were washed once with 1X PBS (Dulbecco's). M-PER Mammalian Protein Extract Reagent (Thermo Scientific) was added for 15 min to lyse cells and extract proteins from each sample. The protein concentration of the lysates was determined using Quick Start Bradford Assay (Bio-Rad) according to manufacturer's instructions. Samples were resuspended with water and Pierce Lane Marker Reducing Sample Buffer and boiled at 95°C for 5 min. Samples were run and analysed as described in the preceding texts. After revealing the Western blot for experimental protein, the membranes were stripped using stripping buffer (Thermo Scientific) for 5 min and reprobed with GAPDH antibodies (Cell Signaling), which also confirmed equal loading of protein for the different lanes of the blot.

Measurement of IL-1β secretion by ELISA

GECs were seeded in 12-well plates and cultured until 75–80% confluence. The cells were then infected with *F. nucleatum* at an MOI of 100. Supernatants were collected at various time points and centrifuged at 800 × *g* for 5 min to remove cellular debris. Cell-free supernatants were used to test for IL-1β by ELISA assay. Human IL-1β was tested by ELISA (eBioscience) according to the manufacturer's instructions.

RNA isolation, reverse transcription and quantitative PCR

Total RNA was isolated from GECs using TRIzol according to the manufacturer's protocol (Invitrogen, Life Technologies). Taqman Reverse Transcription Reagents kit (Applied Biosystem) was used to amplify cDNA from 2 μg RNA. Real-time PCR RT-PCR and quantitative PCR (qPCR) were performed using 1/50 of the prepared cDNA with Mx3000P (Stratagene) and 25 μl of Brilliant QPCR Master Mix (Stratagene). Amplification of cDNA was performed with the addition of sense and antisense primers at 200 nM concentration. Quantitative PCR was conducted at 95°C for 10 min, followed by 40 cycles at 95°C for 30 s, 55°C for 1 min and 72°C for 30 s. The IL-1β gene expression was normalized to GAPDH as instructed by the manufacturer (Stratagene) through comparative cycle threshold method as loading control. The following primers were used for IL-1β: 5′- AAATACCTGTGGCCTTGGGC -3′ and 5′- TTTGGGATCTACACTCTCCAGCT-3′. The primers used for GAPDH are 5′-TTAAAAGCAGCCCTGGTGAC-3′ and 5′-CTCTGCTCCTCCTGTTCGAC-3′.

Immunofluorescence microscopy

F. nucleatum-infected GECs were fixed with 4% paraformaldehyde and permeabilized with 0.1% Triton-X for 40 min. The cells were blocked with 2% BSA for 30 min before applying the primary antibody. Rabbit anti-human NF-κB antibody (Cell Signaling) was then added and incubated for 1 h followed by three washes with PBS containing 0.1% Triton-X. Cells were then incubated with goat anti-rabbit IgG antibody conjugated with red fluorescent Alexa Fluor 546 dye (Invitrogen) for 40 min and stained with DAPI (Millipore) for another 10 min. Finally, the cells were observed by wide-field fluorescence microscope (Leica) or laser scanning confocal microscope (Nikon TE-2000).

Immunofluorescence detection of F. nucleatum *infection in GECs*

Primary GECs were cultured in 4-well culture plates (Nunc) containing round glass inserts (Warner Instruments). Cells at approximately 80% confluence were infected with *F. nucleatum* at an MOI of 100 for 1 h. The cells were fixed in 10% neutral buffered formalin and permeabilized with 0.01% Triton X-100 in PBS. *F. nucleatum* infection was detected using a rabbit anti-*F. nucleatum* polyclonal antibody (Pacific Immunology) at 1:100 dilution and secondary Alexa Fluor 488-conjugated goat anti-rabbit antibody (Invitrogen) at 1:1000 dilution. Actin was labelled using phalloidin–tetramethylrhodamine B isothiocyanate (Sigma). The immunostained cells were mounted onto glass slides using Vectashield mounting medium (Fisher) containing DAPI stain and examined using a Leica confocal microscope and LAS AF (Leica) software.

Immunofluorescence examination of intracellular IL-1β and HMGB1

Primary GECs were cultured in 4-well culture plates containing round glass inserts. Cells were infected at a confluence of 70% with *F. nucleatum* at an MOI of 100 for 2, 6 and 8 h (for IL-1β) or for 3 and 8 h (for HMGB1). The effect of caspase-1 on HMGB1 translocation after 8 h *F. nucleatum*-infection was assessed using the caspase-1 inhibitor z-YVAD-fmk at a 50 μM final concentration for 30 min before infection. All cells were washed three times with PBS, fixed with 4% paraformaldehyde for 15 min and permeabilized using 0.01% Triton X-100 solution in PBS. IL-1β was detected using a FITC-conjugated mouse monoclonal antibody (R&D Systems). HMGB1 was detected using a rabbit polyclonal anti-human HMGB1 antibody and secondary Alexa Fluor® 488-conjugated goat anti-rabbit antibody (Invitrogen). *F. nucleatum* infection was detected using a rabbit anti-*F. nucleatum* polyclonal antibody (Pacific Immunology) and secondary Alexa Fluor® 594-conjugated goat anti-rabbit antibody (Invitrogen). All inserts were mounted onto glass slides using Vectashield mounting medium (Fisher) containing DAPI stain and examined using a Zeiss AxioImager fluorescence microscope connected to a cooled charge-coupled camera controlled by QCAPTURE software

(Surrey). The intensity densities of cytoplasmic IL-1β and HMGB1 staining were measured using NIH-ImageJ. Intensity values at least 2 standard deviations above average were considered significant. Results indicate the average of measurements of at least 25 cells, originating from at least three separate replicate experiments.

Statistical analysis

Data are presented as mean ± standard deviation (SD). Standard *t*-tests were used to determine the statistical significance between groups, with P values < 0.05 considered as statistically significant.

Acknowledgements

This study was supported by intramural funds from the University of the Pacific, NIH/NIDCR grants R01DE019444, R01DE016593 and T90DE021990, and the Fundação de Amparo à Pesquisa do Estado do Rio de Janeiro. We also would like to thank Dr. Nestor Oviedo (UC Merced) for technical support.

References

Andersson, U., and Tracey, K.J. (2011) HMGB1 is a therapeutic target for sterile inflammation and infection. *Annu Rev Immunol* **29**: 139–162.

Atanasova, K.R., and Yilmaz, O. (2015) Prelude to oral microbes and chronic diseases: past, present and future. *Microbes Infect* **17**: 369–377.

Baroja-Mazo, A., Martin-Sanchez, F., Gomez, A.I., Martinez, C.M., Amores-Iniesta, J., Compan, V., *et al.* (2014) The NLRP3 inflammasome is released as a particulate danger signal that amplifies the inflammatory response. *Nat Immunol* **15**: 738–748.

Bartold, P.M., Gully, N.J., Zilm, P.S., and Rogers, A.H. (1991) Identification of components in Fusobacterium nucleatum chemostat-culture supernatants that are potent inhibitors of human gingival fibroblast proliferation. *J Periodontal Res* **26**: 314–322.

Bashir, A., Miskeen, A.Y., Bhat, A., Fazili, K.M., and Ganai, B.A. (2015) Fusobacterium nucleatum: an emerging bug in colorectal tumorigenesis. *Eur J Cancer Prev* **24**: 373–385.

Cassel, S.L., Joly, S., and Sutterwala, F.S. (2009) The NLRP3 inflammasome: a sensor of immune danger signals. *Semin Immunol* **21**: 194–198.

Chen, C.C., Tsai, S.H., Lu, C.C., Hu, S.T., Wu, T.S., Huang, T.T., *et al.* (2012) Activation of an NLRP3 inflammasome restricts Mycobacterium kansasii infection. *PLoS One* **7**: e36292.

Chiang, C.Y., Kyritsis, G., Graves, D.T., and Amar, S. (1999) Interleukin-1 and tumor necrosis factor activities partially account for calvarial bone resorption induced by local injection of lipopolysaccharide. *Infect Immun* **67**: 4231–4236.

Cruz, C.M., Rinna, A., Forman, H.J., Ventura, A.L., Persechini, P.M., and Ojcius, D.M. (2007) ATP activates a reactive oxygen species-dependent oxidative stress response and secretion of proinflammatory cytokines in macrophages. *J Biol Chem* **282**: 2871–2879.

Dommisch, H., Chung, W.O., Rohani, M.G., Williams, D., Rangarajan, M., Curtis, M.A., and Dale, B.A. (2007) Protease-activated receptor 2 mediates human beta-defensin 2 and CC chemokine ligand 20 mRNA expression in response to proteases secreted by *Porphyromonas gingivalis*. *Infect Immun* **75**: 4326–4333.

Franklin, B.S., Bossaller, L., De Nardo, D., Ratter, J.M., Stutz, A., Engels, G., *et al.* (2014) The adaptor ASC has extracellular and 'prionoid' activities that propagate inflammation. *Nat Immunol* **15**: 727–737.

Gomes, M.T., Campos, P.C., Oliveira, F.S., Corsetti, P.P., Bortoluci, K.R., Cunha, L.D., *et al.* (2013) Critical role of ASC inflammasomes and bacterial type IV secretion system in caspase-1 activation and host innate resistance to Brucella abortus infection. *J Immunol* **190**: 3629–3638.

Han, Y.W., Shi, W., Huang, G.T., Kinder Haake, S., Park, N.H., Kuramitsu, H., and Genco, R.J. (2000) Interactions between periodontal bacteria and human oral epithelial cells: Fusobacterium nucleatum adheres to and invades epithelial cells. *Infect Immun* **68**: 3140–3146.

Harijith, A., Ebenezer, D.L., and Natarajan, V. (2014) Reactive oxygen species at the crossroads of inflammasome and inflammation. *Frontiers in physiology* **5**: 352.

Hodge, P., and Michalowicz, B. (2001) Genetic predisposition to periodontitis in children and young adults. *Periodontology* **2000**(26): 113–134.

Huang, P.R., Hung, S.C., Pao, C.C., and Wang, T.C. (2015) N-(1-pyrenyl) maleimide induces bak oligomerization and mitochondrial dysfunction in jurkat cells. *Biomed Res Int* **2015**: 798489.

Hung, S.C., Choi, C.H., Said-Sadier, N., Johnson, L., Atanasova, K.R., Sellami, H., *et al.* (2013) P2X4 assembles with P2X7 and pannexin-1 in gingival epithelial cells and modulates ATP-induced reactive oxygen species production and inflammasome activation. *PLoS One* **8**: e70210.

Janeway, C.A., Jr., and Medzhitov, R. (2002) Innate immune recognition. *Annu Rev Immunol* **20**: 197–216.

Jeng, J.H., Chan, C.P., Ho, Y.S., Lan, W.H., Hsieh, C.C., and Chang, M.C. (1999) Effects of butyrate and propionate on the adhesion, growth, cell cycle kinetics, and protein synthesis of cultured human gingival fibroblasts. *J Periodontol* **70**: 1435–1442.

Ji, S., Shin, J.E., Kim, Y.S., Oh, J.E., Min, B.M., and Choi, Y. (2009) Toll-like receptor 2 and NALP2 mediate induction of human beta-defensins by fusobacterium nucleatum in gingival epithelial cells. *Infect Immun* **77**: 1044–1052.

Johnson, L., Atanasova, K.R., Bui, P.Q., Lee, J., Hung, S.C., Yilmaz, O., and Ojcius, D.M. (2015) *Porphyromonas gingivalis* attenuates ATP-mediated inflammasome activation and HMGB1 release through expression of a nucleoside-diphosphate kinase. *Microbes Infect* **17**: 369–377.

Kim, J.J., and Jo, E.K. (2013) NLRP3 inflammasome and host protection against bacterial infection. *J Korean Med Sci* **28**: 1415–1423.

Koontz, L. (2014) TCA precipitation. *Methods Enzymol* **541**: 3–10.

Lamkanfi, M., and Dixit, V.M. (2014) Mechanisms and functions of inflammasomes. *Cell* **157**: 1013–1022.

Lamkanfi, M., Sarkar, A., Vande Walle, L., Vitari, A.C., Amer, A.O., Wewers, M.D., *et al.* (2010) Inflammasome-dependent release of the alarmin HMGB1 in endotoxemia. *J Immunol* **185**: 4385–4392.

Lee, H.J., Kang, I.K., Chung, C.P., and Choi, S.M. (1995) The subgingival microflora and gingival crevicular fluid cytokines in refractory periodontitis. *J Clin Periodontol* **22**: 885–890.

Liu, H., Redline, R.W., and Han, Y.W. (2007) Fusobacterium nucleatum induces fetal death in mice via stimulation of TLR4-mediated placental inflammatory response. *J Immunol* **179**: 2501–2508.

Lotze, M.T., and Tracey, K.J. (2005) High-mobility group box 1 protein (HMGB1): nuclear weapon in the immune arsenal. *Nat Rev Immunol* **5**: 331–342.

Lu, B., Nakamura, T., Inouye, K., Li, J., Tang, Y., Lundback, P., *et al.* (2012) Novel role of PKR in inflammasome activation and HMGB1 release. *Nature* **488**: 670–674.

Oda, D., Bigler, L., Lee, P., and Blanton, R. (1996) HPV immortalization of human oral epithelial cells: a model for carcinogenesis. *Exp Cell Res* **226**: 164–169.

Oliver, R.C., Brown, L.J., and Loe, H. (1998) Periodontal diseases in the United States population. *J Periodontol* **69**: 269–278.

Pihlstrom, B.L., Michalowicz, B.S., and Johnson, N.W. (2005) Periodontal diseases. *Lancet* **366**: 1809–1820.

Pilot, T. (1998) The periodontal disease problem. A comparison between industrialised and developing countries. *Int Dent J* **48**: 221–232.

Qin, S., Wang, H., Yuan, R., Li, H., Ochani, M., Ochani, K., *et al.* (2006) Role of HMGB1 in apoptosis-mediated sepsis lethality. *J Exp Med* **203**: 1637–1642.

Richards, D. (2013) Oral diseases affect some 3.9 billion people. *Evid Based Dent* **14**: 35.

Richards, D. (2014) Review finds that severe periodontitis affects 11% of the world population. *Evid Based Dent* **15**: 70–71.

Said-Sadier, N., and Ojcius, D.M. (2012) Alarmins, inflammasomes and immunity. *Biomed J* **35**: 437–449.

Saini, R., Marawar, P.P., Shete, S., and Saini, S. (2009) Periodontitis, a true infection. *J Glob Infect Dis* **1**: 149–150.

Santana, P., Martel, J., Lai, H.C., Perfettini, J.L., Kanellopoulos, J., Young, J.D., *et al.* (2015) Is the inflammasome relevant for epithelial cell function? *Microbes Infect* (in press).

Signat, B., Roques, C., Poulet, P., and Duffaut, D. (2011) Fusobacterium nucleatum in periodontal health and disease. *Curr Issues Mol Biol* **13**: 25–36.

Sims, G.P., Rowe, D.C., Rietdijk, S.T., Herbst, R., and Coyle, A.J. (2010) HMGB1 and RAGE in inflammation and cancer. *Annu Rev Immunol* **28**: 367–388.

Srinivasula, S.M., Poyet, J.L., Razmara, M., Datta, P., Zhang, Z., and Alnemri, E.S. (2002) The PYRIN-CARD protein ASC is an activating adaptor for caspase-1. *J Biol Chem* **277**: 21119–21122.

Strauss, J., Kaplan, G.G., Beck, P.L., Rioux, K., Panaccione, R., Devinney, R., *et al.* (2011) Invasive potential of gut mucosa-derived Fusobacterium nucleatum positively correlates with IBD status of the host. *Inflamm Bowel Dis* **17**: 1971–1978.

Takeda, K., and Akira, S. (2005) Toll-like receptors in innate immunity. *Int Immunol* **17**: 1–14.

Taxman, D.J., Swanson, K.V., Broglie, P.M., Wen, H., Holley-Guthrie, E., Huang, M.T., *et al.* (2012) *Porphyromonas gingivalis* mediates inflammasome repression in polymicrobial cultures through a novel mechanism involving reduced endocytosis. *J Biol Chem* **287**: 32791–32799.

Tschopp, J., and Schroder, K. (2010) NLRP3 inflammasome activation: The convergence of multiple signalling pathways on ROS production? *Nature reviews. Immunology* **10**: 210–215.

Tsung, A., Tohme, S., and Billiar, T.R. (2014) High-mobility group box-1 in sterile inflammation. *J Intern Med* **276**: 425–443.

Vande Walle, L., Kanneganti, T.D., and Lamkanfi, M. (2011) HMGB1 release by inflammasomes. *Virulence* **2**: 162–165.

Velsko, I.M., Chukkapalli, S.S., Rivera-Kweh, M.F., Chen, H., Zheng, D.H., Bhattacharyya, I., *et al.* (2015) Fusobacterium nucleatum alters atherosclerosis risk factors and enhances inflammatory markers with an atheroprotective immune response in ApoE(null) mice. *Plos One* **10**: e0129795.

Willingham, S.B., Allen, I.C., Bergstralh, D.T., Brickey, W.J., Huang, M.T., Taxman, D.J., *et al.* (2009) NLRP3 (NALP3, Cryopyrin) facilitates in vivo caspase-1 activation, necrosis, and HMGB1 release via inflammasome-dependent and -independent pathways. *J Immunol* **183**: 2008–2015.

Yang, H., Antoine, D.J., Andersson, U., and Tracey, K.J. (2013) The many faces of HMGB1: molecular structure-functional activity in inflammation, apoptosis, and chemotaxis. *J Leukoc Biol* **93**: 865–873.

Yilmaz, O., Jungas, T., Verbeke, P., and Ojcius, D.M. (2004) Activation of the phosphatidylinositol 3-kinase/Akt pathway contributes to survival of primary epithelial cells infected with the periodontal pathogen *Porphyromonas gingivalis*. *Infect Immun* **72**: 3743–3751.

Yilmaz, O., Sater, A.A., Yao, L., Koutouzis, T., Pettengill, M., and Ojcius, D.M. (2010) ATP-dependent activation of an inflammasome in primary gingival epithelial cells infected by *Porphyromonas gingivalis*. *Cell Microbiol* **12**: 188–198.

Yin, L., and Chung, W.O. (2011) Epigenetic regulation of human beta-defensin 2 and CC chemokine ligand 20 expression in gingival epithelial cells in response to oral bacteria. *Mucosal Immunol* **4**: 409–419.

Zaborina, O., Li, X., Cheng, G., Kapatral, V., and Chakrabarty, A.M. (1999) Secretion of ATP-utilizing enzymes, nucleoside diphosphate kinase and ATPase, by Mycobacterium bovis BCG: sequestration of ATP from macrophage P2Z receptors? *Mol Microbiol* **31**: 1333–1343.

Supporting information

Additional Supporting Information may found in the online version of this article at the publisher's web-site:

Fig. S1. Time course of gingival epithelial cell (GEC) viability. GECs were stained with Trypan blue to assess viability with a hemocytometer after incubation in Opti-MEM media for 0, 2, 4, 6 and 8 h. Cell viability data shown represents three independent experiments counted in duplicates, giving similar results. Error bars represent the mean + SD.

Fig. S2. Immunofluorescence of NF-κB translocation time course. Localization of NF-κB in GECs induced by *Fusobacterium nucleatum* (MOI of 100) at 30 min, 1 and 2 h of infection. The images are representative of at least 100 cells from at three separate experiments. Bar represents 100 μm.

Fig. S3. Pro-IL-1β Western blot and loading control Pro-IL-1β protein (31 kDa) was extracted from cell lysates of *F. nucleatum* infected GECs. A time course of 2, 4, 6 and 8 h post-infection was

analysed by Western blot with IL-1β antibodies. Blots were then stripped and probed with GAPDH antibodies as a loading control.

Fig. S4. Western blot confirmation of NLRP3 knockdown efficiency in GECs. Knockdown of NLRP3 expression was confirmed at the level of NLRP3 protein. Western blot analysis showed knockdown efficiency in comparison with controls. Actin was used as a loading control. The data shown represent three independent tests giving similar results.

4.3 *Fusobacterium nucleatum* oral infection recruits macrophages to the dental pulp and induces bone resorption (Manuscript to be submitted for publication)

Larry Johnson[1,2], Christina Maeda Takiya[3], *Cássio* Luiz Coutinho *Almeida*-da-Silva[3], Gustavo, Miranda Rocha[4], Gilberto Weissmüller[4], Julio Scharfstein[3], Robson Coutinho-Silva[3], and David M. Ojcius[1,2]

[1]Department of Biomedical Sciences, University of the Pacific, Arthur Dugoni School of Dentistry, San Francisco, CA 95343, USA

[2]Department of Molecular Cell Biology, University of California, Merced, CA 95343, USA

[3]Immunobiology Program, Instituto de Biofísica Carlos Chagas Filho, Federal University of Rio de Janeiro, Rio de Janeiro 21941-902, Brazil

[4]Structural Biology Program, Instituto de Biofísica Carlos Chagas Filho, Federal University of Rio de Janeiro, Rio de Janeiro 21941-902, Brazil

4.3.1 Introduction

The oral cavity is colonized with hundreds of different species of bacteria to compose the oral microbiome [91, 92]. Some common bacteria found in individuals afflicted with periodontitis include: *Fusobacterium nucleatum, Porphyromonas gingivalis, and Aggregatibacter actinomycetemcomitans* [87, 93]. Gingivitis is diagnosed when the observation of the gingiva, or gums, show signs of swelling, redness, or chronically bleeding [5]. These symptoms of inflammation are associated with infection. However, chronic inflammation can lead to development of periodontitis with signs of deep periodontal pockets, alveolar bone resorption, and tooth loss [94, 95].

The tooth is surrounded with the gingival epithelium protecting against microorganisms. Bacteria can adhere to a tooth and form plaque biofilm. This microenvironment is optimal for growth of anaerobic bacteria and an opportunity for pathogenic bacteria to attach and coaggregate [96]. *F. nucleatum* is one of the predominant bacteria and contributors to biofilm formation [12, 88, 89]. The bacteria utilize adhesion mechanisms of lectin-like and non-lectin-like interactions and adhesion peptides, such as FadA (*Fusobacterium ad*hesin A) for attachment [97-101]. These interactions facilitate coaggregation or infiltration into lymphocytes, polymorphonuclear neutrophils, erythrocytes, epithelial cells, fibroblasts, HeLa cells [12, 57, 97, 99, 102].

The oral epithelium defends against bacteria colonization by secretion of antimicrobial peptides, defensins, [87, 103-105]. β-defensins target bacteria as the peptides are electrostatically attracted to their negative charged membranes and inducing pore formation [87, 103, 106]. The antimicrobial peptides can also recruit other immune cells, neutrophils or T cells, as a chemoattractant [87, 95, 103]. Thus, β-defensins play an active role as part of innate and adaptive response to oral infection.

Gingival epithelial cells (GECs) are also another line of protection from invasive bacteria. They provide more functionality than acting as not only a barrier, but also contributing to immune recognition and response [22, 23]. They express a complexity of receptors to recognition pathogens and respond with release of inflammatory mediators to recruit other immune cells, such as neutrophils and macrophages [24]. When pathogen-associated molecular patterns (PAMPs) of bacteria are recognized by host pathogen recognition receptors (PRRs), such as Toll-like receptors, it activates NF-κB and induces expression of cytokines [27, 37]. Recognition of *F. nucleatum* and *Aggregatibacter actinomycetemcomitans* infection produces cytokines, IL-1β [107, 108]. TNF-α and IL-17 can also synergize together with IL-β to augment expression and production of other cytokines (IL-6) and defensins, along with endothelial activation to enhance immune response [109-114].

Although inflammation aims to resolve of oral infection, it can lead to bone resorption and destruction [115]. Alveolar bone is one most dynamic bone as osteoclasts and osteoblast continually induce bone remodeling to maintain homeostasis [116-119]. Osteoclasts are resorptive cells activated and differentiated by macrophage-colony stimulating factor, RANKL-RANK signaling, interleukins, and TNF-α [117, 118, 120-122]. Once adhered to bone, a ruffled border is created between the activated osteoclast and bone [117, 119]. Osteoclasts degrade the mineral matrix utilizing a pH gradient for acidification through release of H^+ and Cl^- [117, 119]. The secretion of cathepsin K and metalloproteinases further degrades collagen and the organic matrix [117, 119]. Degraded bone matrix is removed as it is transcytosed in vesicles through osteoclasts and fuse with cytoplasmic vesicles containing tartrate-resistant acid phosphatase (TRAP) to be released in the extracellular matrix [117, 123]. Phagocytes remove the debris and osteoblasts are recruited for bone formation after osteoclast detach from the bone [117].

F. nucleatum mechanisms for invasion and host response have been evaluated both *in vitro* and *in vivo* [93, 108, 124-126]. We previously have shown *F. nucleatum* infection induces inflammasome activation and release of cytokines and danger signals in human GECs [108]. However, infection has not been characterized *in vivo* for oral infection. Therefore, we set out to evaluate host immunity to *F. nucleatum* oral infection in BALB/c mice. We hypothesize an upregulation of pro-inflammatory cytokine expression and release of cytokines due to infection.

4.3.2 Methods

Bacteria

Fusobacterium nucleatum (ATCC 25586) was cultured at 37°C under anaerobic conditions in brain-heart infusion broth supplemented with yeast extract (5 mg/mL), hemin (5 g/mL), and menadione (1 mg/mL). Erythromycin (5 mg/ml) was used as a selective agent for *F. nucleatum* as previously described [127]. After 24 hours of growth, bacteria were collected by centrifugation at 6000 *g* for 10 min at 4°C, washed twice and resuspsended with phosphate-buffered saline (PBS). Quantification of bacteria was measured by optical density (OD) to obtain a concentration of 10^9 colony-forming units (CFU)/ml using a reference standard.

Mice and Oral Challenging of *Fusobacterium nucleatum*

BALB/c mice were obtained from the animal facility of the Instituto de Biofísica Carlos Chagas Filho da Universidade Federal do Rio de Janeiro. All protocols used in this study followed the guidelines and were approved by the Institutional Animal Care and Use Committee at Universidade Federal do Rio de Janeiro.

Six- to eight-week-old male BALB/c mice were given ad libitum water containing 10 mL of Bactrim (Roche) comprised of sulfamethoxazole/trimethoprim for 10 days. Then antibiotic-free water was given to the mice for 3 days prior to infection.

The protocol for oral infection was adapted from Baker et al. [128]. On days of infection, mice were anesthetized with ketamine-xylazine (100 mg/ml and 20 mg/ml) by intraperitoneal injection. Anesthetized mice were orally challenged with *F. nucleatum* at 10^9 bacteria in 100 µl of PBS with 2% carboxymethylcellulose (Sigma), or were sham-infected with the same solution containing no bacteria three times over 2-day intervals.

Collection of Maxilla

Maxillas were surgically removed and collected at days 1, 4, and 7 after the last infection day. One half of the maxilla was placed in TRIzol reagent (Life Technologies), while the other half in cell lysis buffer (Sigma) containing protease inhibitor (Roche). Then the samples were macerated and homogenized using TissueLyser LT (Qiagen) for 5 min at 50 Hz. After centrifugation at 1000 *g* for 10 min supernatants were transferred to new tubes and used for experiments. Prior to protein assays, maxilla halves from each group of mice were pooled together and quantified using Pierce BCA Protein Assay Kit (Thermo Fisher Scientific) for equal loading.

RNA Extraction and Quantitative PCR

Following the manufacturer's instructions, total RNA was extracted using Trizol Reagent (Life Technologies). Total RNA was quantified by using NanoDrop (Thermo Fisher Scientific). RNA was converted to cDNA using High-Capacity cDNA Reverse Transcription Kit (Life Technologies). Quantitative PCR was performed using SYBR-green fluorescence quantification system (SYBR Select Master Mix (Life Technologies)). Real-time PCR cycling parameters were as follows: 95°C for 10 min and then 40 cycles of 95°C for 30 s, 60°C for 1min, and 72 °C for 1 min. The following primers were used as previously described: IL-1β forward, 5'- TTCAGGCAGGCAGTATCACTC-3'; IL-1β reverse, 5'-CCACGGGAAAGACACAGGTAG-3'; TNFα forward, 5'-TTCTATGGCCCAGACCCTCA-3'; TNFα reverse, 5'-GTGGTTTGCTACGACGTGGG-3'; IL-6 forward, 5'-TCCTCTCTGCAAGAGACTTCC-3'; IL-6 reverse, 5'-TTGTGAAGTAGGGAAGGCCG-3'; IL-17 forward, 5'-TCAGCGTGTCCAAACACTGAG-3', IL-17 reverse, 5'-GACTTTGAGGTTGACCTTCACAT-3'; GAPDH forward, 5'-GGTCATCCCAGAGCTGAACG-3'; GAPDH reverse, 5'-

TTGCTGTTGAAGTCGCAGGA-3' [129]. Relative expression levels were calculated against GAPDH as the reference gene using the comparative cycle threshold method. Quantification of infected mice results were normalized against control mice.

PCR

The PCR was performed following the protocol from Liu et al. [130]. Maxilla RNA targeted a 360-bp region using *F. nucleatum* forward, 5'-AGAGTTTGATCCTGGCTCAG -3' and reverse, 5'-GTCATCGTGCACACAGAATTGCTG-3' primer sequences. [130]. The samples were amplified using GoTaq Green Master Mix (Promega) under the same conditions of 5 min at 94^{o}C and 30 cycles, with each cycle consisting of denaturation at 94^{o}C for 30 sec, annealing at 58^{o}C for 30 sec, extension at 72^{o}C for 1 min, and final extension for 10 min. PCR products were loaded onto a 2% agrose gel in Tris-acetate buffer with EDTA. The gel was stained with GelRed nucleic acid gel stain (Biotium) and visualized under UV light.

ELISA

Samples from half the maxilla were used for ELISA experiments. IL-1β, IFN-γ, and TNF-α cytokine levels were measured using Mouse IL-1β, IFN-γ, and TNF-α ELISA kits (R&D Systems). ELISAs were performed following manufacturer's instructions.

Western Blot

Protein samples were dissolved in 6X laemmli buffer and boiled. Then they were run on SDS-PAGE gels and transferred to PVDF membranes. Membranes were blocked with 5% BSA and incubated with anti-HMGB1 (Abcam) at 1:10,000 overnight at 4^{o}C. After primary incubation, the membranes were washed and incubated with HRP conjugated anti-goat IgG antibody (Millipore) at 1:40,000 for one hour at RT. Membranes were developed with Luminata Forte (Millipore) substrate. Images were acquired using ImageQuant LAS 4000 system and analyzed using NIH-ImageJ.

Histopathology and Immunohistochemistry

For morphological studies mandibles were collected and were immediately immersed in zinc-formaldehyde for fixation during 72 hours. Next tissues were decalcified in Morse's solution for 7 days. The complete decalcification of bones was manually assessed. Tissues were then washed in water and dehydrated crescent solutions of ethanol, clarified in xylene and embedded in paraffin. Five-micrometer sections were cut and stained with hematoxylin-eosin (H&E). For immunohistochemistry, paraffin sections were collected onto charged histological slides. A rat monoclonal antibody F4/80 (Abd Serotec) was used to detect macrophages at 1:50. Briefly, after dewaxing and rehydrating, sections were submitted to endogenous peroxidase inhibition (15 minutes with 3% H_2O_2 in methanol), followed by an enzymatic antigen retrieval, with a 0.1% trypsin solution containing 0.01% calcium chloride in Tris-buffer pH 7.4 (Sigma-Aldrich) for 5 minutes. After blocking nonspecific binding of immunoglobulins with 5% BSA with 0.05% Tween in PBS, primary antibody was incubated for 14-18 hours, at 4^{o}C, in a humid chamber. The sections were then washed in 0.25% Tween-phosphate saline buffer (PBS) solution for 5 minutes and then the secondary antibody conjugated to peroxidase (Nichirei) were incubated for 1 hour

at RT. The chromogen substrate was diaminobenzidine (Dako). Negative control slides were incubated with rat nonimmune serum or with the antibody diluent solution.

Statistical Analysis

Results are shown as mean ± standard deviation (SD). Statistical significance was calculated by two-tailed Student's *t*-test and differences were considered significant at $P < 0.05$.

4.3.3 Results

***F. nucleatum* infection induces pro-inflammatory cytokine expression in maxilla**

To assess cytokine expression of *F. nucleatum* infected mice, we isolated RNA from the maxilla at various time points post-infection. We have previously described *F. nucleatum* infection in GECs led to increased IL-1β gene expression dependent on time [108]. Therefore, we speculated response to oral infection of *F. nucleatum* in mice would be similar, so we measured IL-1β gene expression over a course of 7 days post-infection (Fig. 1A). We observed a significant induction of IL-1β at day 1 post-infection compared to uninfected mice and a reduction over time. Park et al. demonstrated *F. nucleatum* infected BMDMs triggered cytokine production (IL-1β, TNF-α, IL-6) through the Toll-like receptor signaling pathway, but proposed TIR-domain-containing adapter-inducing interferon- (TRIF)-dependent pathway could also influence cytokine production [131]. To test this idea in our study, we measured IFN-γ and found an upregulation of transcription on day 1 post-infection in infected mice (Fig. 1B). Then we sought to evaluate TNF-α and IL-6 gene regulation as they were also influenced during *F. nucleatum* infection in BMDMs. Our results show a significant increase in gene transcription post-infection at day 4 for TNF-α (Fig. 1C) and day 1 for IL-6 (Fig. 1D). An additional cytokine we evaluated was IL-17 as it has been implicated to activate osteoclasts and play a role in bone resorption [132-135]. Our findings show, we observe an increase of IL-17 expression at day 1 post-infection (Fig. 1E). The results indicated multiple pro-inflammatory cytokines were upregulated during the course of *F. nucleatum* infection.

Cytokine production augmented in the maxilla during *F. nucleatum* infection

To further evaluate cytokine production, we tested the maxilla of infected mice by ELISA. As IL-1β and IFN-γ had increased gene expression at day 1 post-infection, we observed a correlation of cytokine production at day 4 post-infection (Fig 2A and 2B). We also detected an increase for TNF-α at day 4 post-infection, but it was not statistically significant (Fig. 2C). Next, we looked at high mobility group box 1 (HMGB1) because it functions as a transcription regulator, pro-inflammatory cytokine, and macrophage activator [136-138]. IFN-γ, TNF-α, and TGF-β have been shown to augment expression of HMGB1 mRNA in THP-1 macrophages and human peripheral-blood monocytes [137, 139]. As we observed an increase in two of these cytokines during *F. nucleatum* oral infection, it suggested infection may also promote HMGB1 production. We found a significant increase at day 4 post-infection of total HMGB1 from maxilla compared uninfected mice by Western blot (Fig. 3A and 3B). Collectively, the results show most of

pro-inflammatory cytokine expression occurs on day 1 post-infection, while cytokine production occur on day 4 post-infection as a response to *F. nucleatum* infection.

F. nucleatum infection in the mandible recruits immune cells and activates macrophages

Since we found inflammatory cytokine production increased over time due to infection, we aimed to evaluate this association to immune cell recruitment. H&E and immunohistochemistry staining were performed on sections of the mandible from *F. nucleatum* infected mice. Day 1, 4, and 7 post-infection showed more immune cells were present near the alveolar bone than compared to uninfected mice by H&E staining (Fig. 4). F4/80 macrophages staining also revealed an increase in macrophage recruitment for days 1, 4, and 7 post-infection compared to uninfected mice (Fig. 5). The activated macrophages were detected in adipose tissues, skeletal muscle fibers, and periosteal localization. However, we observed macrophage activation was more concentrated in the dental pulp, around periodontal ligaments, and between odontoblasts. This data suggests macrophage recruitment plays a critical role in response to *F. nucleatum* oral infection.

Osteoclasts contribute to bone resorption during _F. nucleatum_ infection

Previous studies have shown IL-β, IFN-γ, and TNF-α production are important to enhancing osteoclast development [120, 140, 141]. As we saw elevated levels in production of these cytokines during *F. nucleatum* infection, we predicted osteoclasts formation. A small recruitment of osteoclasts were found near alveolar bone at day 4 post-infection (data not shown), but they were more present at day 7 post-infection in H&E staining (Fig. 6). Osteoclast activation leads to attachment to the bone, resorption of the bone through its secretory factors, and detachment from the resorption site [142, 143]. Days 4 and 7 post-infection of *F. nucleatum*, bone resorption pits were observed in the alveolar bone (Fig. 7). These results indicate *F. nucleatum* infection contributes to bone resorption by activation of osteoclasts.

4.3.4 Discussion

Studies have characterized mechanisms influencing adhesion and growth interactions between *F. nucleatum* with other periodontal bacteria, such as *P. gingivalis* and *A. actinomycetemcomitans* [13, 14, 144, 145]. It is equally important to understand *F. nucleatum* infection alone as an oral colonizer and facilitator of other periodontal bacteria to propagate. Thus, we investigated innate immune response to *F. nucleatum* oral infection. In this study, we demonstrated *F. nucleatum* can trigger a pro-inflammatory response contributing to macrophage recruitment. We also show osteoclasts played a role in bone resorption as a result of infection.

Different oral bacteria can negatively or positively regulates host production of pro-inflammatory cytokines. While *P. gingivalis* hinders IL-1β and HMGB1 release during infection in GECs, *A. actinomycetemcomitans* stimulates IL-6 and TNF-α production in BMDMs [131, 146]. It has been described *F. nucleatum* triggers cytokine production through Toll-like receptors, TLR2 and TL4 receptors [131, 147, 148]. However, it has also been proposed *F. nucleatum* can also induce cytokines through Toll-like-receptor-

independent pathways [148, 149]. Our results show an upregulation of IL-1β, IL-6, TNF-α, and HMGB1 for *F. nucleatum* infected mice. This is further supported with previous *in vitro* findings of GECs and BMDMs infected with *F. nucleatum* increasing pro-inflammatory cytokines [108, 131].

Given the heightened inflammatory response we measured, it was not surprising to see a recruitment of immune cells to the alveolar bone during infection. Some immune cells, dendritic cells and macrophages, are present in various tissues as initial responders to infection. It is also well characterized macrophages reside in dental pulp [150]. Their activation relies on exposure to IFN-γ, TNF-α, and LPS [151-153]. Interferons, like IFN-γ, are important for antiviral activity and are augmented by lipopolysaccharides (LPS) stimuli [154-156]. We found *F. nucleatum* infection induced significant IFN-γ, which may have also played a role of enhancement for macrophage presence. Immunohistochemistry revealed activated macrophages throughout the oral cavity and suggests *F. nucleatum* penetrated numerous tissues during infection. GECs may have also contributed to recruitment by release of pro-inflammatory cytokines and macrophage recruitment.

It is controversial whether IFN-γ promotes or inhibits osteoclasts activation [118, 140, 157, 158]. However, in our study, we speculate IFN-γ contributed to stimulation of osteoclasts as they were observed localized near the bone after *F. nucleatum* infection, which weren't present in uninfected mice. As mentioned before, TNF-α and IL-17 synergizes with IL-1β. These cytokines can facilitate osteoclast activation, which further supports what we saw in the mandible [135]. Degradation of collagen and increased bone resorption has also been associated with IL-17 [132]. All these factors may have led to the observed bone resorption in *F. nucleatum* infected mice.

4.3.5 Figures

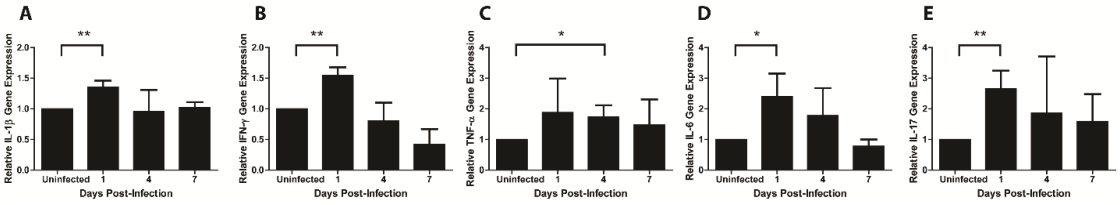

Fig. 1. Gene expression is upregulated in the maxilla during *F. nucleatum* infection
(A-E) Relative IL-1β, IFN-γ, TNF-α, IL-6, and IL-17 mRNA gene expressions compared to control were evaluated by real-time PCR (qPCR) from the maxilla of *F. nucleatum* infected BALB/c mice. Days 1, 4, and 7 post-infection were tested. Results represent an average of three independent experiments with at least 4 mice in each group per experiment. Error bars represent the mean ± SD. (*< 0.05, **<0.01, Student's *t*-test)

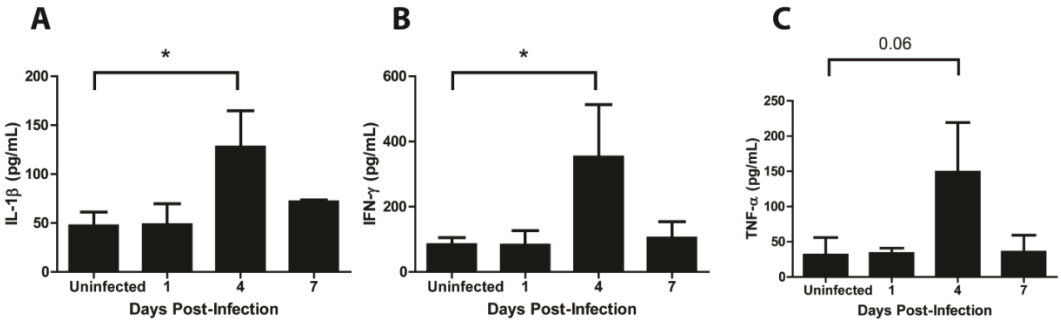

Fig. 2. *F. Nucleatum* infection induces increased cytokine production in the maxilla
(A,B,C) IL-1β ,IFN-γ, and TNF-α cytokines were measured by ELISA for BALB/c mice infected with *F. nucleatum*. Maxilla from days 1, 4, and 7 post-infection were evaluated. Results represent an average of three independent experiments with at least 4 mice in each group per experiment. Error bars represent the mean ± SD. (*< 0.05, **<0.01, Student's *t*-test)

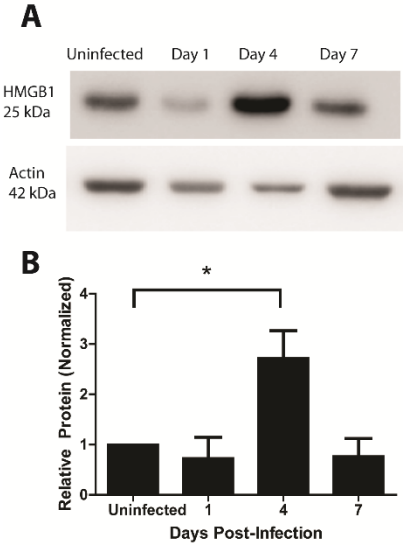

Figure 3. HMGB1 levels augmented at day 4 post-infection of *F. nucleatum* infection
(A) HMGB1 (25 kDA) was detected by Western blot from the maxilla of BALB/c mice infected with *F. nucleatum* over a time-course of day 1, 4, and 7 post-infection. Actin (42 kDa) was used as a loading control. (B) Relative protein was measured by quantification of densitometry using NIH-ImageJ. Results represent an average of three independent experiments with at least 4 mice in each group per experiment. Error bars represent the mean ± SD. (*< 0.05 Student's *t*-test)

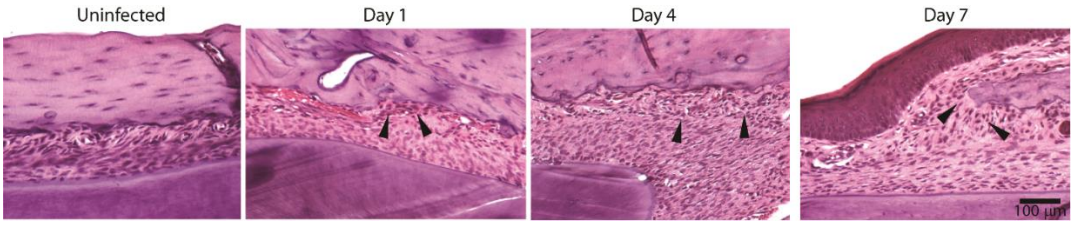

Fig. 4 Immune cells are recruited near the alveolar bone during *F. nucleatum* infection
Sections from mandible of infected BALB/c mice were stained with H&E. Results represent 4 mice in each group. Arrows indicate area of immune cells localized near the bone in dark stain. Bar represents 100 µm.

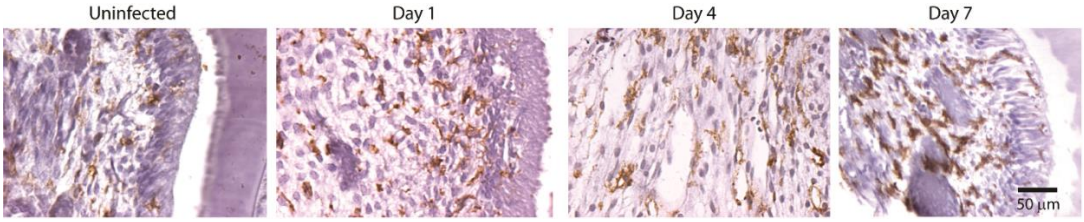

Fig. 5 *F. nucleatum* infection increases macrophage recruitment in the dental pulp
Immunohistochemistry for F4/80 macrophages in the dental pulp of infected BALB/c mice. Bar represents 50 µm.

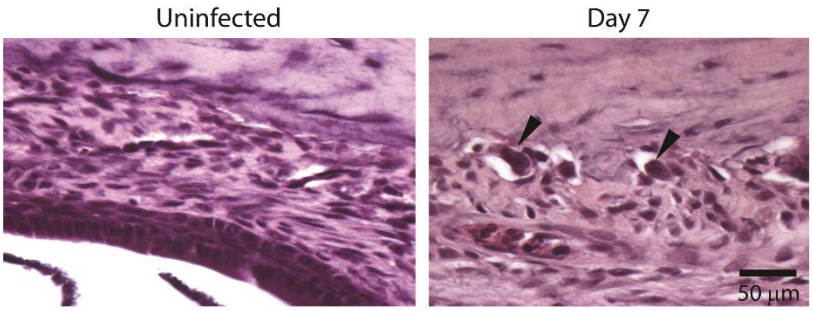

Fig. 6 Osteoclasts recruitment near the alveolar bone in *F. nucleatum* infected mice
Sections from mandible of infected BALB/c mice with H&E staining. Arrows show osteoclasts residing near the bone. Bar represents 50 µm.

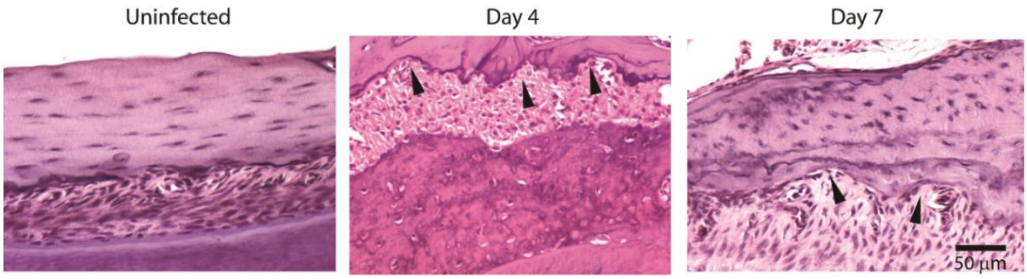

Fig. 7 *F. nucleatum* infection induces bone resorption
Mandible of infected BALB/c mice were stained with H&E. Arrows indicate areas of bone resorption. Bar represents 50 µm.

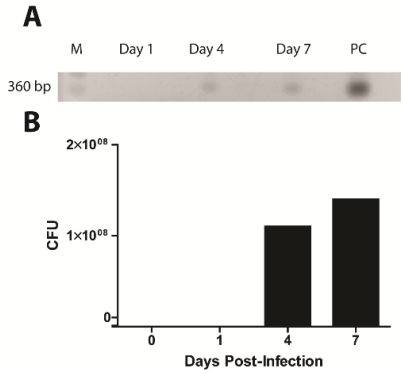

Supplementary Fig. 1 Detecting *F. nucleatum*
(A) Gel electrophoresis of RT-PCR products from maxilla of *F. nucleatum* infected BALB/c mice measuring *F. nucleatum* (360 bp). 10^9 CFU of *F. nucleatum* was loaded for the positive control. (B) Band intensity was measured using NIH-ImageJ. CFU for each day was calculated using relative band intensity compared to the positive control. M: Marker, PC: Positive Control.

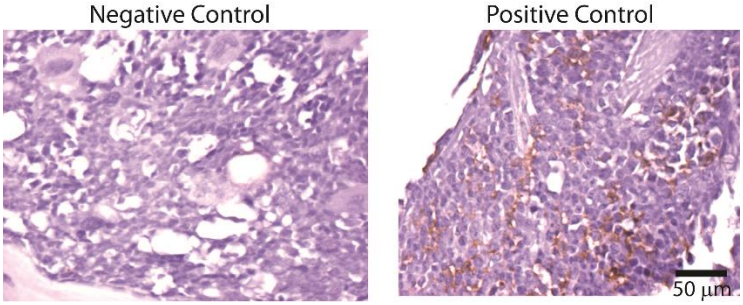

Supplementary Fig. 2 Positive control for F4/80 staining
BALB/c bone marrow was stained for F4/80 macrophages. Negative control slide was prepared similarly to the immunostained ones except that instead of antibody negative control slide was reacted with the normal mice serum or the antibody dilution solution. Absence of reactivity. Positive control slide: maxilla histological sections showing the positive bone marrow monocyte/macrophages for F4/80 antigen. Bar represents 50 µm.

4.4 *Fusobacterium nucleatum* oral infection in caspase-1 knock-out mice (Preliminary data)

Methods*: F. nucleatum* infection and experimental procedures were followed as described in the previous experiments of BALB/c infection. Samples were collected at day 1 post-infection for caspase-1 KO mice experiments.

4.4.1 Results

IL-1β and IFN-γ cytokines showed an increase in response to *F. nucleatum* infection in wild-type C57BL/6 mice (Fig. 1A and 1B). However, their production was significantly less than what we observed BALB/c infected mice. This is consistent with susceptibility of C57BL/6 mice compared to BALB/c mice to other bacterial infections, *B. pseudomallei* and *C. trachomatis* [159, 160]. We postulated inflammasome activation also played a role in the observed cytokine production in *F. nucleatum* oral infected mice. However, our results were not statistically significant. The maxilla were collected at day 1 post-infection, but may have showed more significant if the infection proceed to day 7.

4.4.2 Figures

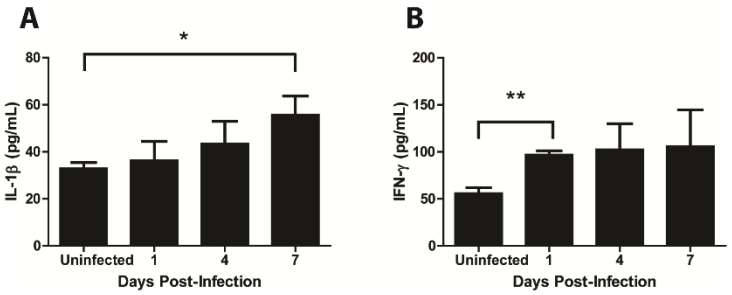

Fig. 1

(A and B) IL-1β and IFN-γ cytokines were measured by ELISA for *F. nucleatum* infected wild-type and caspase-1 KO C57BL/6 mice. Maxilla from day 1 post-infection were evaluated. Results represent an average of three independent experiments with at least 4 mice in each group per experiment. Error bars represent the mean ± SD. (*< 0.05, **<0.01, Student's *t*-test)

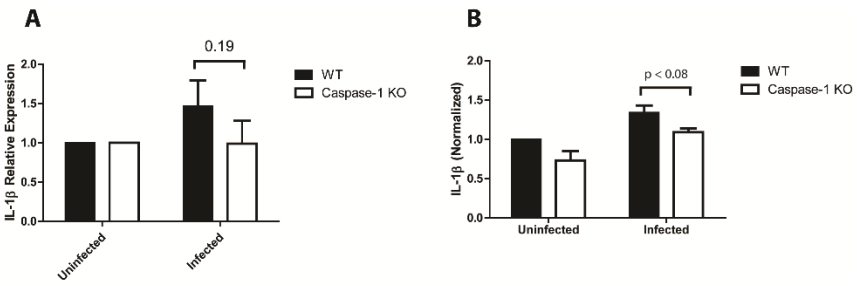

Fig. 2 IL-1β cytokine production in caspase-1 infected mice

(A) Relative IL-1β mRNA gene expression compared to control mice was evaluated by real-time PCR (qPCR) and (B) IL-1β cytokines by ELISA. Infected mice were normalized to the control mice for ELISA. Samples 1 post-infection from the maxilla of *F. nucleatum* infected wild-type and caspase-1 KO C57BL/6 mice were used. Results represent an average of three independent experiments with at least 4 mice in each group per experiment. Error bars represent the mean $\pm$ SD.

Future Perspectives

My research has added to the understanding into why *P. gingivalis* can elude an immune response, while *F. nucleatum* triggers a response during initial infection. We found that NDK homologue of *P. gingivalis* regulates caspase-1 activation and decreases pro-inflammatory cytokine and danger signal release from infected GECs. On the other hand, *F. nucleatum* triggers NLRP3 inflammasome activation and release of pro-inflammatory cytokines. Also, *F. nucleatum* oral infection in mice led to macrophage recruitment to the dental pulp and bone resorption. Using these perspectives, we have modeled host inflammatory and cytokine response to invasion of *P. gingivalis* (Fig. 2) and *F. nucleatum* (Fig. 3) into GECs. We are also the first to characterize the pro-inflammatory response of *F. nucleatum* orally infected mice. However, further study of other potential mechanisms or influences contributing to these infections is still needed.

Figure 2 Proposed model for the role of NDK in HMGB1 localization during *P. gingivalis* infection [146]

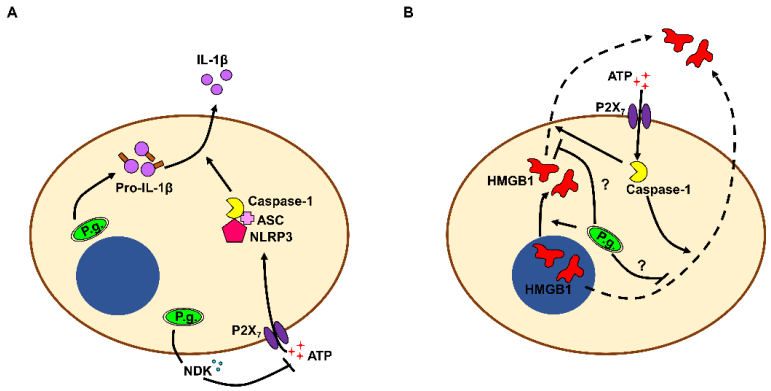

Figure 3 Model of pro-inflammatory cytokine expression and the inflammasome activation cascade during *F. nucleatum* infection [108]

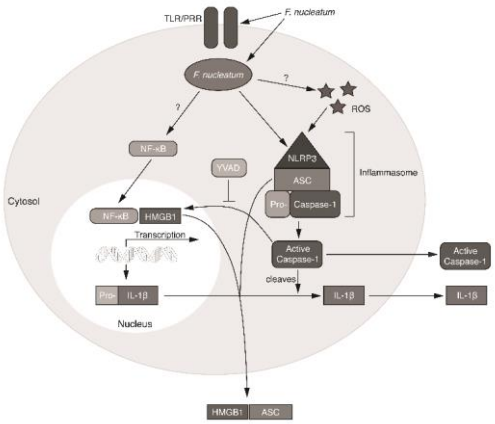

Mitochondria dysfunction can trigger reactive oxygen species (ROS) generation and induce inflammasome activation [161]. However, mitochondrial DNA as another inducer for the inflammasome is of increasing interest. Previous studies have shown *P. gingivalis* masks its presence and proliferates within the host cell by modulating the mitochondrial-dependent apoptosis pathway. Nakhjiri et al. described an upregulation of Bcl-2, an anti-apoptotic protein, and a decrease in Bax, a pro-apoptotic molecule, as one mechanism *P. gingivalis* prevents programmed cell death in GECs [162]. However, it is not well understood how the inflammasome and cytokine secretion is regulated during infection through this pathway. It will also be interesting to evaluate whether *P. gingivalis* can inhibit mitochondrial-dependent inflammasome activation with cells deficient in Bcl-2. This will provide a more detailed model for inhibition of cell death.

Along with the studies of mitochondria dysfunction, upstream intermediates need to be further characterized in this pathway during infection. Hornung et al. described monosodium urate (MSU) crystals, silica crystals, and aluminum salts activate the inflammasome as a result of lysosomal damage [163]. It has been previously described mitochondria malfunction is the intermediate step between lysosomal damage and inflammasome activation [164]. A gap of knowledge can be filled by measuring inflammasome activation during *P. gingivalis* infection with treatment of MSU crystals. Further evaluation of infection with MSU crystal treatment can also incorporate the Bcl-2 knock-down cells to complete an understanding of the pathway for *P. gingivalis* influence and its effects on mitochondrial-dependent inflammasome activation.

Our findings for *F. nucleatum* infection in BALB/c mice showed an enhanced pro-inflammatory response during earlier days after infection. However, our experiments for the wild-type and caspase-1 KO C57BL/6 mice may have not been the most optimal conditions for the best results as we collected samples on day 1. We found IL-1β secretion in wild-type mice showed statistical significance at day 7. This may provide more significant results for KO experiments at this later day of collection. Another change can be more mice per group could be added to account for variability in mouse response to infection. It should also be considered C57BL/6 mice are more naturally resistant to infection than compared to BALB/c mice.

Since we have shown the canonical inflammasome to contribute to maturation of pro-inflammatory cytokines during *F. nucleatum* infection [57]. Another future direction is to study the non-canonical inflammasome. One could also evaluate caspase-11, a non-canonical inflammasome, which has been proposed as an upstream activator of caspase-1 activation [53]. This can be done with adding caspase-11 KO to the caspase-1 KO mice experiments. The hypothesis would be caspase-11 KO mice would induce an intermediate inflammatory response compared to wild-type or caspase-1 KO in *F. nucleatum* infection. Knocking down caspase-4/5 in GECs can also be performed to understand inflammatory response *in vitro*.

It is important to understand the mechanisms for invasion and survival for each periodontal pathogen as it infects its host. Since the oral cavity is colonized with a vast number of organisms, it is also significant to investigate their interactions with one another and how they contribute to homeostasis or dysregulation. *P. gingivalis* has been shown to work synergistically with *F. nucleatum* to induce biofilm formation [13]. It has also been described *F. nucleatum* can create an oxygenated and carbon-dioxide depleted environment

sufficient for *P. gingivalis* to proliferate [14]. The propagation of these infections relies on coordination of time and ratios of bacteria used for infection. *P. gingivalis* infected at earlier or later times than *F. nucleatum* infection in a murine abscess model showed an increase in lesion sizes [165]. A larger multiplicity of infection of *F. nucleatum* than *P. gingivalis* infection showed reduced lesion size, which was speculated to be a result of coaggregration [165]. These factors play a role in determining whether infection can progress into early stages of diseases. However, inflammasome activation and pro-inflammatory response for co-infection of these two bacteria have not been characterized in an oral infection model. This type of study has been performed in bone marrow-derived macrophages, but is more relevant to be studied using GECs as the initial barrier to encounter these pathogens [90]. Therefore, future experiments should examine host response for *F. nucleatum* and *P. gingivalis* co-infection in GECs and in murine models using similar methods as described in our previous publications. Expanding our understanding of host response to pathogenic bacteria is important for limiting progression of periodontitis and other emerging systematic disease linked to these bacteria.

Appendix: Valley fever: danger lurking in a dust cloud

ELSEVIER

Institut Pasteur

Microbes and Infection 16 (2014) 591–600

www.elsevier.com/locate/micinf

Review

Valley fever: danger lurking in a dust cloud

Larry Johnson [a,b,1], Erin M. Gaab [b,1], Javier Sanchez [a,b], Phuong Q. Bui [a,b], Clarissa J. Nobile [a,b], Katrina K. Hoyer [a,b], Michael W. Peterson [c], David M. Ojcius [a,b,*]

[a] Department of Molecular Cell Biology, University of California, Merced, CA 95343, USA
[b] Health Sciences Research Institute, University of California, Merced, CA 95343, USA
[c] Department of Internal Medicine, University of California San Francisco – Fresno, Fresno, CA 93703, USA

Received 1 April 2014; accepted 24 June 2014
Available online 16 July 2014

Abstract

Coccidioides immitis and *Coccidioides posadasii* contribute to the development of Valley Fever. The ability of these fungal pathogens to evade the host immune system creates difficulty in recognition and treatment of this debilitating infection. In this review, we describe the current knowledge of Valley Fever and approaches to improve prevention, detection, and treatment.

Keywords: Innate immunity; Adaptive immunity; Fungal pathogen; Lung infection; *Coccidioides*

1. Introduction

Coccidioidomycosis is an infection caused by inhaling spores of the fungal species *Coccidioides immitis* or *Coccidioides posadasii*. The disease has commonly been termed "Valley Fever," "San Joaquin Valley Fever," "San Joaquin Fever," "desert fever," and "desert rheumatism" [1]. A high incidence of coccidioidomycosis has been reported in the southwestern United States, Central America, and South America [2,3]. The rise in cases has contributed to hospitalization costs totaling over $2 billion for those afflicted with the illness, which include individuals with symptoms ranging from mild local infections to disseminated disease [4].

Although inhalation of *Coccidioides* is the most common mode of transmission, there are rare cases of transmission through transplanted organs or inoculation by penetration of the skin by a sharp object containing the fungus [3,5]. While most infected individuals are asymptomatic, about 40% of individuals show flu-like symptoms, such as fever, cough, headache, skin rash, muscle aches, joint pain, and fatigue [1,3,6,7]. In most cases the immune system resolves the infection without the need for medical intervention. However, without proper diagnosis, disseminated disease may occur, leading to increased severity of symptoms. Laboratory diagnostic testing and clinical evaluation are the most effective measures for determining coccidioidomycosis. Early detection and antifungal drug treatments aid in slowing or inhibiting the development of disease and limit tissue damage, and may prevent morbidity [2]. In this review, we aim to provide a better understanding of coccidioidomycosis and to promote awareness of these pathogenic fungi.

2. Valley fever

2.1. Geographic distribution of coccidioidomycosis

Two types of coccidioidomycosis-causing fungi exist: *C. immitis* and *C. posadasii* [8]. *C. immitis* is mainly endemic to California and is often referred to as the "Californian" strain,

* Corresponding author. Department of Molecular Cell Biology, University of California, 5200 Lake Road, Merced, CA 95343, USA. Tel.: +1 209 228 2948.
E-mail addresses: david.ojcius@gmail.com, dojcius@ucmerced.edu (D.M. Ojcius).
[1] Both authors contributed equally to this work.

http://dx.doi.org/10.1016/j.micinf.2014.06.011
1286-4579/

while *C. posadasii* is distinguished as the "non-Californian" strain [8]. However, *C. immitis* has also been isolated from soil in Venezuela and Washington State, where several patients were suspected of contracting coccidioidomycosis [9,10].

There is a relatively low incidence rate of Valley Fever on a national scale in the United States and a variable status as a reportable disease across endemic regions [11,12]. *Coccidioides* fungi have been found in the Western Hemisphere, mostly in hot, arid areas between latitudes of 40° north and 40° south, including the southwestern United States, Mexico, and Central and South America (Fig. 1) [7,13,14]. Suspected sites of infection have been described as dry plains, hills, prairies, and tropical desert brush land [9]. These areas tend to have temperatures ranging from 5 °C to 45 °C, rainfall averaging between 125 and 500 mm, and altitudes between sea level and 800 m above sea level [9]. With differences in reporting over time and between regions, it is difficult to determine where the fungus was contracted, and which environments propagated the development of the disease [12].

2.2. Geographic distribution in Latin America

In 1892, one of the first described cases of coccidioidomycosis was observed in a 36-year-old Argentinian soldier by a medical intern, Alejandro Posadas, in Buenos Aires [11,15]. However, the more recent incidence and prevalence of coccidioidomycosis in Latin America is unclear [14]. Outside of the United States, other endemic regions include Mexico, Central America, and South America. South American countries that are confirmed to harbor the illness-causing fungus include Argentina, Colombia, Paraguay, and Venezuela, though limited patient data exists to support these claims [9]. The regions of Bolivia, Ecuador, and Peru are also potential sites for harboring the fungus, but even less patient data is clearly documented for these regions.

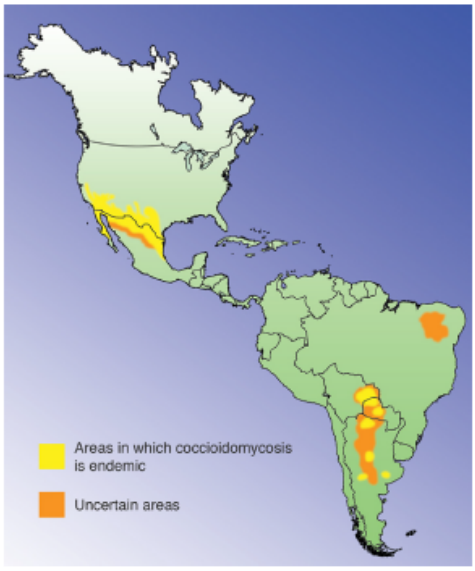

Fig. 1. Geographic distribution of valley fever across the Americas.

2.3. Geographic distribution in North America

The highest rates of coccidioidomycosis cases in North America have been reported in Arizona and California [16]. The illness has also been reported in southern Nevada, southern Texas, Utah, New Mexico, and Washington [7,10,13,17]. Cases reported in Mexico generally tend to originate in the northern region [18]. However, the true incidence of the disease is not known, since coccidioidomycosis was not a reportable disease in Mexico until recently [18].

2.3.1. California

Many of the endemic cases of coccidioidomycosis in the United States are reported in California. The incidence of hospitalizations in California at 0.89 (95% CI 0.79–0.99)/100,000 persons/year likely under represents the extent of the disease in the San Joaquin Valley region, which contains only 10% of California's population [19]. This underrepresentation may be due to this region's population consisting of lower-income inhabitants, who are less likely to seek medical care except in severe cases of infection [19]. Initial reports of coccidioidomycosis in the United States were published in the San Joaquin Valley of California in 1939 [1,20,21]. In the last quarter century, dramatic increases in the reported incidence of Valley Fever in California have brought more public attention to the disease [13,19].

Since the fungus is spread through dust, an increase in the number of reported cases tends to occur during the harvesting season in endemic areas (Fig. 2). During World War II (WWII), several airfield training sites were built in the San Joaquin Valley. The dusty sites were suspected to have caused an 8–25% rate of new infections in those employed by the military, making it the most common cause of hospitalization at several Southwestern airbases [20]. A dust storm in 1977 in the San Joaquin Valley and an earthquake in 1994 in Northridge were also reported to have caused hundreds of cases of

Fig. 2. A tractor disrupting soil and creating a dust cloud, which potentially could be spreading the fungal arthroconidia.

coccidioidomycosis in those areas of California [13]. A six-fold increase in the rates of reported cases occurred in California between 2000 and 2011 [16]. Whether this is due to increased awareness of the illness, changes in the environment, or other factors remains unknown.

2.3.2. Arizona

About 60% of endemic cases in the United States are reported in Arizona (amounting to about 150,000 cases annually) [12]. Only people experiencing symptoms are generally tested, so whether the expression of symptoms in some individuals and not others is due to a large concentration of the fungus or a higher rate of dissemination is unknown. During a six-month period of WWII, as many as 50% of military personnel in Arizona undergoing the coccidioidomycosis skin test showed evidence of infection. At that time, Germany protested that exposure of its prisoners of war to the fungus in work camps violated the Geneva Convention [22]. In recent years, the incidence of coccidioidomycosis has increased in the elderly, even when the increase is adjusted for age [12]. This may be because older adults are more likely to seek medical care (and receive a diagnosis of coccidioidomycosis) or have a greater susceptibility to developing symptoms, and/or may be due to the increased influx of these elderly individuals from non-endemic regions into Arizona to retire, which could affect susceptibility to the fungus (see below) [12].

2.4. Populations affected

Although coccidioidomycosis is most common in the southwestern United States, the Southwest's growing population and tourism industry may result in people from other areas returning home with the disease before developing clinical symptoms [23]. One hypothesis is that people from endemic regions develop immunity against the infection, and visitors to endemic regions are more susceptible to infection. This idea is certainly possible, as individuals living in endemic regions are likely to have been exposed to the fungus, successfully cleared the infection, and developed antibodies. However, evidence for this hypothesis is confounded by the fact that the symptomatology of coccidioidomycosis is non-specific, which may prevent clinicians outside endemic areas from suspecting coccidioidomycosis [24]. Coccidioidomycosis increased from 21 to 91 cases per 100,000 between 1997 and 2006 [12]. Coccidioidomycosis may manifest as acute pneumonia, chronic progressive pneumonia, pulmonary nodules and cavities, or as disseminated extrapulmonary non-meningeal disease and/or meningitis [23].

Ethnicity, disease status, and occupation have been associated with coccidioidomycosis incidence. Hospitalization rates have been reportedly highest among the following groups in the last few decades: African-Americans and Filipinos, males 50-years or older, pregnant individuals, acquired immunodeficiency syndrome (AIDS) patients and other immunosuppressed individuals, and those working in certain outdoor environments, such as construction workers [12,13,25].

2.4.1. Ethnicity

The risk of developing disseminated coccidioidomycosis is about 10–127 times greater in people of African-American and Filipino descent, due to a genetic component contributing to the development of disseminated illness [13,25–29]. Specific genes and blood groups are suspected to influence susceptibility to severe coccidioidomycosis [30]. African-Americans are associated with increased rates of hospitalization [31]. People who identify as Native American and Asian-Pacific Islander have lower rates of dissemination than those who self-identify as white [31].

2.4.2. Age

Although coccidioidomycosis can occur at any stage of life, the risk of developing coccidioidomycosis appears to increase with age [31–33]. In the youngest age group (0–14 years old), the incidence of hospitalization is less than 1 per 100,000 [31]. The rate of hospitalization increases to 7.2 per 100,000 in the 50 years and older group [31]. As a result, coccidioidomycosis has not been well-described in children, despite it causing a substantial disease burden in the children of Central California and elsewhere [34].

2.4.3. Health status

Individuals with primary immune deficiencies and women in their third trimester of pregnancy are at high risk of developing disseminated coccidioidomycosis [13,16,31]. Common concurrent conditions include: having an immunocompromised state, AIDS, Hodgkin's disease, other lymphomas, organ transplantation, and pregnancy [7,16]. Diabetes patients may also be at an increased risk of developing multiple thin-walled chronic lung cavities as a residual effect of infection [35]. Although coccidioidomycosis may cause up to 33% of the cases of community-acquired pneumonia in Arizona, less than 15% of these patients are tested for coccidioidomycosis, perhaps because many healthcare providers lack the experience and knowledge to treat the illness [36].

2.4.4. Occupation

Increased exposure to *Coccidioides* is an occupational hazard faced by individuals who work in outdoor environments close to the soil and dust including: archaeologists, military personnel, construction workers (especially those in excavation and pipeline or highway construction), cotton mill workers, and agricultural workers [13,25,37–40]. In particular, personnel engaged in digging operations in dusty soil are at highest risk for infection [38]. Professions, lifestyles, and hobbies requiring travel to endemic areas also put individuals at risk of exposure to *Coccidioides* [38]. Containing and reducing human exposure to dust has been recommended as a primary measure to reduce the risk of Valley fever [13].

2.5. Biology of pathogen

C. immitis and *C. posadasii* are dimorphic fungi of the phylum Ascomycota, in which most known human fungal pathogens belong. Proper biosafety protocols must be

observed when working with *Coccidioides* as the arthroconidia are very stable, can be viable for years under dry conditions, and are capable of becoming airborne once they are formed. Under most laboratory conditions (Sabouraud-dextrose agar, brain-heart infusion agar, potato-dextrose agar, and blood agar), *C. immitis* and *C. posadasii* require 5–10 days at room temperature to grow, forming a white highly filamentous aerial colony, which then turns tan [41]. This colony contains predominantly arthroconidia and long septated hyphae. Most soil fungi appear morphologically similar to *C. immitis* and *C. posadasii* at room temperature; however, only *Coccidioides* species are known to transition to the endosporulating spherule form (ranging in size from 10 to 100 microns) at mammalian physiological temperatures *in vitro* under inducing conditions and *in vivo* in animal infection models. The most successful technique to induce spherule formation *in vitro* is to culture the fungus in liquid modified Converse medium at 37–40 °C [42].

The sexual cycle of *Coccidioides* species has not yet been elucidated. Although sexual structures have not been observed in the laboratory for *Coccidioides* species, there is molecular and genetic evidence to suggest the existence of a sexual cycle in *Coccidioides*. For example, molecular phylogenetic analyses indicate that different *Coccidioides* strains have undergone recombination (rather than clonal growth) [43–46]. This work was also important in clarifying that *C. immitis* and *C. posadasii*, although very closely related, are distinct species undergoing separate sexual recombination events in nature. Subsequently, work on characterizing the mating type (*MAT*) locus, which is the genomic region regulating sexual reproduction in the fungal kingdom, identified the structure of the *MAT* locus in *C. posadasii* and *C. immitis* [47,48]. These studies found that *C. posadasii* and *C. immitis MAT* loci are arranged similarly to the *MAT* locus of *Histoplasma capsulatum*, suggesting that they have a heterothallic sexual cycle with alternating mating type genes found at a single locus. Indeed, population studies on *C. posadasii* and *C. immitis* isolates identified a 1:1 ratio of mating type alleles [48], providing further evidence for the existence of a sexual cycle in these species in nature.

2.5.1. Life cycle

C. immitis and *C. posadasii* are similar in their development and life cycle. The fungi have been reported to be found clustered around animal burrows and ancient Indian burial sites in high concentrations [49,50]. A mammalian host, such as a rodent, has been suggested to act as a carrier to spread the fungi throughout an endemic area [51]. *Coccidioides* is the only alternating arthroconidia species to contribute to systemic disease. *Coccidioides* species are dimorphic fungi with two distinct life cycle phases: saprophytic and parasitic (Fig. 3) [3,52].

During the saprophytic phase the fungus resides in the soil, where the mycelia, or thread-like hyphae, feed off its surrounding environment of nonliving and organic matter, such as rodent corpses, in the soil [7,51]. As the environment changes due to lack of nutrients or drying of the soil, the mycelia produce arthroconidia in alternating cells, where the arthroconidia are separated by dead cells [7,52,53]. Arthroconidia can remain viable for years in the soil and continue to germinate new mycelia if growth conditions are favorable [3,7]. The fungi are also resistant to harsh conditions, such as high temperatures and high salinity, particularly in the arthroconidia form [54].

Soil disruptions, such as agricultural activities or natural disasters, can disarticulate arthroconidia and release *Coccidioides* into the air to be carried by the wind or spread during dust storms [7,55,56]. Not only does this increase the distribution range of the spores, but also provides the opportunity to infect additional hosts. Inhalation of the arthroconidia leads to

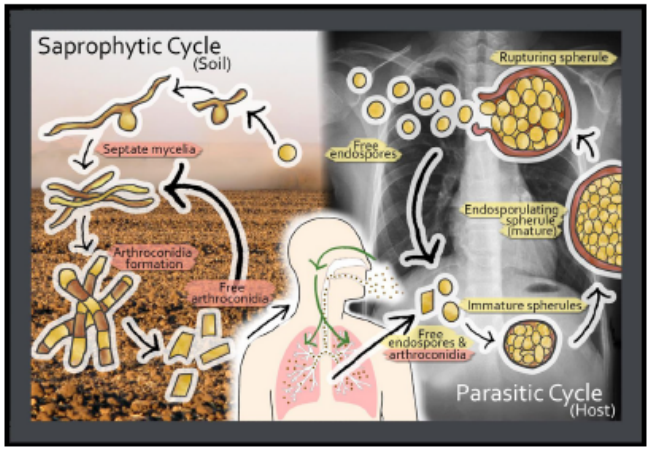

Fig. 3. *Coccidioides immitis* and *Coccidioides posadasii* life cycle in its two phases within the soil and host.

infection in humans, but has also been described to infect horses, rodents, snakes, cats, and dogs [53,57–59].

Once inside the host's body, the fungus transitions into its parasitic phase. The increased temperature and CO_2 concentration in the host contribute to the transformation of arthroconidia [3]. The barrel-shaped, 3–5 μm in size, arthroconidia begin to modify their cell wall to form a spherule with the cells inside rounding and swelling around a vacuole in the middle [3,53]. The structural changes distinguish the fungus in its parasitic phase. Endospores begin to differentiate around the vacuole and expand the spherule for about 3–4 days [3,53]. After developing hundreds of endospores, the spherule can rupture and spread its contents [3,53]. This results in further distribution of infection throughout the body, allowing the parasite to repeat its life cycle.

2.6. Pathology and pathogenesis

As noted above, the primary route of infection for most cases of coccidioidomycosis is through inhalation of arthroconidia into the lungs. Once the arthroconidia lodge in the terminal bronchioles, the fungus reverts to a spherical structure called a spherule; this structure enlarges and becomes filled with mature endospores. After several days of growth, the spherule ruptures releasing endospores into the surrounding tissue. Each endospore is then capable of producing another spherule [60]. Cellular immunity in the host is activated upon spherule formation as is evidenced by increased IL-17, IFNγ and TNFα production [61]. In most cases, the immune response controls the infection, and the infection is resolved without treatment. In biopsied tissue, there may be evidence for non-caseating granulomatous inflammation, and the spherules may be visible on tissue staining (Fig. 4). While the spherules may sometimes be seen on hematoxylin and eosin staining, they are best visualized using silver staining (Fig. 5).

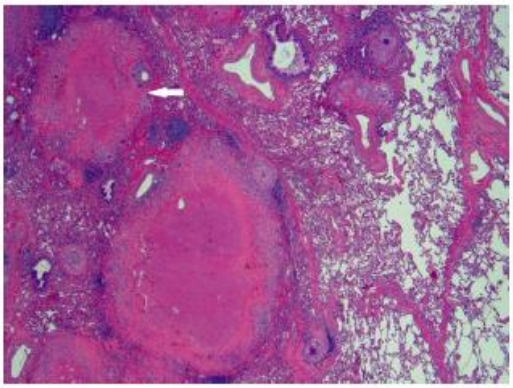

Fig. 4. Hematoxylin and eosin stain of a Valley Fever infected lung, demonstrating granulomatous inflammation. White arrow points to granuloma. Image courtesy of Dr. Williams Pitts (UCSF Fresno).

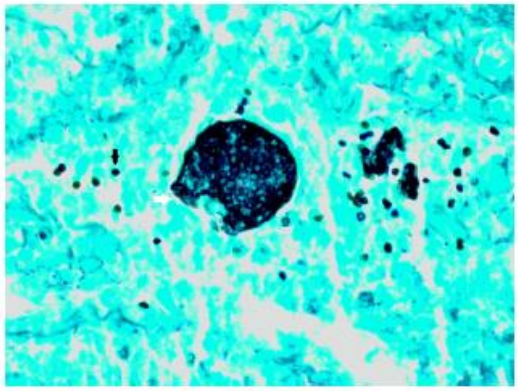

Fig. 5. Silver staining showing a spherule full of endospores with free endospores around it. Black arrow indicates an endospore, white arrow points to a spherule containing many endospores. Image courtesy of Dr. Williams Pitts (UCSF Fresno).

2.7. Immune response

2.7.1. Innate immune responses to Coccidioides

The vast majority of people develop only mild or asymptomatic disease following infection with *Coccidioides*, suggesting that the immune system normally controls infection. However, a subset of infections leads to chronic or severe disseminated disease, likely due to skewed or reduced immune responses that cannot control the fungal spread. Although innate and adaptive immune defects and immunosuppression increase the risk for severe infection, individuals with an apparently normal immune system, for unknown reasons, can also develop chronic and disseminated disease [7,17,62].

The innate immune system acts as the first line of defense against pathogens by recognizing and controlling the infection and activating the adaptive immune response. Little is known about how the innate immune system recognizes, attempts to control, and eliminates the fungal infection, particularly during a productive host immune response. Polymorphonuclear leukocytes (PMNs) are the first responders to *Coccidioides* infection [63]. However, the respiratory burst by these cells kills fewer than twenty percent of the arthroconidia and may drive maturation to the spherule form of *Coccidioides*. Spherules are further resistant to phagocytosis and killing by PMNs due to their large size and potential inhibition of host responses by fungal proteins [64]. Macrophages also phagocytose the arthroconidia and endospores, but may have low killing ability due to specific inhibition of phagosome–lysosome fusion by the fungus [65]. Conflicting results suggest that T cells enhance the ability of macrophages to digest arthroconidia and endospores, but only if T cells are primed before infection. Macrophage functional enhancement by T cells is mediated by IFNγ and TNFα [66].

Different proteins, lipids and genomic material found on and within pathogen subsets termed pathogen-associated molecular patterns (PAMPs) can be recognized by pathogen-

recognition receptors (PRRs) on antigen presenting cells. Recognition of *Coccidioides* by a subset of these PRRs, Toll-like receptor 2 (TLR2) and TLR4, promotes TNFα production and mediates a cell-mediated response to *Coccidioides in vitro* [67,68]. Another PRR important in recognition of fungal invasion, dectin-1, appears to promote innate immune cells to direct T_h1 and T_h17 effector responses in part by reducing inflammatory cytokine production [69]. Additionally, several *Coccidioides* antigens have been identified with variable ability to induce adaptive immune responses [68].

Dendritic cells (DC), as professional antigen presenting cells (APCs), are a critical link between innate and adaptive immune responses. *Coccidioides* antigens induce maturation, and activation of DCs and *Coccidioides* antigen-pulsed DCs can reverse the lymphocyte anergy found in disseminated disease [70]. IL-12-induced T_h1 responses are critical for effective/productive immunity against *Coccidioides* infection. DCs are a major source of IL-12, and activated DCs present antigen and costimulatory signals to naïve T cells; thus, DCs might be expected to play an important role in host immune responses to *Coccidioides*. Together, the few studies evaluating DC responses during coccidioidomycosis suggest that DC activation and antigen presentation is functional in patients with disseminated disease [3]. However, it is unclear whether the DCs in these patients promote an effective or detrimental response to *Coccidioides*. Perhaps the DCs in patients with disseminated disease induce ineffective *T* helper effector responses or promote immune tolerance. One study characterizing DC functions in mouse models of infection found higher TLR2, TLR4 and costimulatory molecule expression and IL-12 production in DCs of resistant mouse strains, compared to susceptible mouse strains [71].

2.7.2. *Adaptive immune responses to* Coccidioides

Coccidioidomycosis induces both cell-mediated and humoral immune responses. Protective immunity requires a strong T_h1 skewed response resulting in production of IFNγ and IgG2a antibodies. Asymptomatic immune patients demonstrate a strong delayed-type hypersensitivity (DTH) reaction and low levels of complement forming antibodies in their serum, while severe disease is usually found in patients with low DTH reactions and high titers of complement forming antibodies [70,72]. Recovery from severe disease is associated with decreased complement forming antibodies and increased DTH reaction [70]. Symptomatic patients develop T cell anergy against *Coccidioides* that is generally specific for this fungus and is reversible with disease remission [70,73,74].

It would therefore appear that humoral immunity plays a weak role in protection against this infection. As outlined above, the titer of complement forming antibodies correlates well with disease severity. In further support, serum from vaccinated mice does not protect from arthrospore infection, or depending upon the analysis, is less critical than T cells for protection [75]. However, using a vaccine model, it was found that vaccine protection is less effective in the absence of B cells, and that a B cell gene expression profile is associated with protection to arthroconidia [76]. Thus, the role of B cells and antibodies in controlling infection or protection against repeat exposure remains unclear.

Further evidence supporting the critical role of T cells in immunity to *Coccidioides* has been demonstrated using mouse models of infection and evaluation of risk severity in patients. Mice lacking $CD4^+$ or $CD8^+$ T cells are more susceptible to disease, and T cells transfer protection to naive animals [77,78]. There is a high risk for dissemination and death in immunosuppressed individuals during organ transplant, HIV infection and neoplasia [79]. In HIV patients, the risk of severe disease increases with lower $CD4^+$ T cell numbers [80].

The type of effector T cell response mounted against *Coccidioides* appears to determine disease severity. T_h1 effector responses, particularly IFNγ and TNFα production, are widely accepted as providing protective immunity against *Coccidioides* that results primarily in mild or asymptomatic disease. Assessment of T cell activation by CD69 expression in coccidioidomycosis correlates with T_h1 effector cytokines and has been suggested to be a potential marker for measuring a productive cellular response to *Coccidioides* [81]. In contrast, T_h2 effector cytokine responses have largely been associated with more severe disease, perhaps in part due to the ability of these cells to suppress macrophage activation and T_h1 differentiation. While T_h2-associated cytokines decrease productive immune responses against *Coccidioides* in mice, in patients it is unclear if T_h2 effectors have any direct effects on immunity to *Coccidioides*, and overall T_h2 cytokines are not produced in response to *Coccidioides* antigens [3,82]. T_h17 effector responses have not yet been measured in patients with coccidioidomycosis; however, evaluation of infection in immunized mice indicates that disease susceptibility increases with the loss of T_h17 functionality [83].

Regulatory T (Treg) cells are known to modulate immunity during infection and their suppressive function can be beneficial or detrimental depending upon the site or stage of an infection. Very little data exists evaluating the impact of Treg cells on coccidioidomycosis. Reduced survival following infection in phagocytic NADPH oxidase-deficient mice correlated with an expanded Treg cell population in the lung [84]. IL-10 producing cells, that may be secreted by Treg cells or T_h2 cells, have been found in clusters adjacent to granulomata during coccidioidomycosis [85]. However, the role and relative importance of IL-10 production in the granuloma and Treg presence in the lung is unknown.

2.7.3. *Immune evasion by* Coccidioides

Most pathogens utilize multiple mechanisms to escape host immune detection, and *Coccidioides* expresses several documented virulence factors that contribute to infection [86,87]. As noted above, arthroconidia and spherules are highly resistant to destruction by PMNs. The outer wall of arthroconidia appears to protect from phagocytosis, as removing the outer wall increases uptake of the arthroconidia. In contrast, the immune system builds a response against the spherule outer wall glycoprotein (SOWgp). *Coccidioides* endospores do not express SOWgp, thus avoiding immune detection by cells responsive to this antigen during a time when *Coccidioides*

can be more efficiently phagocytosed. The spherules are further protected from the immune system by the production of proteases that digest antibodies. Finally, *Coccidioides* produces urease and induces host production of arginase I, both of which contribute to local tissue damage and enhance infection. Thus, while the host immune system fights to actively block infection or eliminate *Coccidioides*, the fungus has its own mechanisms to circumvent, avoid or prevent immune surveillance.

2.8. Diagnosis and treatment

2.8.1. Diagnosis

Early diagnosis of coccidioidomycosis is significant to prevent disseminated disease, to reduce costs of hospitalizations and treatment, and to avoid persistent infection leading to tissue damage or death [2]. However, it is difficult to diagnose early infection for a couple of reasons. As described above, most individuals are asymptomatic. Some people exhibit flu-like symptoms, but do not seek medical evaluation because their immune system resolves the infection over time without medication. This also contributes to an underestimate of reported annual coccidioidomycosis cases. These limitations in self-diagnosis can lead to severe symptoms of chronic pneumonia, meningitis, or bone and joint infection if the infection becomes a disseminated disease [3].

Individuals with coccidioidomycosis also have difficulties obtaining proper diagnosis from clinicians and laboratory testing. One assessment for patients who have persistent lung infection is to obtain a radiographic examination. The results are frequently misinterpreted and patients are diagnosed with lung cancer, even though they may be infected with *Coccidioides*, which gives similar results on the X-ray [88]. There are other laboratory tests used to identify coccidioidomycosis, but they have limitations. Two commonly used diagnostic tests, enzyme immunoassay testing and sputum testing, help determine if a patient has been infected with *Coccidioides*. Enzyme immunoassay testing uses a patient's blood sample to measure *Coccidioides* antibodies. However, as many as 82% false-positive results for coccidioidomycosis have been reported with the antibody test [89]. These findings question the utility of the test for clinicians to diagnose the infection. Sputum culture requires a more invasive procedure to collect the sample, but provides a more accurate result for diagnosis. Doctors can also evaluate patients by performing biopsies, joint effusions, or lumbar punctures [2].

2.8.2. Treatment

Most patients resolve coccidioidomycosis without need of treatment. However, patients with chronic pulmonary or disseminated disease may require antifungal therapy [2]. Common antifungal drugs prescribed include: amphotericin B deoxycholate, lipid formulations of amphotericin, ketoconazole, fluconazole, and itraconazole [2]. Even though treatment is beneficial in clearance of infection, it may come at a cost to the patient, both financially and physically. Patients who require long term medication of antifungal drugs can spend up to $20,000 annually on top of hospital bills [2]. Harmful side effects are associated with using antifungal drugs, such as amphotericin B, which span from mild symptoms of nausea, vomiting, fever, and hypoxia, to severe side effects of anemia, hypertension, hyperthermia, and dyspnea [90]. Routine follow-ups to the physician are recommended after clearance of infection every 3–6 months for about 2 years to prevent developing further complications or disseminated disease [2]. However, chronically-infected patients may need long term follow-up through examinations and laboratory testing.

While there is limited data available for successful outcomes of treatment of immunocompromised individuals, one study demonstrated a significant reduction in relative risk for developing symptomatic coccidioidomycosis among patients treated with infliximab, a TNFα antagonist used for patients with autoimmune disease [91].

2.8.3. Vaccines

The development of a successful coccidioidomycosis vaccine has long been a research goal despite numerous challenges. A successful vaccine should show protective efficacy for both immuno competent and immunocompromised individuals [92]. Many vaccines developed to protect against coccidioidomycosis have failed to show conclusive results for various reasons, some of which we summarize below. Vaccines containing killed organisms have shown optimum protection in animal models but failed in human Phase III trials due to inadequate dosing. These vaccines also resulted in major side effects and pain, which presented an additional issue. One potential solution for improving these killed vaccines is to eliminate side effects while preserving the key immunogens by fractioning the vaccine components [93]. Other vaccine trials in humans, which utilized auxotrophic mutants or attenuated live organisms, showed some survival advantages but failed to completely clear the fungus. Due to the inherent potential risk of reversion to virulence of an attenuated mutant that exists for a live vaccine, recombinant proteins such as rAg_2/Pra, rGel1, and CSA, have been pursued for vaccine trials. The majority of the recombinant antigens of *Coccidioides* have failed to meet the benchmark of protection required in murine vaccine trials [3]. Since these candidate vaccines failed to show necessary protection and ability to stimulate an effective immune response during animal testing, they will not be tested in humans.

Recent research has shown that vaccines with purified plasmid DNA provide superior protection against coccidioidomycosis [92]. Currently, research is focused on pursuing a potential adjuvant vaccine designed to stimulate the appropriate level of immune response [92]. Another line of research for a new potential vaccine involves complementary DNA expression library immunization (ELI), which is under development along with use of parasitic cell wall proteins. Parasitic cell wall proteins can stimulate protective immunity against *C. posadasii* infection in mice and are considered the most protective antigens against coccidioidomycosis thus far [94].

3. Concluding remarks

Research and recognition of coccidioidomycosis has progressed slowly since the first patient was diagnosed in 1892. However, increasing awareness of coccidioidomycosis can contribute to improving methods to prevent and combat this disease. Prevention is the first step to managing this fungal infection. One way to do so is by locating areas with high prevalence of *Coccidioides*. Because the fungus is endemic to certain regions of the United States, researchers can study soil sampling in those areas. In turn, the public can be informed to be cautious when a particular site contains high levels of *Coccidioides*. Further improvement in technology of an on-site test for *Coccidioides* in the soil could add the benefit for turnaround time of evaluating a potential habitat for the fungus. Another preventive measure would be to understand the weather patterns during increased coccidioidomycosis cases. Dry periods after wet winters or summer have been associated with an increase in the rate of coccidioidomycosis cases for California and Arizona [53]. Collecting data on temperature changes and wind patterns, along with reports of coccidioidomycosis, will be informative in assessing correlations between environmental changes and infection rates. With these findings, individuals can consider seeking medical attention if they have symptoms related to Valley Fever during periods of increased likelihood of infection. Remaining indoors during dust storms, for example, provides a preventive approach against exposure to arthroconidia.

Improving diagnostic testing and early detection can also increase prevention of disseminated disease. Not only could patients benefit from early recognition, but also a more accurate number of reported cases could be tracked. Monitoring patients during acute infection could in understanding the mechanisms and progression of disease. This is critical in filling gaps in knowledge of Valley Fever for physicians. One uncertainty is whether a patient needs to be treated with antifungal drugs. If treatment is found to be needed, it is not known which drug is most effective, which dosage should be administrated, and what should be the duration of usage. Another question to be addressed is when a patient has cleared infection, how long should the patient continue to be followed-up?

Further research in the development and proliferation of the fungus in the host can aid in our understanding of an effective approach to clear the pathogen. It is unclear what regulatory events contribute to the transformation of arthroconidia into spherules after entry into the body. Characterizing the signaling for the transformation could contribute to preventing early infection. Studying the fungus could also contribute to the development of a vaccine. A number of vaccines have been developed and tested. Indeed, several coccidioidal antigens have shown protective properties against the fungus in animal models. Thus far, however, a successful vaccine showing long term immunity in humans has not yet been achieved [95–97]. Overall, the approach to resolve this hidden danger in a dust cloud is to improve detection methods for *Coccidioides*, improve reporting of infection cases, and better understand the immune response as a way of predicting which patients are at risk for disseminated disease.

Conflict of interest

The authors declare that they have no conflict of interest.

Acknowledgments

We thank Trevor P. Hirst from the Health Sciences Research Institute (HSRI) at UC Merced for acquiring the photograph of the tractor and creating the map outlining the distribution of coccidioidomycosis. We are grateful to Caroline Chen for her contributions to the graphical design of the fungal life cycle. CJN and KH were supported by the National Institutes of Health (NIH) grants K99AI100896 and R00HL090706, respectively. Research on Valley Fever at UC Merced is supported by the UC Merced Blum Center for Developing Economies, the UC Merced HSRI, a University of California Presidential Chair, and Children's Hospital Central California.

References

[1] Smith CE. Epidemiology of acute coccidioidomycosis with erythema nodosum ("San Joaquin" or "Valley Fever"). Am J Public Health Nations Health 1940;30:600–11.
[2] Galgiani JN, Ampel NM, Blair JE, Catanzaro A, Johnson RH, Stevens DA, et al. Coccidioidomycosis. Clin Infect Dis 2005;41:1217–23.
[3] Cox RA, Magee DM. Coccidioidomycosis: host response and vaccine development. Clin Microbiol Rev 2004;17:804–39.
[4] Sondermeyer G, Lee L, Gilliss D, Tabnak F, Vugia D. Coccidioidomycosis-associated hospitalizations, California, USA, 2000–2011. Emerg Infect Dis 2013;19:1590–8.
[5] Blair JE, Logan JL. Coccidioidomycosis in solid organ transplantation. Clin Infect Dis 2001;33:1536–44.
[6] Williams PL, Sable DL, Mendez P, Smyth LT. Symptomatic coccidioidomycosis following a severe natural dust storm. An outbreak at the Naval Air Station, Lemoore, Calif. Chest 1979;76:566–70.
[7] Hector RF, Laniado-Laborin R. Coccidioidomycosis—a fungal disease of the Americas. PLoS Med 2005;2:e2.
[8] Fisher MC, Koenig GL, White TJ, Taylor JW. Molecular and phenotypic description of *Coccidioides posadasii* sp. nov., previously recognized as the non-California population of *Coccidioides immitis*. Mycologia 2002;94:73–84.
[9] Campins H. Coccidioidomycosis in South America. A review of its epidemiology and geographic distribution. Mycopathol Mycol Appl 1970;41:25–34.
[10] Hurst S, Gade L, Marsden-Haug N, Engelthaler D, Hill H, Ralston C, et al. Molecular detection and isolation of *Coccidioides* immitis from soil in Washington State. In: Cocci study group 58th annual meeting, Phoenix, Arizona; 2014.
[11] Posada A. Un nuevo caso de micosis fungoidea con psorosperm ias. Anales del Circulo Medico Argent 1892;15:585–97.
[12] Sunenshine RH, Anderson S, Erhart L, Vossebrink A, Kelly PC, Engelthaler D, et al. Public health surveillance for coccidioidomycosis in Arizona. Ann N Y Acad Sci 2007;1111:96–102.
[13] Kirkland TN, Fierer J. Coccidioidomycosis: a reemerging infectious disease. Emerg Infect Dis 1996;2:192.
[14] Laniado-Laborin R. Expanding understanding of epidemiology of coccidioidomycosis in the Western hemisphere. Ann N Y Acad Sci 2007;1111:19–34.

[15] Hirschmann JV. The early history of coccidioidomycosis: 1892-1945. Clin Infect Dis 2007;44:1202–7.
[16] Sondermeyer G, Lee L, Gilliss D, Tabnak F, Vugia D. Coccidioidomycosis-associated hospitalizations, California, USA, 2000–2011. Emerg Infect Dis 2013;19.
[17] Stevens DA. Coccidioidomycosis. N Engl J Med 1995;332:1077–82.
[18] Laniado-Laborín R. Coccidioidomycosis and other endemic mycoses in Mexico. Rev Iberoam Micol 2007;24:249.
[19] Seitz AE, Prevots DR, Holland SM. Hospitalizations associated with disseminated coccidioidomycosis, Arizona and California, USA. Emerg Infect Dis 2012;18:1476.
[20] Smith CE, Beard RR. Varieties of coccidioidal infection in relation to the epidemiology and control of the diseases. Am J Public Health Nations Health 1946;36:1394–402.
[21] Faber HK, Smith CE, Dickson EC. Acute coccidioidomycosis with erythema nodosum in children. J Pediatr 1939;15:163–71.
[22] Galgiani JN. Coccidioidomycosis: changing perceptions and creating opportunities for its control. Ann N Y Acad Sci 2007;1111:1–18.
[23] Parish JM, Blair JE. Coccidioidomycosis. In: Mayo Clin Proceedings. Elsevier; 2008. pp. 343–9.
[24] Chaturvedi V, Ramani R, Gromadzki S, Rodeghier B, Chang H-G, Morse DL. Coccidioidomycosis in New York state. Emerg Infect Dis 2000;6:25.
[25] Hector RF, Rutherford GW, Tsang CA, Erhart LM, McCotter O, Anderson SM, et al. The public health impact of coccidioidomycosis in Arizona and California. Int J Environ Res Publ 2011;8:1150–73.
[26] Pappagianis D. Epidemiology of coccidioidomycosis. In: Curr Top Med Mycol. Springer; 1988. pp. 199–238.
[27] Crum NF, Lederman ER, Stafford CM, Parrish JS, Wallace MR. Coccidioidomycosis: a descriptive survey of a reemerging disease. clinical characteristics and current controversies. J Med 2004;83:149–75.
[28] Pappagianis D. Coccidioidomycosis. Semin Dermatol 1993:301.
[29] Pappagianis D, Lindsay S, Beall S, Williams P. Ethnic background and the clinical course of coccidioidomycosis. Am Rev Respir Dis 1979;120:959–61.
[30] Louie L, Ng S, Hajjeh R, Johnson R, Vugia D, Werner SB, et al. Influence of host genetics on the severity of coccidioidomycosis. Emerg Infect Dis 1999;5:672.
[31] Hector R, Rutherford GW. The public health need and present status of a vaccine for the prevention of coccidioidomycosis. Ann N Y Acad Sci 2007;1111:259–68.
[32] Einstein HE, Johnson RH. Coccidioidomycosis: new aspects of epidemiology and therapy. Clin Infect Dis 1993:349–54.
[33] Rosenstein NE, Emery KW, Werner SB, Kao A, Johnson R, Rogers D, et al. Risk factors for severe pulmonary and disseminated coccidioidomycosis: Kern County, California, 1995–1996. Clin Infect Dis 2001;32:708–14.
[34] McCarty JM, Demetral LC, Dabrowski L, Kahal AK, Bowser AM, Hahn JE. Pediatric coccidioidomycosis in central California: a retrospective case series. Clin Infect Dis 2013;56:1579–85.
[35] Baker EJ, Hawkins JA, Waskow EA. Surgery for coccidioidomycosis in 52 diabetic patients with special reference to related immunologic factors. J Thorac Cardiovasc Surg 1978;75:680–7.
[36] Chen S, Erhart LM, Anderson S, Komatsu K, Park B, Chiller T, et al. Coccidioidomycosis: knowledge, attitudes, and practices among healthcare providers-Arizona, 2007. Med Mycol 2011;49:649–56.
[37] Petersen LR, Marshall SL, Barton C, Hajjeh RA, Lindsley MD, Warnock DW, et al. Coccidioidomycosis among workers at an archeological site, northeastern Utah. Emerg Infect Dis 2004;10:637.
[38] Sipsas NV, Kontoyiannis DP. Occupation, lifestyle, diet, and invasive fungal infections. J Infect 2008;36:515–25.
[39] Cummings KC, McDowell A, Wheeler C, McNary J, Das R, Vugia DJ, et al. Point-source outbreak of coccidioidomycosis in construction workers. Epidemiol Infect 2010;138:507–11.
[40] Gehlbach SH, Hamilton JD, Conant NF. Coccidioidomycosis: an occupational disease in cotton mill workers. Arch Intern Med 1973;131:254.
[41] Welsh O, Vera-Cabrera L, Rendon A, Gonzalez G, Bonifaz A. Coccidioidomycosis. Clin Dermatol 2012;30:573–91.
[42] Depiazzi LJ, Roberts WD, Hawkins CD, Palmer MA, Pitman DR, McQuade NC, et al. Severity and persistence of footrot in Merino sheep experimentally infected with a protease thermostable strain of *Dichelobacter nodosus* at five sites. Aust Vet J 1998;76:32–8.
[43] Burt A, Carter DA, Koenig GL, White TJ, Taylor JW. Molecular markers reveal cryptic sex in the human pathogen *Coccidioides immitis*. Proc Natl Acad Sci U S A 1996;93:770–3.
[44] Fisher MC, Koenig G, White TJ, Taylor JW. A test for concordance between the multilocus genealogies of genes and microsatellites in the pathogenic fungus *Coccidioides immitis*. Mol Biol Evol 2000;17:1164–74.
[45] Koufopanou V, Burt A, Taylor JW. Concordance of gene genealogies reveals reproductive isolation in the pathogenic fungus *Coccidioides immitis*. Proc Natl Acad Sci U S A 1997;94:5478–82.
[46] Koufopanou V, Burt A, Szaro T, Taylor JW. Gene genealogies, cryptic species, and molecular evolution in the human pathogen *Coccidioides immitis* and relatives (Ascomycota, Onygenales). Mol Biol Evol 2001;18:1246–58.
[47] Fraser JA, Stajich JE, Tarcha EJ, Cole GT, Inglis DO, Sil A, et al. Evolution of the mating type locus: insights gained from the dimorphic primary fungal pathogens *Histoplasma capsulatum*, *Coccidioides immitis*, and *Coccidioides posadasii*. Eukaryot Cell 2007;6:622–9.
[48] Mandel MA, Barker BM, Kroken S, Rounsley SD, Orbach MJ. Genomic and population analyses of the mating type loci in *Coccidioides* species reveal evidence for sexual reproduction and gene acquisition. Eukaryot Cell 2007;6:1189–99.
[49] Lacy GH, Swatek FE. Soil ecology of *Coccidioides immitis* at Amerindian middens in California. Appl Microbiol 1974;27:379–88.
[50] Maddy KT. The geographic distribution of *Coccidioides immitis* and possible ecologic implications. Ariz Med 1958;15:178–88.
[51] Greene DR, Koenig G, Fisher MC, Taylor JW. Soil isolation and molecular identification of *Coccidioides immitis*. Mycologia 2000;92:406–10.
[52] Huppert M, Sun SH, Harrison JL. Morphogenesis throughout saprobic and parasitic cycles of *Coccidioides immitis*. Mycopathologia 1982;78:107–22.
[53] Nguyen C, Barker BM, Hoover S, Nix DE, Ampel NM, Frelinger JA, et al. Recent advances in our understanding of the environmental, epidemiological, immunological, and clinical dimensions of coccidioidomycosis. Clin Microbiol Rev 2013;26:505–25.
[54] Egeberg RO, Elconin AE, Egeberg MC. Effect of salinity and temperature on *Coccidioides immitis* and three antagonistic soil saprophytes. J Bacteriol 1964;88:473–6.
[55] Schieffelin JS, Torrellas M, Lartchenko S, Gill F, Garcia-Diaz J, McGoey R. How natural disasters change natural patterns: coccidioidomycosis imported to New Orleans. J La State Med Soc 2013;165:145–9.
[56] Centers for Disease Control and Prevention, (CDC). Sources of coccidioidomycosis (Valley fever); 2013.
[57] Ziemer EL, Pappagianis D, Madigan JE, Mansmann RA, Hoffman KD. Coccidioidomycosis in horses: 15 cases (1975–1984). J Am Vet Med Assoc 1992;201:910–6.
[58] Graupmann-Kuzma A, Valentine BA, Shubitz LF, Dial SM, Watrous B, Tornquist SJ. Coccidioidomycosis in dogs and cats: a review. J Am Anim Hosp Assoc 2008;44:226–35.
[59] Timm KI, Sonn RJ, Hultgren BD. Coccidioidomycosis in a Sonoran gopher snake, *Pituophis melanoleucus affinis*. J Med Vet Mycol 1988;26:101–4.
[60] Saubolle MA, McKellar PP, Sussland D. Epidemiologic, clinical, and diagnostic aspects of coccidioidomycosis. J Clin Microbiol 2007;45:26–30.
[61] Nesbit LA, Knox KS, Nguyen CT, Roesch J, Wheat LJ, Johnson SM, et al. Immunological characterization of bronchoalveolar lavage fluid in patients with acute pulmonary coccidioidomycosis. J Infect Dis 2013;208:857–63.
[62] Ampel NM. New perspectives on coccidioidomycosis. Proc Am Thorac Soc 2010;7:181–5.

[63] Drutz DJ, Huppert M. Coccidioidomycosis: factors affecting the host-parasite interaction. J Infect Dis 1983;147:372–90.
[64] Frey CL, Drutz DJ. Influence of fungal surface components on the interaction of *Coccidioides immitis* with polymorphonuclear neutrophils. J Infect Dis 1986;153:933–43.
[65] Beaman L, Holmberg CA. In vitro response of alveolar macrophages to infection with *Coccidioides immitis*. Infect Immun 1980;28:594–600.
[66] Beaman L. Effects of recombinant gamma interferon and tumor necrosis factor on in vitro interactions of human mononuclear phagocytes with *Coccidioides immitis*. Infect Immun 1991;59:4227–9.
[67] Viriyakosol S, Fierer J, Brown GD, Kirkland TN. Innate immunity to the pathogenic fungus *Coccidioides posadasii* is dependent on Toll-like receptor 2 and Dectin-1. Infect Immun 2005;73:1553–60.
[68] Ampel NM. The complex immunology of human coccidioidomycosis. Ann N Y Acad Sci 2007;1111:245–58.
[69] Viriyakosol S, Jimenez Mdel P, Gurney MA, Ashbaugh ME, Fierer J. Dectin-1 is required for resistance to coccidioidomycosis in mice. MBio 2013;4. e00597–12.
[70] Cox RA, Vivas JR. Spectrum of in vivo and in vitro cell-mediated immune responses in coccidioidomycosis. Cell Immunol 1977;31:130–41.
[71] Awasthi S, Magee DM. Differences in expression of cell surface co-stimulatory molecules, Toll-like receptor genes and secretion of IL-12 by bone marrow-derived dendritic cells from susceptible and resistant mouse strains in response to *Coccidioides posadasii*. Cell Immunol 2004;231:49–55.
[72] Ampel NM. Measurement of cellular immunity in human coccidioidomycosis. Mycopathologia 2003;156:247–62.
[73] Smith CE, Beard RR, Saito MT. Pathogenesis of coccidioidomycosis with special reference to pulmonary cavitation. Ann Intern Med 1948;29:623–55.
[74] Ibrahim AB, Pappagianis D. Experimental induction of anergy to coccidioidin by antigens of *Coccidioides immitis*. Infect Immun 1973;7:786–94.
[75] Beaman LV, Pappagianis D, Benjamini E. Mechanisms of resistance to infection with *Coccidioides immitis* in mice. Infect Immun 1979;23:681–5.
[76] Magee DM, Friedberg RL, Woitaske MD, Johnston SA, Cox RA. Role of B cells in vaccine-induced immunity against coccidioidomycosis. Infect Immun 2005;73:7011–3.
[77] Beaman L, Pappagianis D, Benjamini E. Significance of T cells in resistance to experimental murine coccidioidomycosis. Infect Immun 1977;17:580–5.
[78] Fierer J, Waters C, Walls L. Both CD4+ and CD8+ T cells can mediate vaccine-induced protection against *Coccidioides immitis* infection in mice. J Infect Dis 2006;193:1323–31.
[79] Centers for Disease Control and Prevention, (CDC). Coccidioidomycosis (Valley fever) (*Coccidioides* spp.); 2012.
[80] Ampel NM, Dols CL, Galgiani JN. Coccidioidomycosis during human immunodeficiency virus infection: results of a prospective study in a coccidioidal endemic area. Am J Med 1993;94:235–40.
[81] Ampel NM, Kramer LA, Li L, Carroll DS, Kerekes KM, Johnson SM, et al. In vitro whole-blood analysis of cellular immunity in patients with active coccidioidomycosis by using the antigen preparation T27K. Clin Diagn Lab Immunol 2002;9:1039–43.
[82] Corry DB, Ampel NM, Christian L, Locksley RM, Galgiani JN. Cytokine production by peripheral blood mononuclear cells in human coccidioidomycosis. J Infect Dis 1996;174:440–3.
[83] Hung CY, Gonzalez A, Wuthrich M, Klein BS, Cole GT. Vaccine immunity to coccidioidomycosis occurs by early activation of three signal pathways of T helper cell response (Th1, Th2, and Th17). Infect Immun 2011;79:4511–22.
[84] Gonzalez A, Hung CY, Cole GT. Absence of phagocyte NADPH oxidase 2 leads to severe inflammatory response in lungs of mice infected with *Coccidioides*. Microb Pathog 2011;51:432–41.
[85] Li L, Dial SM, Schmelz M, Rennels MA, Ampel NM. Cellular immune suppressor activity resides in lymphocyte cell clusters adjacent to granulomata in human coccidioidomycosis. Infect Immun 2005;73:3923–8.
[86] Hung CY, Xue J, Cole GT. Virulence mechanisms of *Coccidioides*. Ann N Y Acad Sci 2007;1111:225–35.
[87] Galgiani JN. Coccidioidomycosis. West J Med 1993;159:153–71.
[88] Petrini B, Skold CM, Bronner U, Elmberger G. Coccidioidomycosis mimicking lung cancer. Respiration 2003;70:651–4.
[89] Kuberski T, Herrig J, Pappagianis D. False-positive IgM serology in coccidioidomycosis. J Clin Microbiol 2010;48:2047–9.
[90] Laniado-Laborin R, Cabrales-Vargas MN. Amphotericin B: side effects and toxicity. Rev Iberoam Micol 2009;26:223–7.
[91] Bergstrom L, Yocum DE, Ampel NM, Villanueva I, Lisse J, Gluck O, et al. Increased risk of coccidioidomycosis in patients treated with tumor necrosis factor alpha antagonists. Arthritis Rheum 2004;50:1959–66.
[92] Cole GT, Hung CY, Sanderson SD, Hurtgen BJ, Wuthrich M, Klein BS, et al. Novel strategies to enhance vaccine immunity against coccidioidomycosis. PLoS Pathog 2013;9:e1003768.
[93] Yoon HJ, Clemons KV. Vaccines against *coccidioides*. Korean J Intern Med 2013;28:403–7.
[94] Tarcha EJ, Basrur V, Hung CY, Gardner MJ, Cole GT. Multivalent recombinant protein vaccine against coccidioidomycosis. Infect Immun 2006;74:5802–13.
[95] Pappagianis D. Evaluation of the protective efficacy of the killed *Coccidioides immitis* spherule vaccine in humans. The Valley fever vaccine study Group. Am Rev Respir Dis 1993;148:656–60.
[96] Levine HB, Miller RL, Smith CE. Influence of vaccination on respiratory coccidioidal disease in cynomolgus monkeys. J Immunol 1962;89:242–51.
[97] Johnson SM, Lerche NW, Pappagianis D, Yee JL, Galgiani JN, Hector RF. Safety, antigenicity, and efficacy of a recombinant coccidioidomycosis vaccine in cynomolgus macaques (*Macaca fascicularis*). Ann N Y Acad Sci 2007;1111:290–300.

References

1. Petersen, P.E. and H. Ogawa, *The global burden of periodontal disease: towards integration with chronic disease prevention and control.* Periodontol 2000, 2012. **60**(1): p. 15-39.
2. Petersen, P.E., et al., *Global oral health of older people--call for public health action.* Community Dent Health, 2010. **27**(4 Suppl 2): p. 257-67.
3. Loesche, W.J. and N.S. Grossman, *Periodontal disease as a specific, albeit chronic, infection: diagnosis and treatment.* Clin Microbiol Rev, 2001. **14**(4): p. 727-52, table of contents.
4. Weidlich, P., et al., *Association between periodontal diseases and systemic diseases.* Braz Oral Res, 2008. **22 Suppl 1**: p. 32-43.
5. Armitage, G.C., *Periodontal diagnoses and classification of periodontal diseases.* Periodontol 2000, 2004. **34**: p. 9-21.
6. Socransky, S.S. and A.D. Haffajee, *Evidence of bacterial etiology: a historical perspective.* Periodontol 2000, 1994. **5**: p. 7-25.
7. Darveau, R.P., *Periodontitis: a polymicrobial disruption of host homeostasis.* Nat Rev Microbiol, 2010. **8**(7): p. 481-90.
8. Hasegawa, Y., et al., *Gingival epithelial cell transcriptional responses to commensal and opportunistic oral microbial species.* Infect Immun, 2007. **75**(5): p. 2540-7.
9. DiRienzo, J.M., *Breaking the Gingival Epithelial Barrier: Role of the Aggregatibacter actinomycetemcomitans Cytolethal Distending Toxin in Oral Infectious Disease.* Cells, 2014. **3**(2): p. 476-99.
10. Yilmaz, O., et al., *Intercellular spreading of Porphyromonas gingivalis infection in primary gingival epithelial cells.* Infect Immun, 2006. **74**(1): p. 703-10.
11. Kuboniwa, M. and R.J. Lamont, *Subgingival biofilm formation.* Periodontol 2000, 2010. **52**(1): p. 38-52.
12. Zilm, P.S. and A.H. Rogers, *Co-adhesion and biofilm formation by Fusobacterium nucleatum in response to growth pH.* Anaerobe, 2007. **13**(3-4): p. 146-52.
13. Saito, Y., et al., *Stimulation of Fusobacterium nucleatum biofilm formation by Porphyromonas gingivalis.* Oral Microbiol Immunol, 2008. **23**(1): p. 1-6.
14. Diaz, P.I., P.S. Zilm, and A.H. Rogers, *Fusobacterium nucleatum supports the growth of Porphyromonas gingivalis in oxygenated and carbon-dioxide-depleted environments.* Microbiology, 2002. **148**(Pt 2): p. 467-72.
15. Rosen, G. and M.N. Sela, *Coaggregation of Porphyromonas gingivalis and Fusobacterium nucleatum PK 1594 is mediated by capsular polysaccharide and lipopolysaccharide.* FEMS Microbiol Lett, 2006. **256**(2): p. 304-10.
16. Park, O.J., et al., *Pyrosequencing Analysis of Subgingival Microbiota in Distinct Periodontal Conditions.* J Dent Res, 2015.
17. Ali, R.W., et al., *Prevalence of 6 putative periodontal pathogens in subgingival plaque samples from Romanian adult periodontitis patients.* J Clin Periodontol, 1996. **23**(2): p. 133-9.
18. Saito, A., et al., *Fusobacterium nucleatum enhances invasion of human gingival epithelial and aortic endothelial cells by Porphyromonas gingivalis.* FEMS Immunol Med Microbiol, 2008. **54**(3): p. 349-55.

19. Socransky, S.S., *Criteria for the infectious agents in dental caries and periodontal disease.* J Clin Periodontol, 1979. **6**(7): p. 16-21.
20. Socransky, S.S., et al., *Microbial complexes in subgingival plaque.* J Clin Periodontol, 1998. **25**(2): p. 134-44.
21. Shaykhiev, R. and R. Bals, *Interactions between epithelial cells and leukocytes in immunity and tissue homeostasis.* J Leukoc Biol, 2007. **82**(1): p. 1-15.
22. Rao, M.R., et al., *Gingival Epithelial Cell Responses to Microbial Infections – AnOverview.* Journal of Research and Advancement in Dentistry, 2014. **3**(2s): p. 53-56.
23. Dale, B.A., *Periodontal epithelium: a newly recognized role in health and disease.* Periodontol 2000, 2002. **30**: p. 70-8.
24. Laube, D.M., et al., *Differential regulation of innate immune response genes in gingival epithelial cells stimulated with Aggregatibacter actinomycetemcomitans.* J Periodontal Res, 2008. **43**(1): p. 116-23.
25. McClure, R. and P. Massari, *TLR-Dependent Human Mucosal Epithelial Cell Responses to Microbial Pathogens.* Front Immunol, 2014. **5**: p. 386.
26. Broz, P. and D.M. Monack, *Newly described pattern recognition receptors team up against intracellular pathogens.* Nat Rev Immunol, 2013. **13**(8): p. 551-65.
27. Medzhitov, R., *Toll-like receptors and innate immunity.* Nat Rev Immunol, 2001. **1**(2): p. 135-45.
28. Vance, R.E., R.R. Isberg, and D.A. Portnoy, *Patterns of pathogenesis: discrimination of pathogenic and nonpathogenic microbes by the innate immune system.* Cell Host Microbe, 2009. **6**(1): p. 10-21.
29. Takeuchi, O. and S. Akira, *Pattern recognition receptors and inflammation.* Cell, 2010. **140**(6): p. 805-20.
30. Mogensen, T.H., *Pathogen recognition and inflammatory signaling in innate immune defenses.* Clin Microbiol Rev, 2009. **22**(2): p. 240-73, Table of Contents.
31. Janssens, S. and R. Beyaert, *Role of Toll-like receptors in pathogen recognition.* Clin Microbiol Rev, 2003. **16**(4): p. 637-46.
32. Kawai, T. and S. Akira, *The role of pattern-recognition receptors in innate immunity: update on Toll-like receptors.* Nat Immunol, 2010. **11**(5): p. 373-84.
33. Lim, K.H. and L.M. Staudt, *Toll-like receptor signaling.* Cold Spring Harb Perspect Biol, 2013. **5**(1): p. a011247.
34. Takeda, K. and S. Akira, *Toll-like receptors in innate immunity.* Int Immunol, 2005. **17**(1): p. 1-14.
35. Takeuchi, O., et al., *Differential roles of TLR2 and TLR4 in recognition of gram-negative and gram-positive bacterial cell wall components.* Immunity, 1999. **11**(4): p. 443-51.
36. Dziarski, R. and D. Gupta, *Role of MD-2 in TLR2- and TLR4-mediated recognition of Gram-negative and Gram-positive bacteria and activation of chemokine genes.* J Endotoxin Res, 2000. **6**(5): p. 401-5.
37. Kawai, T. and S. Akira, *Signaling to NF-kappaB by Toll-like receptors.* Trends Mol Med, 2007. **13**(11): p. 460-9.
38. Takeda, K. and S. Akira, *TLR signaling pathways.* Semin Immunol, 2004. **16**(1): p. 3-9.
39. Trautmann, A., *Extracellular ATP in the immune system: more than just a "danger signal".* Sci Signal, 2009. **2**(56): p. pe6.
40. Ghaemi-Oskouie, F. and Y. Shi, *The role of uric acid as an endogenous danger signal in immunity and inflammation.* Curr Rheumatol Rep, 2011. **13**(2): p. 160-6.

41. Klune, J.R., et al., *HMGB1: endogenous danger signaling.* Mol Med, 2008. **14**(7-8): p. 476-84.
42. Abdul-Sater, A.A., et al., *Inflammasomes bridge signaling between pathogen identification and the immune response.* Drugs Today (Barc), 2009. **45 Suppl B**: p. 105-12.
43. Franchi, L., et al., *Function of Nod-like receptors in microbial recognition and host defense.* Immunol Rev, 2009. **227**(1): p. 106-28.
44. Martinon, F., A. Mayor, and J. Tschopp, *The inflammasomes: guardians of the body.* Annu Rev Immunol, 2009. **27**: p. 229-65.
45. Kanneganti, T.D., *The inflammasome: firing up innate immunity.* Immunol Rev, 2015. **265**(1): p. 1-5.
46. Schroder, K. and J. Tschopp, *The inflammasomes.* Cell, 2010. **140**(6): p. 821-32.
47. Davis, B.K., H. Wen, and J.P. Ting, *The inflammasome NLRs in immunity, inflammation, and associated diseases.* Annu Rev Immunol, 2011. **29**: p. 707-35.
48. Latz, E., T.S. Xiao, and A. Stutz, *Activation and regulation of the inflammasomes.* Nat Rev Immunol, 2013. **13**(6): p. 397-411.
49. Said-Sadier, N. and D.M. Ojcius, *Alarmins, inflammasomes and immunity.* Biomed J, 2012. **35**(6): p. 437-49.
50. Man, S.M. and T.D. Kanneganti, *Regulation of inflammasome activation.* Immunol Rev, 2015. **265**(1): p. 6-21.
51. Sollberger, G., et al., *Caspase-1: the inflammasome and beyond.* Innate Immun, 2014. **20**(2): p. 115-25.
52. Miao, E.A., J.V. Rajan, and A. Aderem, *Caspase-1-induced pyroptotic cell death.* Immunol Rev, 2011. **243**(1): p. 206-14.
53. Kayagaki, N., et al., *Non-canonical inflammasome activation targets caspase-11.* Nature, 2011. **479**(7371): p. 117-21.
54. Schmid-Burgk, J.L., et al., *Caspase-4 mediates non-canonical activation of the NLRP3 inflammasome in human myeloid cells.* Eur J Immunol, 2015. **45**(10): p. 2911-7.
55. Lorenz, G., M.N. Darisipudi, and H.J. Anders, *Canonical and non-canonical effects of the NLRP3 inflammasome in kidney inflammation and fibrosis.* Nephrol Dial Transplant, 2014. **29**(1): p. 41-8.
56. Broz, P. and D.M. Monack, *Noncanonical inflammasomes: caspase-11 activation and effector mechanisms.* PLoS Pathog, 2013. **9**(2): p. e1003144.
57. Martinon, F., K. Burns, and J. Tschopp, *The inflammasome: a molecular platform triggering activation of inflammatory caspases and processing of proIL-beta.* Mol Cell, 2002. **10**(2): p. 417-26.
58. Lamkanfi, M., *Emerging inflammasome effector mechanisms.* Nat Rev Immunol, 2011. **11**(3): p. 213-20.
59. Hung, S.C., et al., *P2X4 assembles with P2X7 and pannexin-1 in gingival epithelial cells and modulates ATP-induced reactive oxygen species production and inflammasome activation.* PLoS One, 2013. **8**(7): p. e70210.
60. Junger, W.G., *Immune cell regulation by autocrine purinergic signalling.* Nat Rev Immunol, 2011. **11**(3): p. 201-12.
61. Surprenant, A. and R.A. North, *Signaling at purinergic P2X receptors.* Annu Rev Physiol, 2009. **71**: p. 333-59.
62. Burnstock, G., *Purinergic signalling.* Br J Pharmacol, 2006. **147 Suppl 1**: p. S172-81.

63. Tozaki-Saitoh, H., M. Tsuda, and K. Inoue, *Role of purinergic receptors in CNS function and neuroprotection.* Adv Pharmacol, 2011. **61**: p. 495-528.
64. Ralevic, V. and G. Burnstock, *Involvement of purinergic signaling in cardiovascular diseases.* Drug News Perspect, 2003. **16**(3): p. 133-40.
65. Burnstock, G. and M. Williams, *P2 purinergic receptors: modulation of cell function and therapeutic potential.* J Pharmacol Exp Ther, 2000. **295**(3): p. 862-9.
66. Burnstock, G., *Purine and pyrimidine receptors.* Cell Mol Life Sci, 2007. **64**(12): p. 1471-83.
67. Ralevic, V. and G. Burnstock, *Receptors for purines and pyrimidines.* Pharmacol Rev, 1998. **50**(3): p. 413-92.
68. Weisman, G.A., et al., *P2Y receptors in the mammalian nervous system: pharmacology, ligands and therapeutic potential.* CNS Neurol Disord Drug Targets, 2012. **11**(6): p. 722-38.
69. Pelegrin, P. and A. Surprenant, *Pannexin-1 mediates large pore formation and interleukin-1beta release by the ATP-gated P2X7 receptor.* EMBO J, 2006. **25**(21): p. 5071-82.
70. Jiang, R., et al., *Tightening of the ATP-binding sites induces the opening of P2X receptor channels.* EMBO J, 2012. **31**(9): p. 2134-43.
71. Riteau, N., et al., *ATP release and purinergic signaling: a common pathway for particle-mediated inflammasome activation.* Cell Death Dis, 2012. **3**: p. e403.
72. Gombault, A., L. Baron, and I. Couillin, *ATP release and purinergic signaling in NLRP3 inflammasome activation.* Front Immunol, 2012. **3**: p. 414.
73. Heid, M.E., et al., *Mitochondrial reactive oxygen species induces NLRP3-dependent lysosomal damage and inflammasome activation.* J Immunol, 2013. **191**(10): p. 5230-8.
74. Martinon, F., *Signaling by ROS drives inflammasome activation.* Eur J Immunol, 2010. **40**(3): p. 616-9.
75. Chen, K., et al., *ATP-P2X4 signaling mediates NLRP3 inflammasome activation: a novel pathway of diabetic nephropathy.* Int J Biochem Cell Biol, 2013. **45**(5): p. 932-43.
76. Soto, F., et al., *P2X4: an ATP-activated ionotropic receptor cloned from rat brain.* Proc Natl Acad Sci U S A, 1996. **93**(8): p. 3684-8.
77. Yilmaz, O., *The chronicles of Porphyromonas gingivalis: the microbium, the human oral epithelium and their interplay.* Microbiology, 2008. **154**(Pt 10): p. 2897-903.
78. Al-Younes, H.M., V. Brinkmann, and T.F. Meyer, *Interaction of Chlamydia trachomatis serovar L2 with the host autophagic pathway.* Infect Immun, 2004. **72**(8): p. 4751-62.
79. Amano, A., I. Nakagawa, and T. Yoshimori, *Autophagy in innate immunity against intracellular bacteria.* J Biochem, 2006. **140**(2): p. 161-6.
80. Birmingham, C.L., et al., *Listeria monocytogenes evades killing by autophagy during colonization of host cells.* Autophagy, 2007. **3**(5): p. 442-51.
81. Yilmaz, O., et al., *Gingival epithelial cell signalling and cytoskeletal responses to Porphyromonas gingivalis invasion.* Microbiology, 2003. **149**(Pt 9): p. 2417-26.
82. Belanger, M., et al., *Autophagy: a highway for Porphyromonas gingivalis in endothelial cells.* Autophagy, 2006. **2**(3): p. 165-70.
83. Coutinho-Silva, R. and D.M. Ojcius, *Role of extracellular nucleotides in the immune response against intracellular bacteria and protozoan parasites.* Microbes Infect, 2012.
84. Schwiebert, E.M. and A. Zsembery, *Extracellular ATP as a signaling molecule for epithelial cells.* Biochim Biophys Acta, 2003. **1615**(1-2): p. 7-32.

85. Choi, C.H., et al., *Porphyromonas gingivalis-nucleoside-diphosphate-kinase inhibits ATP-induced reactive-oxygen-species via P2X7 receptor/NADPH-oxidase signalling and contributes to persistence.* Cell Microbiol, 2013. **15**(6): p. 961-76.
86. Zhang, J., et al., *IL-8 degradation by Porphyromonas gingivalis proteases.* Microb Pathog, 1999. **26**(5): p. 275-80.
87. Signat, B., et al., *Fusobacterium nucleatum in periodontal health and disease.* Curr Issues Mol Biol, 2011. **13**(2): p. 25-36.
88. Karpathy, S.E., et al., *Genome sequence of Fusobacterium nucleatum subspecies polymorphum - a genetically tractable fusobacterium.* PLoS One, 2007. **2**(7): p. e659.
89. Al-Ahmad, A., et al., *The in vivo dynamics of Streptococcus spp., Actinomyces naeslundii, Fusobacterium nucleatum and Veillonella spp. in dental plaque biofilm as analysed by five-colour multiplex fluorescence in situ hybridization.* J Med Microbiol, 2007. **56**(Pt 5): p. 681-7.
90. Taxman, D.J., et al., *Porphyromonas gingivalis mediates inflammasome repression in polymicrobial cultures through a novel mechanism involving reduced endocytosis.* J Biol Chem, 2012. **287**(39): p. 32791-9.
91. Dewhirst, F.E., et al., *The human oral microbiome.* J Bacteriol, 2010. **192**(19): p. 5002-17.
92. Bik, E.M., et al., *Bacterial diversity in the oral cavity of 10 healthy individuals.* ISME J, 2010. **4**(8): p. 962-74.
93. Han, Y.W., et al., *Interactions between periodontal bacteria and human oral epithelial cells: Fusobacterium nucleatum adheres to and invades epithelial cells.* Infect Immun, 2000. **68**(6): p. 3140-6.
94. Silva, N., et al., *Host response mechanisms in periodontal diseases.* J Appl Oral Sci, 2015. **23**(3): p. 329-55.
95. Arigbede, A.O., B.O. Babatope, and M.K. Bamidele, *Periodontitis and systemic diseases: A literature review.* J Indian Soc Periodontol, 2012. **16**(4): p. 487-91.
96. Hasan, A. and R.M. Palmer, *A clinical guide to periodontology: pathology of periodontal disease.* Br Dent J, 2014. **216**(8): p. 457-61.
97. Han, Y.W., et al., *Identification and characterization of a novel adhesin unique to oral fusobacteria.* J Bacteriol, 2005. **187**(15): p. 5330-40.
98. Tuttle, R.S., et al., *A non-lectin-like mechanism by which Fusobacterium nucleatum 10953 adheres to and activates human lymphocytes.* Oral Microbiol Immunol, 1992. **7**(2): p. 78-83.
99. Mangan, D.F., et al., *Lectinlike interactions of Fusobacterium nucleatum with human neutrophils.* Infect Immun, 1989. **57**(11): p. 3601-11.
100. Temoin, S., et al., *Signal peptide of FadA adhesin from Fusobacterium nucleatum plays a novel structural role by modulating the filament's length and width.* FEBS Lett, 2012. **586**(1): p. 1-6.
101. Xu, M., et al., *FadA from Fusobacterium nucleatum utilizes both secreted and nonsecreted forms for functional oligomerization for attachment and invasion of host cells.* J Biol Chem, 2007. **282**(34): p. 25000-9.
102. Ozaki, M., et al., *Binding specificity of Fusobacterium nucleatum to human erythrocytes, polymorphonuclear leukocytes, fibroblasts, and HeLa cells.* J Periodontal Res, 1990. **25**(3): p. 129-34.
103. Diamond, G. and L. Ryan, *Beta-defensins: what are they really doing in the oral cavity?* Oral Dis, 2011. **17**(7): p. 628-35.

104. Mathews, M., et al., *Production of beta-defensin antimicrobial peptides by the oral mucosa and salivary glands.* Infect Immun, 1999. **67**(6): p. 2740-5.
105. Dale, B.A. and S. Krisanaprakornkit, *Defensin antimicrobial peptides in the oral cavity.* J Oral Pathol Med, 2001. **30**(6): p. 321-7.
106. Gomes Pde, S. and M.H. Fernandes, *Defensins in the oral cavity: distribution and biological role.* J Oral Pathol Med, 2010. **39**(1): p. 1-9.
107. Kelk, P., et al., *IL-1beta secretion induced by Aggregatibacter (Actinobacillus) actinomycetemcomitans is mainly caused by the leukotoxin.* Int J Med Microbiol, 2008. **298**(5-6): p. 529-41.
108. Bui, F.Q., et al., *Fusobacterium nucleatum infection of gingival epithelial cells leads to NLRP3 inflammasome-dependent secretion of IL-1beta and the danger signals ASC and HMGB1.* Cell Microbiol, 2015.
109. Griffin, G.K., et al., *IL-17 and TNF-alpha sustain neutrophil recruitment during inflammation through synergistic effects on endothelial activation.* J Immunol, 2012. **188**(12): p. 6287-99.
110. McGee, D.W., et al., *A synergistic relationship between TNF-alpha, IL-1 beta, and TGF-beta 1 on IL-6 secretion by the IEC-6 intestinal epithelial cell line.* Immunology, 1995. **86**(1): p. 6-11.
111. Guilloteau, K., et al., *Skin Inflammation Induced by the Synergistic Action of IL-17A, IL-22, Oncostatin M, IL-1{alpha}, and TNF-{alpha} Recapitulates Some Features of Psoriasis.* J Immunol, 2010.
112. Awane, M., et al., *NF-kappa B-inducing kinase is a common mediator of IL-17-, TNF-alpha-, and IL-1 beta-induced chemokine promoter activation in intestinal epithelial cells.* J Immunol, 1999. **162**(9): p. 5337-44.
113. Palmqvist, P., et al., *IL-1beta and TNF-alpha regulate IL-6-type cytokines in gingival fibroblasts.* J Dent Res, 2008. **87**(6): p. 558-63.
114. Saperstein, S., et al., *IL-1beta augments TNF-alpha-mediated inflammatory responses from lung epithelial cells.* J Interferon Cytokine Res, 2009. **29**(5): p. 273-84.
115. Hardy, R. and M.S. Cooper, *Bone loss in inflammatory disorders.* J Endocrinol, 2009. **201**(3): p. 309-20.
116. Vignery, A. and R. Baron, *Dynamic histomorphometry of alveolar bone remodeling in the adult rat.* Anat Rec, 1980. **196**(2): p. 191-200.
117. Hienz, S.A., S. Paliwal, and S. Ivanovski, *Mechanisms of Bone Resorption in Periodontitis.* J Immunol Res, 2015. **2015**: p. 615486.
118. Soysa, N.S., et al., *Osteoclast formation and differentiation: an overview.* J Med Dent Sci, 2012. **59**(3): p. 65-74.
119. Goltzman, D., *Discoveries, drugs and skeletal disorders.* Nat Rev Drug Discov, 2002. **1**(10): p. 784-96.
120. Boyce, B.F., et al., *TNF-alpha and pathologic bone resorption.* Keio J Med, 2005. **54**(3): p. 127-31.
121. Hwang, S.Y. and J.W. Putney, Jr., *Calcium signaling in osteoclasts.* Biochim Biophys Acta, 2011. **1813**(5): p. 979-83.
122. Blair, H.C., L.J. Robinson, and M. Zaidi, *Osteoclast signalling pathways.* Biochem Biophys Res Commun, 2005. **328**(3): p. 728-38.
123. Hayman, A.R., *Tartrate-resistant acid phosphatase (TRAP) and the osteoclast/immune cell dichotomy.* Autoimmunity, 2008. **41**(3): p. 218-23.

124. Lee, H.R., et al., *In-vivo-induced antigenic determinants of Fusobacterium nucleatum subsp. nucleatum.* Mol Oral Microbiol, 2011. **26**(2): p. 164-72.
125. Kostic, A.D., et al., *Fusobacterium nucleatum potentiates intestinal tumorigenesis and modulates the tumor-immune microenvironment.* Cell Host Microbe, 2013. **14**(2): p. 207-15.
126. Dharmani, P., et al., *Fusobacterium nucleatum infection of colonic cells stimulates MUC2 mucin and tumor necrosis factor alpha.* Infect Immun, 2011. **79**(7): p. 2597-607.
127. Zaborina, O., et al., *Secretion of ATP-utilizing enzymes, nucleoside diphosphate kinase and ATPase, by Mycobacterium bovis BCG: sequestration of ATP from macrophage P2Z receptors?* Mol Microbiol, 1999. **31**(5): p. 1333-43.
128. Baker, P.J., et al., *Heterogeneity of Porphyromonas gingivalis strains in the induction of alveolar bone loss in mice.* Oral Microbiol Immunol, 2000. **15**(1): p. 27-32.
129. Ramos-Junior, E.S., et al., *A Dual Role for P2X7 Receptor during Porphyromonas gingivalis Infection.* J Dent Res, 2015. **94**(9): p. 1233-42.
130. Liu, P., et al., *Detection of fusobacterium nucleatum and fadA adhesin gene in patients with orthodontic gingivitis and non-orthodontic periodontal inflammation.* PLoS One, 2014. **9**(1): p. e85280.
131. Park, S.R., et al., *Diverse Toll-like receptors mediate cytokine production by Fusobacterium nucleatum and Aggregatibacter actinomycetemcomitans in macrophages.* Infect Immun, 2014. **82**(5): p. 1914-20.
132. Kotake, S., et al., *IL-17 in synovial fluids from patients with rheumatoid arthritis is a potent stimulator of osteoclastogenesis.* J Clin Invest, 1999. **103**(9): p. 1345-52.
133. Lee, Y., *The role of interleukin-17 in bone metabolism and inflammatory skeletal diseases.* BMB Rep, 2013. **46**(10): p. 479-83.
134. Huang, H., et al., *IL-17 stimulates the proliferation and differentiation of human mesenchymal stem cells: implications for bone remodeling.* Cell Death Differ, 2009. **16**(10): p. 1332-43.
135. Yago, T., et al., *IL-17 induces osteoclastogenesis from human monocytes alone in the absence of osteoblasts, which is potently inhibited by anti-TNF-alpha antibody: a novel mechanism of osteoclastogenesis by IL-17.* J Cell Biochem, 2009. **108**(4): p. 947-55.
136. Andersson, U., et al., *HMGB1 as a DNA-binding cytokine.* J Leukoc Biol, 2002. **72**(6): p. 1084-91.
137. Lotze, M.T. and K.J. Tracey, *High-mobility group box 1 protein (HMGB1): nuclear weapon in the immune arsenal.* Nat Rev Immunol, 2005. **5**(4): p. 331-42.
138. Erlandsson Harris, H. and U. Andersson, *Mini-review: The nuclear protein HMGB1 as a proinflammatory mediator.* Eur J Immunol, 2004. **34**(6): p. 1503-12.
139. Kalinina, N., et al., *Increased expression of the DNA-binding cytokine HMGB1 in human atherosclerotic lesions: role of activated macrophages and cytokines.* Arterioscler Thromb Vasc Biol, 2004. **24**(12): p. 2320-5.
140. Gao, Y., et al., *IFN-gamma stimulates osteoclast formation and bone loss in vivo via antigen-driven T cell activation.* J Clin Invest, 2007. **117**(1): p. 122-32.
141. Zupan, J., M. Jeras, and J. Marc, *Osteoimmunology and the influence of pro-inflammatory cytokines on osteoclasts.* Biochem Med (Zagreb), 2013. **23**(1): p. 43-63.
142. Vaananen, K., *Mechanism of osteoclast mediated bone resorption--rationale for the design of new therapeutics.* Adv Drug Deliv Rev, 2005. **57**(7): p. 959-71.
143. Teitelbaum, S.L., *Bone resorption by osteoclasts.* Science, 2000. **289**(5484): p. 1504-8.

144. Periasamy, S. and P.E. Kolenbrander, *Aggregatibacter actinomycetemcomitans builds mutualistic biofilm communities with Fusobacterium nucleatum and Veillonella species in saliva.* Infect Immun, 2009. **77**(9): p. 3542-51.
145. Metzger, Z., et al., *Synergistic pathogenicity of Porphyromonas gingivalis and Fusobacterium nucleatum in the mouse subcutaneous chamber model.* J Endod, 2009. **35**(1): p. 86-94.
146. Johnson, L., et al., *Porphyromonas gingivalis attenuates ATP-mediated inflammasome activation and HMGB1 release through expression of a nucleoside-diphosphate kinase.* Microbes Infect, 2015. **17**(5): p. 369-77.
147. Toussi, D.N., X. Liu, and P. Massari, *The FomA porin from Fusobacterium nucleatum is a Toll-like receptor 2 agonist with immune adjuvant activity.* Clin Vaccine Immunol, 2012. **19**(7): p. 1093-101.
148. Liu, H., R.W. Redline, and Y.W. Han, *Fusobacterium nucleatum induces fetal death in mice via stimulation of TLR4-mediated placental inflammatory response.* J Immunol, 2007. **179**(4): p. 2501-8.
149. Quah, S.Y., G. Bergenholtz, and K.S. Tan, *Fusobacterium nucleatum induces cytokine production through Toll-like-receptor-independent mechanism.* Int Endod J, 2014. **47**(6): p. 550-9.
150. Iwasaki, Y., et al., *In situ proliferation and differentiation of macrophages in dental pulp.* Cell Tissue Res, 2011. **346**(1): p. 99-109.
151. Mosser, D.M. and X. Zhang, *Activation of murine macrophages.* Curr Protoc Immunol, 2008. **Chapter 14**: p. Unit 14 2.
152. Mosser, D.M. and J.P. Edwards, *Exploring the full spectrum of macrophage activation.* Nat Rev Immunol, 2008. **8**(12): p. 958-69.
153. Mosser, D.M., *The many faces of macrophage activation.* J Leukoc Biol, 2003. **73**(2): p. 209-12.
154. Schroder, K., et al., *Interferon-gamma: an overview of signals, mechanisms and functions.* J Leukoc Biol, 2004. **75**(2): p. 163-89.
155. Kamijo, R., et al., *Mice that lack the interferon-gamma receptor have profoundly altered responses to infection with Bacillus Calmette-Guerin and subsequent challenge with lipopolysaccharide.* J Exp Med, 1993. **178**(4): p. 1435-40.
156. Shtrichman, R. and C.E. Samuel, *The role of gamma interferon in antimicrobial immunity.* Curr Opin Microbiol, 2001. **4**(3): p. 251-9.
157. Takayanagi, H., et al., *T-cell-mediated regulation of osteoclastogenesis by signalling cross-talk between RANKL and IFN-gamma.* Nature, 2000. **408**(6812): p. 600-5.
158. Boyle, W.J., W.S. Simonet, and D.L. Lacey, *Osteoclast differentiation and activation.* Nature, 2003. **423**(6937): p. 337-42.
159. Ulett, G.C., N. Ketheesan, and R.G. Hirst, *Cytokine gene expression in innately susceptible BALB/c mice and relatively resistant C57BL/6 mice during infection with virulent Burkholderia pseudomallei.* Infect Immun, 2000. **68**(4): p. 2034-42.
160. Pal, S., E.M. Peterson, and L.M. de la Maza, *Susceptibility of mice to vaginal infection with Chlamydia trachomatis mouse pneumonitis is dependent on the age of the animal.* Infect Immun, 2001. **69**(8): p. 5203-6.
161. Tschopp, J., *Mitochondria: Sovereign of inflammation?* Eur J Immunol, 2011. **41**(5): p. 1196-202.

162. Nakhjiri, S.F., et al., *Inhibition of epithelial cell apoptosis by Porphyromonas gingivalis.* FEMS Microbiol Lett, 2001. **200**(2): p. 145-9.
163. Hornung, V., et al., *Silica crystals and aluminum salts activate the NALP3 inflammasome through phagosomal destabilization.* Nat Immunol, 2008. **9**(8): p. 847-56.
164. Yin, L., R. Stearns, and B. Gonzalez-Flecha, *Lysosomal and mitochondrial pathways in H2O2-induced apoptosis of alveolar type II cells.* J Cell Biochem, 2005. **94**(3): p. 433-45.
165. Feuille, F., et al., *Mixed infection with Porphyromonas gingivalis and Fusobacterium nucleatum in a murine lesion model: potential synergistic effects on virulence.* Infect Immun, 1996. **64**(6): p. 2094-100.